PREPARATION OF ASYMMETRIC TiO_2 BASED NANO/ULTRAFILTRATION MEMBRANES FOR WASTEWATER TREATMENT

A Thesis Submitted to
the Graduate School of Engineering and Sciences of
İzmir Institute of Technology
in Partial Fulfillment of the Requirements for the Degree of

MASTER OF SCIENCE

in Chemical Engineering

by
İklima ODABAŞI

July 2017
İZMİR

We approve the thesis of **İklima ODABAŞI**

Examining Committee members:

Prof. Dr. Muhsin ÇİFTÇİOĞLU
Department of Chemical Engineering, İzmir Institute of Technology

Assist. Prof. Dr. Ayben TOP
Department of Chemical Engineering, İzmir Institute of Technology

Assoc.Prof.Dr.Mücahit SÜTÇÜ
Department of Materials Science and Engineering, İzmir Katip Çelebi University

24 July 2017

Prof. Dr. Muhsin ÇİFTÇİOĞLU
Supervisor, Department of Chemical Engineering,
İzmir Institute of Technology

Prof. Dr. Fehime ÇAKICIOĞLU ÖZKAN
Head of the Department of
Chemical Engineering

Prof. Dr. Aysun SOFUOĞLU
Dean of the Graduate School of
Engineering and Sciences

ACKNOWLEDGEMENTS

I would like to express my deepest gratitude to my advisor, Prof. Dr. Muhsin ÇİFTÇİOĞLU for his support, guidance, encouragement and motivation during my thesis.

I would like to express my gratitude to Assist. Prof. Selçuk ÖZCAN for his support, motivation and encouragement.

I am especially grateful to my laboratory colleagues, Safiye YALDIZ, Pınar ÇETİN, Kaan YALTRIK, Öncel KIRKBAŞ, Kenan YILMAZ for their assistance and support during this study.

I would also like to thank Burcu ALP and Rukiye ÇİFTÇİOĞLU for their assistance, support during my thesis.

I would like to thank İzmir Institute of Technology Environmental Development Application and Research Center for providing technical help and support.

Lastly, I offer sincere thanks to my family Kemal Yalçın ODABAŞI, Sibel ODABAŞI and Kemal Erdem ODABAŞI for their continuous support, deepest love, invaluable patience all throughout my life.

This study was supported by The Scientific and Technological Research Council of Turkey (TUBITAK) within the context of ÇAYDAG 113Y344 project.

ABSTRACT

PREPARATION OF ASYMMETRIC TiO_2 BASED NANO/ULTRAFILTRATION MEMBRANES FOR WASTEWATER TREATMENT

Fresh water scarcity have been the most fundamental problem in the world and is already affecting mankind and human activities. This problem forced an increasing effort in the reuse of wastewater originating from municipal, agricultural, and industrial activities. The textile industry demands large amounts of water and produces large quantities of wastewater. Adsorption, filtration, ozonation and photocatalysis techniques are currently used for wastewater treatment and safe discharge to the environment. Although membrane filtration necessitates a high initial setup cost, it has a high potential and may cause significant cost savings through the reuse of water and salts. The membrane based technologies are widely accepted to be the best method when compared with the currently available technologies for wastewater treatment.

Extruded tubular alumina supports were coated by stable colloidal sols and polymeric sols prepared by using sol-gel based techniques for the formation of selective micro/ultra/nanofiltration layers in this work. Textile wastewater treatment (with and without pre-treatment) and membrane fouling analysis was conducted. The performances of the membranes were determined through the characterization of permeates by a spectrophotometer. The reduction of colors (Pt-Co, m^{-1}), turbidity and suspended solids content were about 99%, 100% and 100%, respectively. The incorporation of a coagulation stage by using $Al_2(SO_4)_3$ followed by a successive filtration reduced the membrane/irreversible fouling levels in the MF/UF membranes significantly. The Pt-Co 455 values of permeates were determined to be in the 15-260 range which are below the discharge criteria bringing the possibility of the reuse of some of these permeates.

ÖZET

TEKSTİL ATIKSU ARITIMI İÇİN TiO_2 BAZLI NANO/ULTRAFİLTRASYON MEMBRANLARIN HAZIRLANMASI

Temiz su kıtlığı dünyadaki en önemli problemlerden biri olmuş ve insanoğlunu ve aktivitelerini etkilemektedir. Bu problem kentsel, tarımsal ve endüstriyel faaliyetlerden kaynaklanan atıksuyun tekrar kullanımına yönelik giderek artan çabaları zorunlu kılmıştır. Tekstil çok yüksek miktarlarda su kullananılan ve atıksu üreten bir endüstridir. Adsorpsiyon, filtrasyon, ozonlama ve fotokataliz gibi teknikler bugünlerde atıksu arıtımı ve arıtılan suyun çevreye güvenli bir şekilde deşarjı için kullanılmaktadır. Membran filtrasyonu yüksek kurulum maliyetine ihtiyaç duymasına ragmen yüksek bir potansiyele sahiptir ve su/tuzların tekrar kullanımıyla maaliyette önemli azalmalara neden olabilir. Atıksu arıtımı için halen kullanılmakta olan teknolojiler ile membran teknolojisi kıyaslandığında membran teknolojileri yaygın bir biçimde en iyi method olara kabul görmektedir.

Bu çalışmada seçici micro/ultra/nanofiltrasyon tabakalarının oluşumları için sol-jel teknikleri esas alınarak hazırlanmış kararlı kolloidal ve polimerik sollerle ekstrüde alümina destekler kaplandı. Tekstil atıksu arıtımı (önarıtmalı ve önarıtmasız) ve membran tıkanma analizleri yapıldı. Membranların performansları spektrofotometre tarafından karakterize edilen süzüntüler vasıtasıyla belirlendi. Katı madde miktarı, bulanıklık ve renkteki (Pt-Co, m^{-1}) azalışlar yaklaşık olarak sırasıyla %100, %100 ve %99'dur. MF/UF membranlarında geri dönüşümsüz/membran tıkanıklık seviyeleri koagülasyon katılımı olan $Al_2(SO_4)_3$ kullanımını takip eden filtrasyonda önemli oranda azalmıştır. Süzüntülerin Pt-Co 455 değerleri deşarj kriterlerinin altında 15-215 arasında belirlenmiş olup bu süzüntülerden bazılarının tekrar kullanımı olasıllığı bulunmaktadır.

TABLE OF CONTENTS

LIST OF FIGURES viii

LIST OF TABLES xii

CHAPTER 1. INTRODUCTION 1

CHAPTER 2. CERAMIC MEMBRANES 4
- 2.1. History of Membranes 4
- 2.2. Ceramic Membranes 6
- 2.3. Materials Used In Membrane Preparation 8
  - 2.3.1. Polymeric Organic Membranes 8
  - 2.3.2. Inorganic Membranes 8
- 2.4. Classification of Membranes 9
- 2.5. Preparation of Ceramic Membranes 11
- 2.6. Preparation of Titania Nanofiltration Ceramic Membranes 12

CHAPTER 3. MEMBRANE TECHNOLOGY 14
- 3.1. Membrane Working Principle 14
- 3.2. Membrane Fouling 17
  - 3.2.1. Nature of Flux Decline 17

CHAPTER 4. MEMBRANE SEPARATION FOR TEXTILE WASTEWATER TREATMENT 19

CHAPTER 5. EXPERIMENTAL 23
- 5.1. Materials 23
- 5.2. Method 24
  - 5.2.1. Preparation of the Selective Layers 25
  - 5.2.2. Thermal Behaviour of Selective Layer 31
  - 5.2.3. Filtration Experiments 31

CHAPTER 6. RESULTS AND DISCUSSION 34
- 6.1. Preparation of The Selective Layers 34
  - 6.1.1. Characterization of Ceramic Asymmetric Membrane Layers 35

6.1.2. Characterization of the Dip-Coating Sols 36
6.2. Characterization of Textile Wastewater 41
6.3. Determination of the Pre-treatment Methods 41
6.3.1. Analyses of Filter Papers 41
6.3.2. Determination of the effective $Al_2(SO4)_3$ coagulant addition in pretreatment.....45
6.4. Membrane Performance 48
6.4.1. Effect of Pre-treatment on Membrane Performance For the First tubular membrane set 48
6.4.1.1. Analyses of Membrane Fouling with Pre-treatment 55
6.4.2. Textile Wastewater Treatment With/Without Pre-Treatment For The Second Tubular Membrane Series.....58
6.4.2.1. Fouling Analyses of the Textile wastewater treatment with/without pre-treatment for the second tubular membrane series 67

CHAPTER 7. CONCLUSIONS 73

REFERENCES 76

LIST OF FIGURES

Figure **Page**

Figure 2.1. The first ceramic filter in 800 B.C. for serving liquids from Israeli National Museum(Source: Vitaliy Gidis, 2016). 4
Figure 2.2. Historical timeline of ceramic membrane applications(Source: Vitaliy Gidis, 2016). 5
Figure 2.3. Timeline of ceramic membrane development(Source: Vitaliy Gidis, 2016). 6
Figure 2.4. The pore content distribution of a tubular ceramic membrane with pore size(Source: Li, 2007). 7
Figure 2.5. The four major types of pressure-driven membrane processes(Source: Tim Van Gestel et al. 2003)..... 11
Figure 3.1. Filtration mechanism of membrane (Source: Kırkbaş, 2016). 14
Figure 3.2. The total resistance modelling of membrane (Source: Kırkbaş, 2016). 16
Figure 5.1. The layers of the asymmetric ceramic tubular membrane..... 24
Figure 5.2. Schematic representation of the first α-alumina MF layer preparation..... 26
Figure 5.3. Schematic representation of the AKP-50 MF layer preparation. 26
Figure 5.4. Schematic representation of the disperal UF-1 layer preparation. 27
Figure 5.5. Schematic representation of P2 UF-1 layer preparation 28
Figure 5.6. Schematic representation of TiO_2 UF-2 layer preparation. 29
Figure 5.7. Schematic representation of TiO_2 (TTB) UF-2 layer preparation. 29
Figure 5.8. Schematic representation of the polymeric titania-zirconia layer preparation. 30
Figure 5.9. The cross flow filtration set-up (1-pump, 2-feed tank, 3- recycle, 4-gauge, 5-flowmeter, 6-cross-flow membrane module)..... 32
Figure 6.1. The extruded tubular α-alumina supports..... 34
Figure 6.2. Top surface and cross-sectional SEM images of the MF layer. 35
Figure 6.3. Top surface SEM images of the UF-1 selective layer. 36

Figure 6.4. Top surface and cross-sectional SEM images of the UF-2 selective layer. . 36

Figure 6.5. The particle size distribution of the CT3000SG α-alumina colloidal suspension (wt 7% α-alumina, 0.8% PVA). 37

Figure 6.6. The particle size distribution of the AKP-50 colloidal suspension (wt 7% AKP-50). 38

Figure 6.7. The particle size distribution of the disperal colloidal suspension (wt 0.6% Boehmite (disperal), 0.8% PVA). 38

Figure 6.8. The particle size distribution of the P2 colloidal suspension (wt 0.6% P2). 39

Figure 6.9. The particle size distribution of the TTIP hydrosol (TTIP:DEA:HNO_3:H_2O:Propanol 1:0.8:2.4:1000:10). 39

Figure 6.10. The particle size distribution of the TTB hydrosol. 40

Figure 6.11. The particle size distribution of the titania/zirconia polymeric sols. 40

Figure 6.12. The rejection percentage of Color (Pt-Co) after filter paper pretreatment. 42

Figure 6.13. The rejection percentage of Admi Color (m^{-1}) after filter paper pretreatment. 43

Figure 6.14. The rejection percentage of Suspended Solids (mg/L) after filter paper pretreatment. 43

Figure 6.15. The rejection percentage of Turbidity (NAU) after filter paper pretreatment. 44

Figure 6.16. The rejection percentage of Pt-Co 410 Color (mg/L) after filter paper pretreatment. 44

Figure 6.17. The variation of the rejection percentage of 455 Pt-Co color values with coagulant addition level. 46

Figure 6.18. The variation of rejection percentage of Admi color (m^{-1}) with coagulant amount..... 46

Figure 6.19. The variation of rejection percentage of Pt-Co color with coagulant amount..... 47

Figure 6.20. The variation of rejection percentage of turbidity with coagulant amount..... 47

Figure 6.21. The variation of rejection percentage of Suspended Solids (mg/L) with coagulant amount. 48

Figure 6.22. Variation of clean water flux at TMP-2 (support, α-alumina, AKP-50, disperal and P2)..... 49
Figure 6.23. Variation of clean water flux at TMP-2 (TTIP, TTB, NF (one, two, three, four and five layers))..... 49
Figure 6.24. Wastewater flux decline of membranes at TMP-2 (support, α-alumina, AKP-50, disperal and P2). 50
Figure 6.25. Wastewater flux decline of membranes at TMP-2 (TTIP, TTB, NF (one, two, three, four and five layers))..... 50
Figure 6.26. Rejection percentage of suspended solids (wastewater with pre-treatment). 51
Figure 6.27. Rejection percentage of suspended solids (wastewater with pre-treatment). 52
Figure 6.28. Rejection percentage of Admi Color (m^{-1}) of wastewater with pre-treatment..... 52
Figure 6.29. Rejection percentage of Admi Color (m^{-1}) of the wastewater with pre-treatment..... 53
Figure 6.30. Rejection percentage of Color (Pt-Co) of the wastewater with pre-treatment..... 53
Figure 6.31. Rejection percentage of Color (Pt-Co) of the wastewater with pre-treatment..... 54
Figure 6.32. The color change of wastewater (with pre-treatment) (from left to right; for a; original wastewater, $Al_2(SO_4)_3$+fitler paper, support, MF, AKP-50, UF-1 (disperal and P2),for b; UF-2 (TTIP and TTB), NF (one, two, three, four and five layers), respectively). 54
Figure 6.33. The variation of the filtration resistance for wastewater with pre-treatment with membrane type..... 58
Figure 6.34. The variation of the filtration resistance for wastewater with pre-treatment with membrane type..... 58
Figure 6.35. Variation of clean water flux at TMP=2 (UF-1 (disperal), UF-1 (P2), UF-2 (TTB), NF (one, two, three and four layers)) (without pre-treatment)..... 59
Figure 6.36. Wastewater flux variation of membranes at TMP-2 with time (UF-1 (disperal), UF-1 (P2), UF-2 (TTB) and NF (one, two, three and four layers)) (without pre-treatment)..... 60
Figure 6.37. Rejection percentage of suspended solids (without pre-treatment)..... 61

Figure 6.38. Rejection percentage of Color (Pt-Co) (without pre-treatment)..... 62
Figure 6.39. Rejection percentage of Admi Color (m^{-1}) (without pre-treatment). 62
Figure 6.40. Color change of wastewater (without pre-treatment) (from left to right; original wastewater, UF-1 (disperal, P2), UF-2 (TTB), NF (one, two, three and four layers, respectively)). 62
Figure 6.41. Variation of clean water flux at TMP=2 (P2 and NF(four layers)). 63
Figure 6.42. Wastewater flux decline of membranes at TMP-2 (UF-1 (P2) and NF (four layers)) (with pre-treatment). 64
Figure 6.43. Rejection percentage of Suspended solids (with pre-treatment). 65
Figure 6.44. Rejection percentage of Admi Color (m^{-1}) (with pre-treatment)..... 66
Figure 6.45. Rejection percentage of Color (Pt-Co) (with pre-treatment)..... 66
Figure 6.46. Color change of wastewater (with pre-treatment) (from left to right; original wastewater, $Al_2(SO_4)_3$+filter paper, UF-1 (P2), NF (four layers)). 67
Figure 6.47. The distribution of the resistances for the second tubular membrane series without pre-treatment (Route 1)..... 70
Figure 6.48. The distribution of the filtration resistance for wastewater with pre-treatment (UF-1(P2) and NF (four layers)). 72

LIST OF TABLES

Table **Page**

Table 2.1. The characteristics of hollow fibre, plate-and-frame and tubular modules(Source: Wade et al., 2007). 7

Table 2.2. Pressure-driven processes and their characteristics.(Source: Tim Van Gestel et al. 2003) 9

Table 4.1. the discharge criteria of textile wastewater (Source: Damas et al., 2010).....20

Table 4.2. The reuse criteria of textile wastewater (Source: Capar et al., 2006).....20

Table 5.1. The materials and their properties. 23

Table 5.2. The flux decline analysis equations. 33

Table 6.1. Textile wastewater characterization results……....41

Table 6.2. The percent rejection values of the filter papers. 42

Table 6.3. The variation of percent rejection values with $Al_2(SO_4)_3$ addition level. 45

Table 6.4. The cumulative percent rejection values of the wastewater with pre-treatment after the NF (five layers) treatment. 51

Table 6.5. The various fluxes and flux recoveries of the membranes (support, MF, AKP-50, UF-1 (disperal and P2), UF-2 (TTIP and TTB) and NF (one, two, three, four and five layers)). 55

Table 6.6. The fouling (irreversible, reversible) and concentration polarization flux decline percentages of Support, MF, AKP-50, UF-1 (disperal and P2), UF-2 (TTIP and TTB) and NF (one, two, three, four and five layers) membranes with pre-treatment. 56

Table 6.7. The filtration resistance of Support, MF, AKP-50, UF-1 (disperal and P2), UF-2 (TTIP and TTB) and NF (one, two, three, four and five layers) membranes with pre-treatment. 57

Table 6.8. The cumulative percent rejection values of the wastewater without pre-treatment after the NF (four layers) treatment. 61

Table 6.9. The cumulative percent rejection values of the wastewater with pre-treatment after the NF (four layers) treatment. 65

Table 6.10. The flux decline of the membranes (UF-1 (disperal and P2), UF-2 (TTB) and NF (one, two, three and four layers)) (without pre-treatment)..... 68

Table 6.11. The flux decline and its distribution with fouling (irreversible, reversible) and concentration polarization of membranes without pre-treatment. 69
Table 6.12. The filtration resistances of the membranes without pre-treatment. 69
Table 6.13. The fluxes and flux recovery for the UF-1 (P2) and NF (four layers) membranes with pre-treatment..... 70
Table 6.14. The flux decline distribution with fouling (irreversible, reversible) and concentration polarization of UF-1 (P2) and NF (four layers) membranes with pre-treatment. 71
Table 6.15. The filtration resistance of UF-1 (P2) and NF (four layers) membranes with pre-treatment. 72

CHAPTER 1

INTRODUCTION

Fresh water scarcity have been the most fundamental problem in the world and is already affecting mankind and human activities. This problem forced an increasing effort in the reuse of wastewater originating from municipal, agricultural, and industrial activities. The households consume roughly 50% of the water and the other 50% of the water is used by agricultural and industrial activities. Various water reclamation applications necessitate specific water qualities. The increasing world population contributed to a series of fresh water related concerns in the industry. The most important concern is about the unforbidable fact of reclamation and water reuse in industrial activities in order to solve water scarcity and environmental problems. This is vital for the sustainable growth and continuation of industrial production.

The textile industry demands large amounts of water and produces large quantities of wastewater. The color and concentration of dissolved solids which may be organic /inorganic in nature may vary significantly in textile wastewater. The color in the wastewater is not easily removed by conventional treatment techniques like adsorption, filtration, ozonation, biological treatment and photocatalysis. The treated wastewater is finally diluted with clean water and then discharged to the nature or sewage systems.

Although membrane treatment requires a high initial setup cost, significant cost savings can be achieved through the reuse of permeates and salts. The membrane fouling problems can be overcome by regular cleaning techniques, the use of pre-filters and through the choice of the most suitable membrane system (Tang & Chen, 2002).

Membrane based technologies have been proven to be capable of separating macromolecules and ions from wastewater and considered to be superior to the existing treatment techniques (Moliner-Salvador, Deratani, Palmeri, & Sanchez, 2012). Membrane based technologies are widely accepted to be the Best Available Techniques (BAT) for textile wastewater treatment and reclamation in a recent Reference Document

issued by European Union (Barredo-Damas, Alcaina-Miranda, Iborra-Clar, & Mendoza-Roca, 2012).

Ceramic membranes have high chemical, thermal and mechanical stability, a long life-time (low fouling rate) compared to polymeric membranes (Zeidler, Puhlfürß, Kätzel, & Voigt, 2014). Ceramic membranes with high permeability can be provided in the asymmetric structure. The asymmetric configuration has a multilayered structure with a macroporous support which mainly provides the mechanical strength to the system. The intermediate layers decrease the defects on the support surface. The intermediate layer also prevents leaking of the top layer coating sols into the pores of the support. The top layer is the final selective layer and its pore size determines the separation abilities and flux of the membrane system. Alumina (Al_2O_3), silica (SiO_2), titania (TiO_2) and zirconia (ZrO_2) are widely used for the formation of the asymmetric intermediate/top layer structures in ceramic membranes. Sol-gel based methods are commonly used for the preparation of sols used for fabricating the selective top layers. Sol-gel derived methods make the preparation of selective layers/films with a close control/design of the pore structure possible with lower heat treatment temperatures, creating the possibility of multicomponent film production and a high degree of chemical homogeneity (Benito, Conesa, Rubio, & Rodríguez, 2005).

Leenaars et al. (1984, 1985) applied the first sol-gel process in the ceramic ultrafiltration membrane preparation. The phase pure alumina (Al_2O_3) and titania (TiO_2) membranes were prepared and applied by Anderson et al. (1988), Moosemiller et al. (1989), Zaspalis et al. (1992), Kumar (1993), Chang et al. (1994), Schaep et al. (1999) and Chuah et al. (2000). Alumina-titania mixed oxide membranes have been investigated by Van gestel et al. (2002). The alumina-titania membranes were developed due to their good thermal, chemical, and mechanical stability (Sh. Akbarnezhad, 2010).

The selective layers of tubular membranes which were composed of two microfiltration (α-alumina), two ultrafiltration (boehmite and titania hydrosol) and several nanofiltration (titania polymeric sol) were formed on the inner surfaces of extruded and heat treated Al_2O_3 supports in this work. The particle sizes of the stable dip-coating suspensions/sols used for the formation of these layers were determined by Dynamic light scattering (DLS Zetasizer). The unsupported membrane micro/nano structures were characterized by scanning electron microscope (SEM). The textile wastewater was treated in cross-flow operation by a pilot scale set-up. The wastewater

was treated successively with the support, microfiltration, ultrafiltration-1, ultrafiltration-2, and nanofiltration tubular membranes. A number of important permeate properties such as chemical oxygen demand, color, conductivity, and suspended solids content were determined by a spectrophotometer. The fouling analysis of the membranes were also conducted.

CHAPTER 2

CERAMIC MEMBRANES

2.1. History of Membranes

A membrane is a semipermeable structure which retains some the components such as bacteria, sugar, or salt allowing the others to permeate present in a liquid or gaseous mixture. The first membranes were synthesized in 1700's. Graham used a pioneering type of membrane in the improvement of the diffusion law in 1848. The improvement and application of membranes evolved into a scientific discipline in the 1950's. Membrane based separations with relatively lower energy requirements are attracting increased interest nowadays. These membrane based processes are becoming an alternative to the well known separation methods such as crystallization, distillation, adsorption, absorption, extraction etc.

Ceramics are in general compounds formed by non-metallic and metallic elements [like alumina (Al_2O_3), zirconia (ZrO_2), silica (SiO_2)]. The first ceramics were found in Czechoslovakia and were made from animal fat, bone ash and clays. The first use of ceramics in the form of containers was for storing grains. The Sumerians wrote on ceramic stone plaques about 5000 years ago. The ceramic amphora was invented for the storage and transport of liquids such as olive oil and wine in Greece. The first ceramic filter used in history is shown in Figure 2.1.

Figure 2.1. The first ceramic filter in 800 B.C. for serving liquids from Israeli National Museum (Source: Vitaliy Gidis, 2016).

The production and use of ceramic articles dates back to thousands of years ago but the ceramic technology has improved significantly in the last century and evolved into a science rather than an art. Technical ceramics are used in various industries and applications such as membrane separations, electronic devices, biomaterials, engines, artificial bones. The first large scale application of ceramic membranes was in the separation of U-238 and U-235 isotopes for making nuclear weapons and fuels in the 1940's and 1950's. The separation of U-238 and U-235 isotopes was conducted at high temperatures.

Loeb and Sourirajan proposed an idea which divided the membrane structure into a skin and a porous substructure and this created a new interest in ceramic membranes as a new generation of separation technology materials in 1962. The ceramic membranes had layers like an onion. The combination of the relatively thin selective separation layers and the support which gives the mechanical strength improved the permeate fluxes significantly in the new asymmetric membrane structure.

Burgraff and Cot improved a concept and procedure in the 1980's for the fabrication of the intermediate layers. This development led to new applications in gas separation, food/beverage industries and biotechnologies. The ceramic membranes have become a worthful component of fuel cells in the past two decades affecting hydrogen economy. Water and wastewater purification applications started in 1998 in Japan. These purification applications started in The USA and Europe recently. Ceramic membranes have been developed and produced by a number of companies for new applications in chemical, water/wastewater treatment, and petrochemical industries. A timeline of ceramic membrane applications and types is given in Figures 2.2 and 2.3.

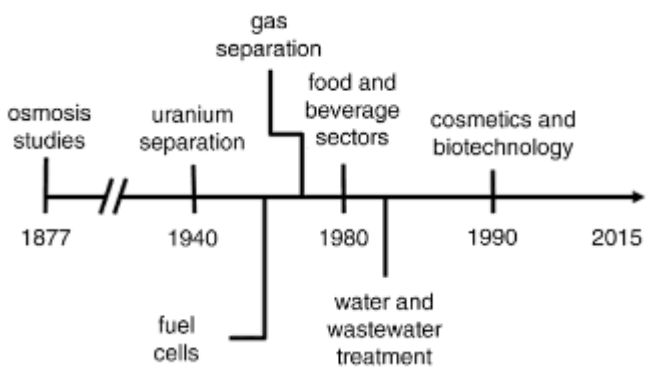

Figure 2.2. Historical timeline of ceramic membrane applications(Source: Vitaliy Gidis, 2016).

2.2. Ceramic Membranes

Membrane industry was dominated by polymeric organic membranes but in recent years inorganic membranes are increasing their share in the market due to their advantages. Ceramic membranes are the major type of inorganic membranes and have been used in some industries such as biotechnology, petrochemical, electronic, pharmaceutical industry (Vitaliy Gidis, 2016). Ceramic membranes nowadays are presenting energy efficient and environmental friendly alternatives for a large number of separation applications. Ceramic membranes have superior chemical and thermal stability, higher recoveries, longer lifetime, higher flux compared to their polymeric counterparts (Vitaliy Gidis, 2016).

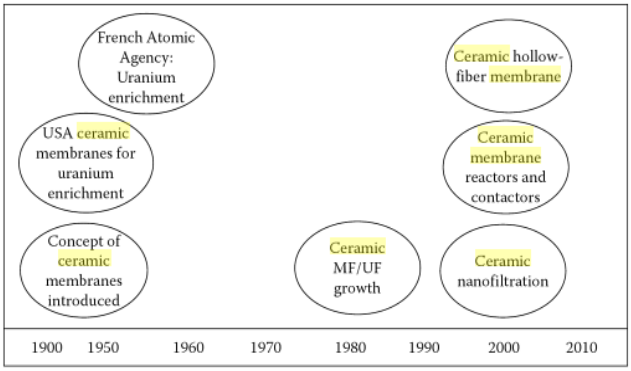

Figure 2.3. Timeline of ceramic membrane development (Source: Vitaliy Gidis, 2016).

Membranes can be classified as symmetric and asymmetric membranes according to their structure. Ceramic membranes commonly have an asymmetric structure due to their chemical and thermal stability, higher recoveries, longer lifetime and higher flux (Van der Bruggen, Vandecasteele, Van Gestel, Doyen, & Leysen, 2003). Asymmetric membrane structure is formed from a macroporous support and a number of selective thinner layers with decreasing pore sizes in the meso/micro pore size range (Li, 2007). The pore content of an asymmetric ceramic membrane as a function of pore size is shown in Figure 2.4. Ceramic membranes are produced in different geometries such as disc, tube, and sheet. The advantages and disadvantages of various modules are given in Table 2.1. The effective separation with high flux necessitates high surface area to volume ratio. Tubular ceramic membrane configuration has a reasonably high surface area to volume ratio.

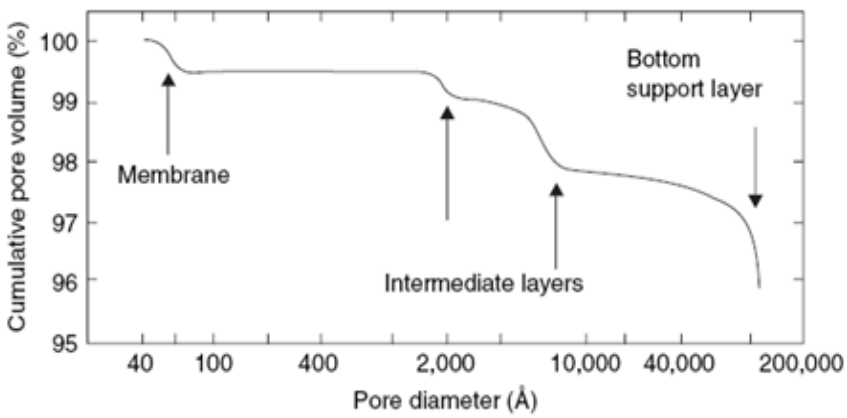

Figure 2.4. The pore content distribution of a tubular ceramic membrane with pore size(Source: Li, 2007).

Table 2.1. The characteristics of hollow fibre, plate-and-frame and tubular modules(Source:Wade et al., 2007).

	Hollow fibre	Plate-and-frame	Tubular
Cost/area	Low	High	Low
Membrane replacement cost	Moderate	Low	Moderate/low
Flux (l/(m^2 h))	Good	Low	Low
Packing density (m^2/m^3)	Excellent	Good/fair	Good
Hold-up volume	Low	Medium	Medium
Cleaning in place	Good	Fair/poor	Fair/poor

The most important advantage of ceramic membranes is their high thermal stability. Ceramic membranes can be operated at high temperatures (ranging from 200°C to 1000 °C) while organic membranes can only be operated at low temperatures (Wade et al., 2007). Chemical and mechanical stability of ceramic membranes also is higher than organic membranes. Ceramic membranes have higher fluxes because of their higher porosity and hydrophilic surfaces. Ceramic membranes also have longer operational life than organic membranes. Organic membranes are cheaper than ceramic membranes. Ceramic membranes may have sealing problems due to differences in thermal expansions between material couples (Abadi et al, 2011).

2.3. Materials Used In Membrane Preparation

2.3.1. Polymeric Organic Membranes

Polymeric membrane was introduced in the 1960s and they have the largest market share in the separation industry since 1960. Polymeric membranes are more economical than other membranes. There are some important parameters such as chain rigidity, stereoregularity, interactions of chains and polarity of their functional groups in the production of suitable polymeric membranes. Cellulose acetate is an example of polymeric membrane material. Polyether sulfone, polyamide, polyvinylidene fluoride and polyacrylonitrile are commonly used in the preparation of polymeric membranes. Track etching, coating, phase inversion (the most common technique) and polymerization are some of the techniques used for the preparation of polymeric membranes.

2.3.2. Inorganic Membranes

Inorganic membranes are attracting increasing interest in recent years. The application and research on inorganic membranes have been developed rapidly because of their advantages over organic membranes. These membranes can be classified in there main groups such as ceramic, glass and metallic. These membranes can be operated at higher temperatures and in wider pH ranges than their polymeric counterparts. Inorganic membranes can be operated for a long lifetime by using cleaning operations commonly known as backwashing. Backwashing is conducted by reversing the flow direction and the application of high transmembrane pressures. The main advantage of ceramic inorganic membrane is its extended lifetime. Their major disadvantages are their high capital cost and brittle nature.

Inorganic membranes can be classified in two main groups. These are porous membranes made from ceramic materials and dense membranes produced by using palladium and its alloys/other metals. Porous ceramic membranes are made from metal oxides like alumina (Al_2O_3), titania (TiO_2), silica (SiO_2), zirconia (ZrO_2) and their

composites and can be used in harsh conditions such as high temperatures and chemically corrosive environments.

2.4. Classification of Membranes

A membrane separation process is focused on different driving forces and porous membrane separation is a pressure driven process. Pressure-driven membrane processes can be sorted by several criteria such as pore size, charge and size of the maintained molecules or particles, pressure exerted on the membrane. The four major types of pressure-driven membrane processes are microfiltration (MF), ultrafiltration (UF), nanofiltration (NF) and reverse osmosis (RO). These four types are summarized in Table 2.2. (Tim Van Gestel et al., 2003) and their separation abilities are schmetically shown in Figure 2.5. The most important property is the pore size of the membrane structure in this classification. The molecular weight cut-off (MWCO) in daltons (where a Dalton is equal to 1 g/mol) is commonly used as a measure of the effective membrane pore size in separation applications.

Table 2.2. Pressure-driven processes and their characteristics.(Source: Tim Van Gestel et al. 2003)

	Microfiltration (MF)	**Ultrafiltration (UF)**	**Nanofiltration (NF)**	**Reverse Osmosis (RO)**
Permeability (l/h.m^2.bar)	>1,000	10-1,000	1.5-30	0.05-1.5
Pressure (bar)	0.1-2	0.1-5	3-20	5-120
Pore size (nm)	100-10,000	2-100	0.5-2	<0.5
Rejection				
• Monovalent ions	-	-	-	+
• Multivalent ions	-	-/+	+	+
• Small organic compounds	-	-	-/+	+
• Macromolecules	-	+	+	+
• Particles	+	+	+	+
Separation mechanism	Sieving	Sieving	Sieving Charge effects	Solution-Diffusion
Applications	Clarification, Pretreatment, Removal of bacteria	Removal of macromolecules bacteria, viruses	Removal of (multivalent) ions and relatively small organics	Ultrapure water, desalination
Type of membrane	Porous	Porous	Porous	Nonporous

Microfiltration (MF) membranes have the largest pores in the100-10,000 nm range. MF membranes have the highest permeability which is higher than 1,000l/h.m^2.bar. A sieving mechanism is responsible for the removal of the components which are larger than the pore size. Microfiltration membranes act as a molecular sieve preventing bacteria, suspended solids, colloids to pass, but cannot retain germs and viruses and they are commonly used in biotechnology and food/dairy industries.

Pore sizes of ultrafiltration membranes are smaller than microfiltration membranes (from 2 nm to 100 nm) and their permeability is lower than MF membranes. These membranes operate at higher pressures. Generally, macromolecules and colloidal particles are removed from liquids with ultrafiltration processes which are called purification processes. The ultrafiltration processes are applied in food industries for the purification of streams and separation of proteins.

Pore sizes of nanofiltration (NF) membranes are smaller than ultrafiltration membranes (from 0.5 to 2 nm) which are between ultrafiltration and reverse osmosis processes. Permeability is lower than ultrafiltration. NF membranes operate at higher pressures than UF membranes. Common applications of NF are in the separation of small species/molecules (about 1 nm in size) and some salts which are monovalent and divalent salts in wastewater treatment and desalination.

Reverse osmosis (RO) membranes have a dense structure. Permeation is the slowest in RO membranes with a low permeability and rejection is not a result of molecular sieving. NF processes work at high pressures in the 5-120 bar range. Separation is accomplished through a solution-diffusion process in these membranes. Reverse osmosis membranes can remove dissolved salts and ions and they are used in the textile, pulp and paper, chemical industries.

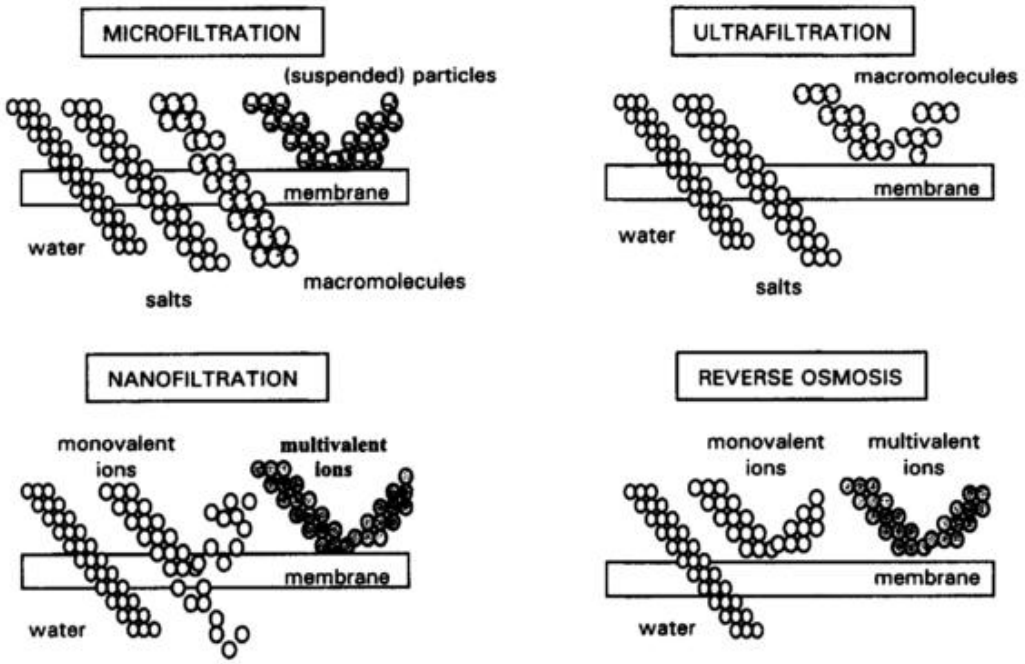

Figure 2.5. The four major types of pressure-driven membrane processes(Source: Tim Van Gestel et al. 2003).

2.5. Preparation of Ceramic Membranes

There are various methods such as leaching, slipcasting, extrusion, and sintering used for ceramic membrane support preparation. Ceramic powders and varieties of additives prepared by hydrothermal treatment, sol-gel synthesis, and chemical vapor deposition are used in these support preparation methods (Vitaliy Gidis, 2016). α-alumina is usually used for the preparation of ceramic membrane supports by using extrusion, tape casting or slipcasting due to the millimeter-depth thickness and micrometer-size pores. Smaller particle size γ-alumina is used for the preparation of intermediate layers which are 300-400 μm thick and contains nanometer sized pores by using dip coating. The order of the intermediate layers is determined by considering the particle sizes of sols. The top layer which is responsible from the membrane's separation abilities is above the intermediate layers. This layer can be made by using different methods such as sol-gel synthesis, chemical vapour deposition, pyrolysis and oxidation (Moliner-Salvador et al., 2012).

2.6. Preparation of Titania Nanofiltration Ceramic Membranes

There are different types of processes for developing ceramic nanofiltration membranes but the key technique is the sol-gel process. Voigt et al. were the first to improve a titania nanofiltration membrane. They used the polymeric route and measured molecular weight cut-off which was smaller than 500 Da. Sekulic et al. prepared a titania nanofiltration membrane and pore sizes of these membranes were ≤0.8 nm with the polymeric route. Tsuru et al. prepared titania nanofiltration membranes series (molecular weight cut-offs of 250 Da, 400 Da, 500 Da, 600 Da and 1000 Da) via the polymeric sol-gel technique. The colloidal route is more preferable than other routes for industrial scale production because of its easy operation, low volatilization and non-toxicity. The colloidal route was used in the preparation of titania nanofiltration membranes in many studies due to the above stated reasons. The most important challenge is the prevention of particle aggregation when colloidal sol-gel technique is used for producing titania nanofiltration membranes by using stable sols. The particle size of the stable titania hydrosol should be below 10 nm depending on the packing models of random closed packed systems. The nanosized stable titania hydrosols were prepared via the sol-gel techniques. Mohammadi et al. fabricated the stable TiO_2 hydrosol and measured a hydrodynamic diameter of 13 nm. They used titanium (IV) isopropoxide (TTIP), hydrochloric acid (HCl) and water (H_2O). The molar ratio of the stable titania sol was TTIP:HCl:H_2O=1:0.6:534. The titania sol was peptized at 50 °C for 2h. The crystallite size of this material was 1.3 nm and this material was 95% anatase. Katoch et al. prepared long term stable titania sols and by adjusting H_2O to Ti molar ratio. Anatase titania nanocrystallites 3-5 nm in diameter was obtained in their work. These crystallites were uniformly dispersed in the stable titania sol. Most of the colloidal sols were prepared with acid in the reported literature. The nanoparticles are formed rapidly with a high surface energy and completed hdyrolysis during the colloidal sol-gel process. These nanoparticles produced large particles due to the agglomeration and formed a precipitated hydrate. The peptization process should be controlled for fragmentization to the primary agglomerates. Many studies were conducted on the production of ultrafine colloidal sols by controlling the amount of acid necessary for peptization (Cai, Wang, Chen, Qiu, & Fan, 2015).

Anatase is the low temperature phase of TiO_2 and transforms to the rutile phase at high temperature. The transformation temperature depends on the preparation method, morphology of the particles and nature of the precursor. The anatase phase has a higher catalytic activity than rutile. These transormations also end up with a dense rutile phase. The dense rutile phase is not useful as a sensing material or catalyst. The anatase phase is the useful phase for catalytic applications because of its higher specific area. Many studies was conducted on the production of nanocrystalline anatase TiO_2 through changing chemical preparation parameters in recents years. Chemseddine and Moritz produced anatase titania nanocrystals which were 12 nm in size and used titanium (IV) isopropoxide (TTIP): (IV) methylammonium hydroxide (Me_4NOH):1.14:0.82 molar ratio by using reflux at 90-100 °C for 6 h. Chemseddine and Moritz controlled the crystal size, structure, shape and organization of titania nanocrystals via wet chemistry. They obtained large anatase titania nanocrystals of different shapes and sizes via changing some process parameters like the pressure, the relative concentrations of Me_4NOH and TTIP and the reaction temperature. Zhang et al. studied 93% anatase titania powder. The powder was heated up to 500 °C and the average particle size of this powder was 18 nm. They used the polymeric sol-gel method and hydrolyzed titanium ethoxide in water at 70 °C with ethanol and acetic acid. Pottier et al. produced nanoparticles of anatase titania and the mean size of anatase titania was between 5 and 10 nm. They used stabilizing agents and ligands (surfactants or sulfate) in aqueous medium for precipitation of $TiCl_4$. Also, the anatase phase which has the high surface area is reached by chemical technique using different additives like a polymeric agents. Sivakumar et al. produced anatase titania powder. The anatase titania powder was heated up to 600 °C and its crystallite size and surface area were 10.3 nm, 104 $m^{-2}g^{-1}$ respectively. They prepared a titania sol by dispersing the precipitates. The TiO_2 sol was prepared from titanyl sulfate aqueous solution. 10% HNO_3 and hot distilled water were added to this solution. Iwasaki et al prepared nanocrystalline anatase titania with surface area of 68 $m^{-2}g^{-1}$ and its crystallite size was between 2 and 7 nm. They synthesized these powders by thermal hydrolysis of titanyl sulfate in the presence of alcohol and water (Mohammadi, Fray, & Mohammadi, 2008).

CHAPTER 3

MEMBRANE TECHNOLOGY

3.1. Membrane Working Principle

A membrane or, more properly, a semipermeable membrane, is a thin layer of material capable of separating substances when a driving force is applied across the membrane. The feed is separated to permeate and retentate streams in membrane separation. Phases at both sides of the membrane can be either in liquid or gas form. Dissolved solids and compounds can be retained totally or partially in retentate. The shape, size, surface charge of the particles and selective membrane surface are important in membrane separations. Dominant filtration mechanism is based on particle/species size as schematically shown in Figure 3.1. When the particle size is smaller than pore size, particles can pass through the membrane. If the particle size is bigger than pore size, particles cannot pass through the membrane (Kırkbaş, 2016).

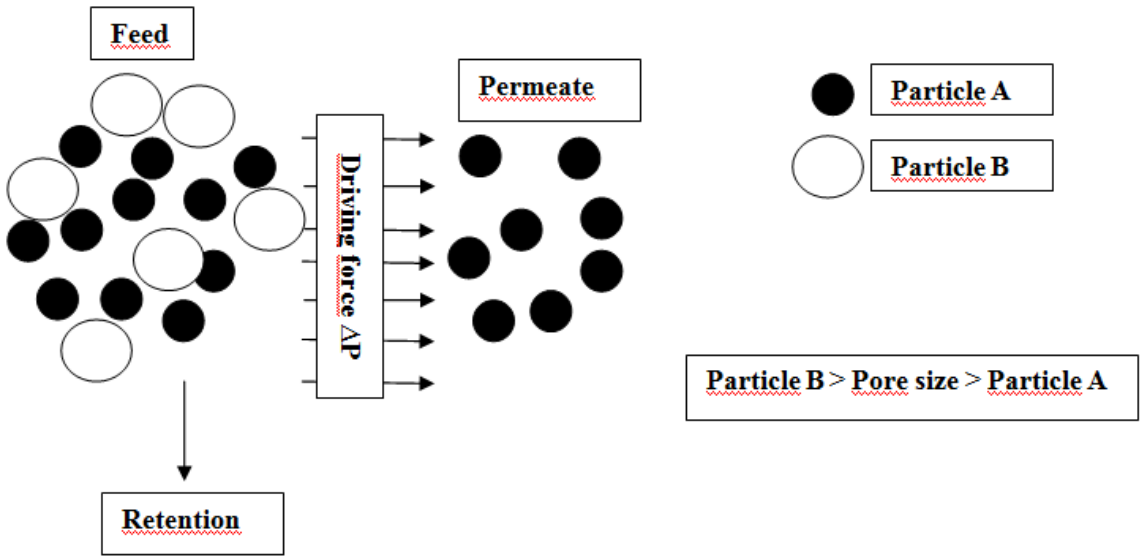

Figure 3.1. Filtration mechanism of membrane (Source: Kırkbaş, 2016).

Pressure, electrical field and concentration diffrences are the major driving forces for the transport through the membranes. Membrane acts like a sieving barrier. The ratio between the size of the dissolved species and the membrane pores controls the selective transport through the membrane. Membrane performance involves two main factors as selectivity and permeability. Permeability can be measured as flux ($L/m^2.h$). Permeability and selectivity depend on the nature of the membrane and the design.

Flux can calculated by using the following equations:

$$J_t = \frac{Q_p}{A} \tag{3.1.}$$

where

J_t = flux at t time ($L/m^2.h$)

Q_p = Permeate flow rate at t time (L/h)

A = Total membrane surface area (m^2)

$$J = \frac{TMP}{\mu R_t} \tag{3.2.}$$

J = Permeate flux

TMP = Transmembrane pressure (bar) or ΔP which is the Driving force

R_t = The total resistance to flow

μ = Dynamic viscosity of permeate (Ns/m^2)

TMP is called the transmembrane pressure and is calculated by using the following equation:

$$TMP = \frac{(P_f + P_r)}{2} - P_p \tag{3.3.}$$

where

P_f = Pressure on the membrane module inlet (bar)

P_p = Permeate pressure (bar)

P_r = Pressure on the membrane module exit (bar)

R_t is called the total resistance of the membrane which consists of several resistances as R_m, R_c, R_f. The cause of irreversible/reversible fouling is the particles present in the wastewater which forms the cake layer. The total resistances of the membrane is schematically shown in Figure 3.2.

$$R_t = R_m + R_c + R_f \quad (3.4.)$$

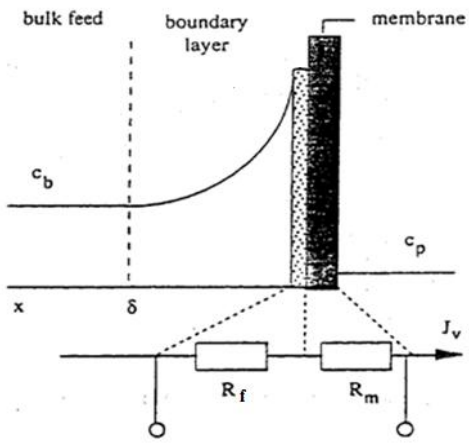

Figure 3.2. The total resistance modelling of membrane (Source: Kırkbaş, 2016).

where :

R_t = Total resistance

R_f = Fouling resistance

R_m = Membrane resistance

R_c = Cake resistance

R_f is caused by solute adsorption into the membrane pore and can be cleaned by chemical cleaning operation. R_c is formed by the cake layer and can be separated for cleaning mechanism by physical membrane.

$$R_f = \frac{\Delta P}{\mu J_{ww}} - R_m \quad (3.5.)$$

$$R_{irrev} = \frac{\Delta P}{\mu J_{cwc}} - R_m \quad (3.6.)$$

$$R_{rev} = R_f - R_{irrev} \quad (3.7.)$$

$$R_{cp} = R_t - R_m - R_f \quad (3.8.)$$

Selectivity is another important performance factor. Selectivity of the membrane is determined by using the concentration difference between feed and the permeate. Selectivity of membrane is calculated by the following equation. The determination of the membrane performance is based on selectivity and flux values.

$$\mathrm{R}\ (\%) = 100 \times \left(\frac{\mathrm{C_f} - \mathrm{C_p}}{\mathrm{C_f}}\right) = 100 \times \left(1 - \frac{\mathrm{C_p}}{\mathrm{C_f}}\right) \quad (3.9.)$$

3.2. Membrane Fouling

Complex interactions present between the foulant and the membrane must be known for determining the best procedure for membrane cleaning. Trial-and-error methods are implemented on most cleaning studies and a more methodical approach is needed to contemplate the different parts of fouling control. Also, it is essential to consider the financial effect of cleaning methods, including the expenses of the cleaning handle itself alongside the impact of the methods on membrane lifetime and productivity (Shi, Tal, Hankins, & Gitis, 2014).

3.2.1. Nature of Flux Decline

Concentration polarization and fouling affect the membrane flux under constant driving force. Concentration polarization occurs in the mass transfer boundary layer where aggregation of rejected particles or solutes happen adjacent to the membrane surface. Ultrafiltration membranes especially have this serious problem while low molecular weight macromolecules or solutes are being filtrated. The solutes are transported towards the membrane surface while the solvent passes through the membrane. The smaller solutes pass through the membrane whereas the larger species are rejected and retained by the membrane. These rejected molecules which induces a concentration gradient above the membrane surface are slow to diffuse back to the bulk solution. It is a reversible and inevitable event affecting the membrane performance significantly.

The other important effect is membrane fouling. The particals/species present in the feed solution are retained and membrane fouling takes place due deposition on the membrane surface or inside the membrane porous structure. Membrane fouling leads to the accumulation of material in a membrane as external fouling on the surface or in the pore structure of a membrane as internal fouling. The membrane fouling can result in irreversible loss of the permeability although concentration polarization is reversible. The nature of fouling can be defined in terms of its reversibility. Extensive research is conducted on the development of a better understanding of the reversible/irreversible nature of fouling which is of fundamental for determining the best backwashing/cleaning methods. Irreversible fouling continues after the cleaning but reversible fouling can be eliminated with cleaning methods easily. The irreversible part

of fouling is called as hydraulically irreversible fouling or chemically irreversible fouling after chemical cleaning (Shi et al., 2014).

CHAPTER 4

MEMBRANE SEPARATION FOR TEXTILE WASTEWATER TREATMENT

Textile industries use high quantities of fresh water (160-500 m^3/ton). Membrane technologies have been used for water reclamation in textile industries (Capar, Yilmaz, & Yetis, 2008). The BAT reference document reviewed the treatment methods for water reclamation in textile industries (Barredo-Damas et al., 2012; Capar et al., 2008). The membrane technologies are more commonly used after the BAT reference document. Dyeing process which includes fiber/fabric colorization is a main process in the textile industry. Dyes, tar and petroleum-based synthetic compounds are used in the textile dyeing process. The dyes resist to ozon, peroxide, compounds of chlorine and light. The number of dyeing baths is connected with the amount of wastewater from the bleaching or laundering processes (Schrank, Santos, Souza, & Souza, 2007). The bleaching and laundering processes involve high dye and low organic particles. Generally, these chemical groups are functional and chromofores. The structure of chromofores have chemical bonds and these bonds can change. The chromofores provide light absorption in visible region and they luster to dye. Other chemicals in the textile wastewater contain of sulphur and indigo dyes which are used for paint adherence. The practice of indigo dyes which are used in jeans are usually a complicated process because they cannot be dissolved easily in water. The indigo dyes can be dissolved with reduction reaction in water. Sodium dithionite ($Na_2S_2O_4$) is used in the reduction reaction. The wastewater treatment is difficult with classical processes because of these chemicals and reaction products. The increase in the amount of textile wastewater is connected with the variety and amount of productions of textile products. The amount and composition of textile wastewater can change based on the methods used in textile production. The textile wastewater essentially contains non-biodegradable organic matters, paint particles, inhibitory compounds and their salts. Discharge and reuse (Barredo-Damas et al., 2010; Capar, Yilmaz, & Yetis, 2006) criteria of textile wastewater are given in Tables 4.1 and 4.2.

Table 4.1. The discharge criteria of textile wastewater (Source: Damas et al., 2010).

Parameters	**Discharge Criteria**
Chemical Oxygen Demand (COD) (mg/L)	250-400
pH	6-9
Turbidity (NTU)	1
Color (Pt-Co)	260-280
Suspended Solids (mg/L)	140-400

Table 4.2. The reuse criteria of textile wastewater (Source: Capar et al., 2006).

Parameters	**Reuse Criteria (G.Capar et al)**	**Reuse Criteria (S. Barredo-Domas et al.)**
Chemical Oxygen Demand (COD) (mg/L)	80	60-80
pH	6-8	6-8
Turbidity (NTU)	1	1
Color (Pt-Co)	None	None
Suspended Solids (mg/L)	5	5

The performance of polymeric MF-UF-NF and RO(Debik, Kaykioglu, Coban, & Koyuncu, 2010; Kurt, Koseoglu-Imer, Dizge, Chellam, & Koyuncu, 2012; Uzal, Yilmaz, & Yetis, 2009; Uzal, Yılmaz, & Yetis, 2010) and ceramic UF membranes (Barredo-Damas et al., 2010; Cheïma Fersi & Dhahbi, 2008; Cheima Fersi, Gzara, & Dhahbi, 2009) were investigated. The flux reduction due to fouling were observed to be reduced with pre-treatment practices in NF membranes. The traditional pre-treatment practices were chemical precipitation, sand filtration and ozonization. The use of ceramic MF and UF membrane treatments have been considered to be effective alternatives to these traditional pre-treatment practices. The ceramic MF membranes can effectively remove suspended solids. Smaller particles and macromolecules can be removed by ceramic UF membranes and finally ceramic NF membranes may have the potential to decrease the color levels close to the reuse criteria.

The textile wastewater collected from dyeing wash processes were treated by using a pilot-scale membrane system for removing color, COD and salt with polymeric

NF270 and RO-XLE membranes in batch and continuous modes in a recent study. The initial values of COD, conductivity and color analyses varied due to the variation of the quality of print processes production in the batch system. The wastewater from the washing bath was also cooled to 30-40 °C in the pilot-system as the maximum working temperature of the polymeric membrane was at 45 °C. The values of COD, conductivity and color in NF membrane were 96%, 77.4%, 99% in batch system, respectively. Also, the values of COD, conductivity and color in NF membrane 99.3%, 65.3%, 99.1% in the continuos system, respectively. The values of COD, conductivity and color in RO-XLE membrane were 99.3%, 97.1%, 99.4% in batch system, respectively. Also, the values of COD, conductivity and color in RO-XLE membrane 99.9%, 96.9%, 99.9% in the continuos system, respectively. The textile wastewater was refined with pressure-driven membrane and it was used again. The membrane fouling sources were concluded to be inorganic pollution and concentration polarization related with increasing osmotic pressure (Kurt et al., 2012).

The ceramic tubular membranes were used in the textile wastewater treatment where mainly printing, finishing and dyeing activities were performed. Borreda-Damas et al. used an asymmetric ceramic tubular membrane which had 8 channels. The external diameter of these membranes were 25 mm and they were 580 mm long. The asymmetric structure consisted of a titania support and a zirconia-titania active layer. The MWCO (molecular weight cut-offs) of these membranes were determined (30, 50 and 150 kDa). Pleated (30 μm) and string wound PP(polypropylene) cartridge filters (5 μm) were used for pre-treatment and UF membrane was used for treatment. These pre-treatments prevented bigger particles, module damage and membrane fouling. The pilot system was tested with a set crossflow velocity of 3 m/sec. COD, turbidity, flux and color measurements were conducted in this study and COD, color and turbidiy retntions were found as 70%, 93% and 96% , respectively. The UF membrane treatment were concluded to be satisfactory for the reduction of COD, color and turbidity before NF and RO treatment (Barredo-Damas et al., 2012).

Debik et al. compared the performances of the UF and NF membranes with different pre-treatment processes in textile wastewater treatment. The textile wastewater was treated with membrane filtration directly and then an aerobic treatment and a laboratory scale anaerobic treatment were compared with NF and UF membranes. The results showed that the aerobic pre-treatment was better separation than the other pre-

treatment processes before membrane filtration and the UF membranes must be used before NF membranes (Debik et al., 2010).

CHAPTER 5

EXPERIMENTAL

5.1. Materials

The materials and their properties used in this work are given in Table 5.1.

Table 5.1. The materials and their properties.

Materials	Property
Alumina Powder α-Al_2O_3	High purity ALMATIS CT 3000 SG
Alumina Powder α-Al_2O_3	High purity Sumitomo AKP-50
Ethanol	High purity FW: 46.7, d: 0.81, Merck
Nitric Acid, HNO_3	65% FW: 63.01, d: 1.4, Aldrich
Polyvinyl alcohol, PVA	80% hydrolysed, MW: 9000-10000, Aldrich
Boehmite Powder AlO(OH)	Sasol Company, High purity acid dispersible Disperal and P2
1-Propanol	High purity, FW:60.10, d:0.8 ,Riedel
Titanium (IV) isopropoxide(TTIP)	97 %, Aldrich
Diethanolamin	Merck
Dolapix CE 64	Eurokimya A.Ş
Defoamer	Dağlar Kimya A.Ş
Zirconium (IV) propoxide (ZTP)	70%, Aldrich
Titanium (IV) butoxide (TTB)	97%, Aldrich
$Al_2(SO_4)_3$	98%, Aldrich
Filter paper	Filrtak

5.2. Method

The alumina supports used in this work was prepared by using commercial α-alumina powders (5μm, 1.3 μm and 0.5 μm), boehmite (Disperal), methocel, glycerol and water. The powders were mixed and water and glycerol were added to the powder mixture. The mixture was kneaded by a screw extruder for preparing a cylindrical paste which was placed into the barrel of the piston extruder for forming tubular ceramic membrane supports (L:20 mm, ID:16mm OD:25 mm). The tubular supports were dried at room temperature overnight and heat treated at 1525°C (Yılmaz, 2016).

The tubular alumina supports were dip-coated with α-alumina, AKP-50, boehmite (disperal and P2), and titania (TTIP and TTB) sols. The tubular asymmetric ceramic membranes were coated with three intermediate layers and a thin top layer. The asymmetric ceramic membrane structure is illustrated schematically in Figure 5.1.

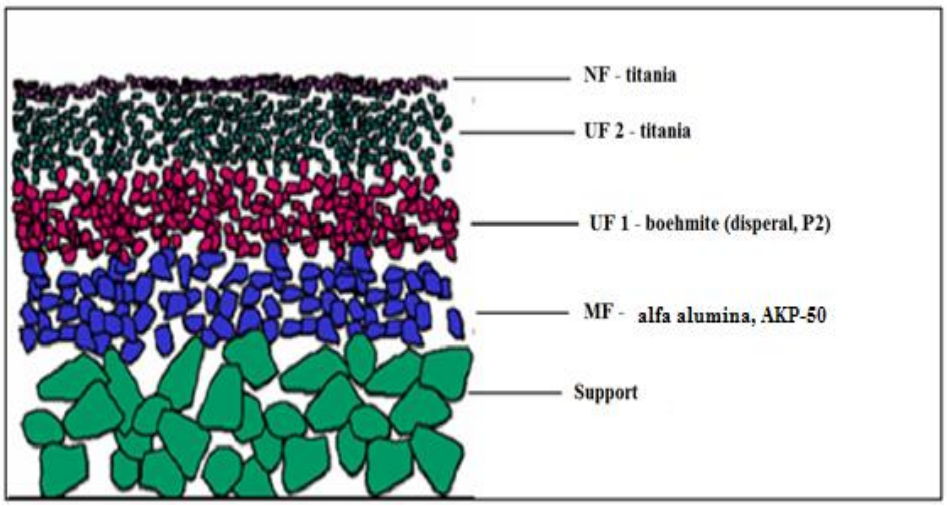

Figure 5.1. The layers of the asymmetric ceramic tubular membrane.

Microfiltration (MF) selective layers were prepared by using 0.5 μm CT3000SG and 0.18μm AKP-50 stable colloidal suspensions. Selective intermediate ultrafiltration layers were prepared by boehmite (disperal and P2) colloidal suspensions and titania (TTIP and TTB) colloidal hydrosols. The thin top layer which was the selective nanofiltration layer was prepared by using titania and zirconia polymeric sols (stable alcoholic suspensions of nanosized polymeric species) synthesized by sol-gel based methods. The particle sizes of the polymeric species in these sols were determined by Zetasizer-DLS(Malvern 3000HSA). The supports were coated with the

suspensions/sols by dip coating method and were further dried. Micro/nano structures were investigated with SEM. The phase structures were characterized with XRD. The sol coated membrane surface images were obtained by optical microscopy (Olympus BX60M). A filtration set-up was used for the determination of clean water permeabilities and separation performances. Hach Lange spectrophotometer was used for the determination of various important wastewater and permeate properties like color(Pt-Co and Admi at selected wavelengths), suspended solids, conductivity, etc.

5.2.1. Preparation of the Selective Layers

The microfiltration layer included two layers formed from α-alumina (CT3000 SG and AKP-50) powder suspensions. The stable α-alumina colloidal sol was prepared by using 7 wt % 0.5 μm CT3000 SG α-alumina, 0.8 wt % polyvinyl alcohol (PVA) (M_w = 9000-10000), dolapix and defoamer. PVA was added as a binder/drying control additive. The dolapix addition was for steric stabilization of the powder particles. The defoamer was added for the minimization of the air bubble formation during the coating process. These two additives were added slowly drop by drop.The powder suspension was ultrasonically treated 2 hours in an ultrasonic bath for the complete dispersion/deagglomeration of the powder. The AKP-50 suspension was prepared by using 7 wt % AKP-50 and water. The powder suspension was ultrasonically treated 2 hours in an ultrasonic bath for the satisfactory dispersion and deagglomeration of the powder. Dynamic light scattering (DLS Malvern Zetasizer 3000 HSA) was used for the determination of the particle size distribution of the α-alumina (0.5 μm CT3000SG and AKP-50) colloidal suspensions. The microfiltration layer was prepared from 0.5 μm Almatis and AKP-50 suspensions as schematically shown in Figures 5.2 and 5.3. The tubular ceramic support was coated with α-alumina suspension 10 minutes and was dried at room temperature for about 24 hours. The dried α-alumina coated support was heat treated at 1200°C in a furnace (Carbolite CWF 1300). The furnace was heated from room temperature to 110°C with 2°C/min heating rate, from 110°C to 1000°C with 2.7°C/min heating rate, from 1000°C to 1200°C with 2°C/min heating rate followed by a final dwell for 60 min at 1200 °C. This tubular ceramic membrane was further coated with AKP-50 colloidal suspension for 10 minutes and dried at room temperature for about 24 hours. The dried AKP-50 coated membrane was heated at 1000°C in a furnace

(Carbolite CWF 1300). The furnace was heated from room temperature to 500°C with 2°C/min heating rate, from 500°C to 800°C with 3°C/min heating rate, from 800°C to 1000°C with 2°C/min heating rate followed by a dwell time of 60 min at 1000°C.

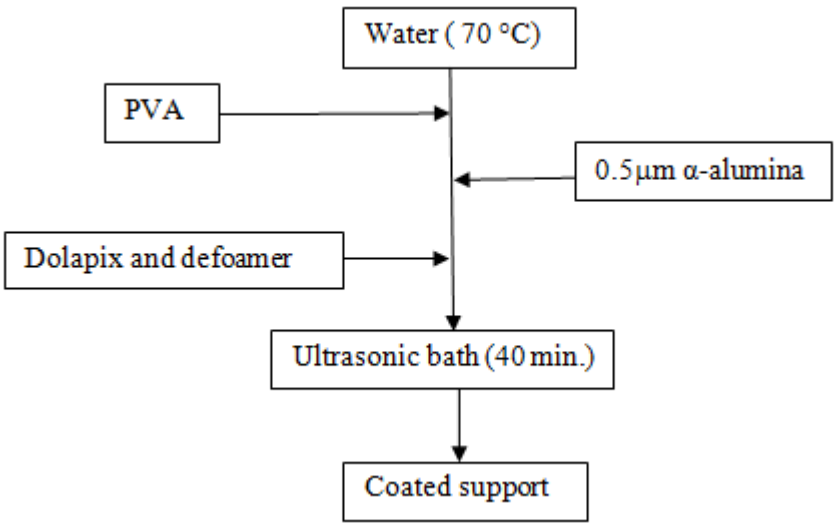

Figure 5.2. Schematic representation of the first α-alumina MF layer preparation.

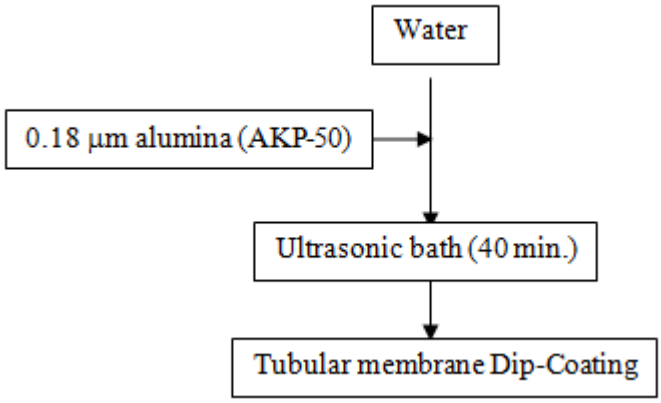

Figure 5.3. Schematic representation of the AKP-50 MF layer preparation.

The UF-1 layer was formed from two selective layers. These layers were formed by using stable disperal and P2 sols. The water based disperal sol was prepared by using 0.8 wt % disperal, 0.25 wt % PVA. Nitric acid (3 ml 1 M) was also added dropwise for peptization. Disperal powder peptization was conducted by stirring for 20 min. followed by 20 minutes ultrasonic treatment which was repeated 3 times. The particle size of the disperal sol was determined by Zetasizer-DLS. The heat treated AKP-50 layer was dip-

coated for 10 seconds with the disperal sol. The disperal coated AKP-50 layer was dried at room temperature for 24 hours. The dried disperal coated tube was heat treated at 600°C in the furnace. The furnace was heated from room temperature to 200°C with 2°C/min heating rate, from 200°C to 400°C with 1°C/min heating rate, from 400°C to 600 °C with 2°C/min heating rate. Finally the tube was dwelled at 600°C for 1 hour. One of the two UF-1 layers was prepared from disperal sol as schematically shown in Figure 5.4.

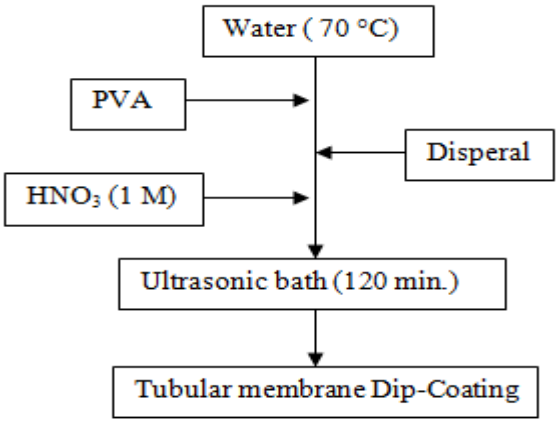

Figure 5.4. Schematic representation of the disperal UF-1 layer preparation.

The water based P2 sol was prepared by using 0.8 wt % P2. P2 powders were peptized by stirring for 20 min and were treated in an ultrasonic bath for 20 min. This procedure was repeated 3 times. The particle size of the P2 sol was determined by Zetasizer-DLS. The disperal coated layer was coated with P2 sol for 10 seconds. The P2 coated disperal layer was dried at room temperature for 24 hours. The dried P2 coated tube was heated at 600°C in the furnace. The furnace was heated from room temperature to 200°C with 2°C/min heating rate, from 200°C to 400°C with 1°C/min heating rate, from 400°C to 600°C with 2°C/min heating rate. Finally the tube was dwelled at 600°C for 1 hour in the furnace. The second UF-1 layer was prepared from P2 sol as schematically shown in Figure 5.5.

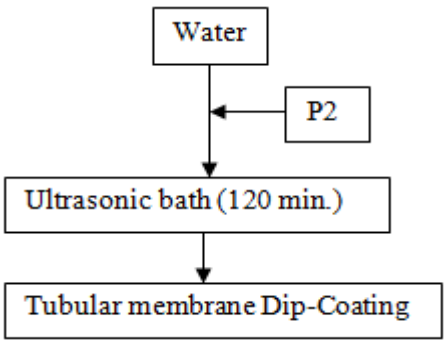

Figure 5.5. Schematic representation of P2 UF-1 layer preparation .

The UF-2 layer was prepared with two techniques. TiO_2 hydrosol was used in one of the techniques as schematically shown in Figure 5.6. Two solutions were prepared separately in this technique. Titanium tetraisopropoxide (TTIP), diethanolamine (DEA) and isopropanol was mixed for 1 hour in the preparation of the first solution of the titania hydrosol preparation. Water was heated to 45°C and used as the second solution. The well mixed first solution was added dropwise to the precipitant hot water under constant stirring. The mixture was further stirred for 1 hour by using a magnetic stirrer. Nitric acid (14 M) was added drop by drop to peptize the titania hydrosol. The molar ratio of titania sol was 1:0.3:2.5:1000:20 (TTIP:DEA:HNO_3:H_2O: Isopropanol). The particle sizes of the titania hydrosols were determined as a function of the molar ratio of water to DEA. The particle size distributions of the titania hydrosols were determined by Zetasizer-DLS.

The UF-1 (P2 coated) membrane was dip-coated for 10 seconds with the prepared TTIP based hydrosol. The coated UF-2 layer was dried at room temperature for 24 hours. The dried UF-2 layer was heat treated at 400°C in the furnace. The furnace was heated from room temperature to 400°C with 1°C/min heating rate. The tubes were dwelled at 400°C for 1 h.

The TTB (Titanium (IV) Butoxide) hydrosol preparation is schematically shown in Figure 5.7 and was used in the second route. Water was heated to 60 °C and HNO_3 (14 M) was added dropwise along with glycerol. This solution was stirred for 2 minutes. TTB was added drop by drop to the solution. The hydrosol was stirred vigorously for 30 minutes initially. The hydrosol was stirred slowly for an extra 1 hour. The molar ratio of the TTB hydrosol was 1:1:556:3.2 (TTB:Glycerol:H_2O:HNO_3). The TTIP sol coated membranes were further dip-coated for 10 seconds with the prepared TTB hydrosol. The coated TTB layer was dried at room temperature for 24 hours. The dried TTB

hydrosol layer was finally heat treated at 400°C in the furnace. The furnace was heated from room temperature to 400°C with 1°C/min heating rate. The tubes were dwelled at 400°C for 1 h in the furnace.

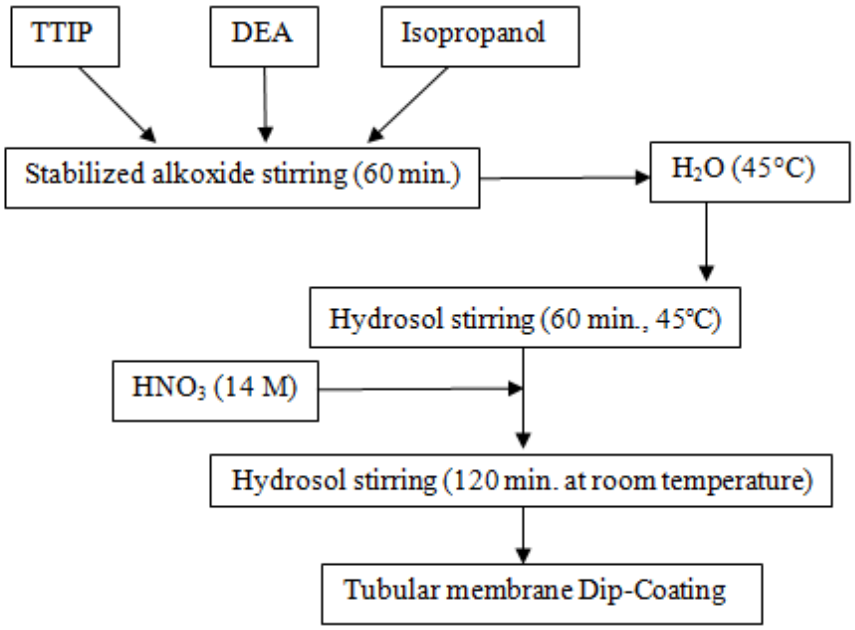

Figure 5.6. Schematic representation of TiO_2 UF-2 layer preparation.

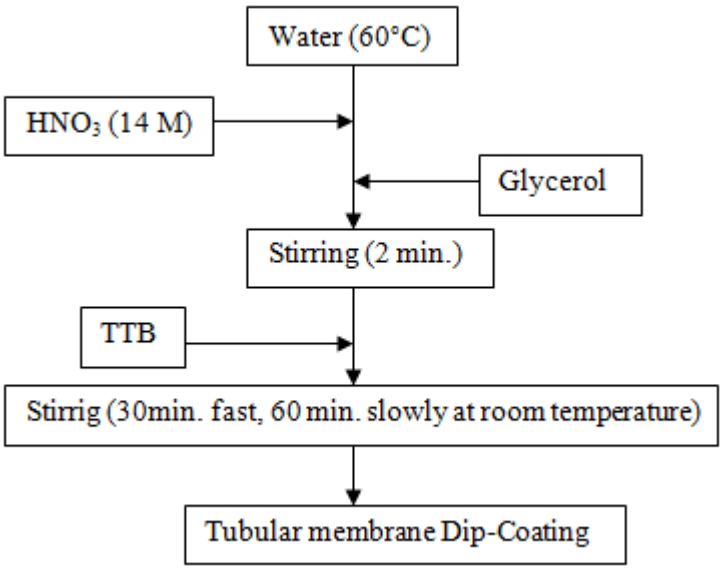

Figure 5.7. Schematic representation of TiO_2 (TTB) UF-2 layer preparation.

Nanofiltration layers were prepared by polymeric titania sol and titania-zirconia sol as shown schematically in Figures 5.8 and 5.9. One of the NF layers was prepared by using the polymeric titania sol. This polymeric sol was prepared by using two separate solutions. TTIP and ethanol were mixed 15 minutes for the formation of the first solution. Nitric acid (14 M), ethanol and water were mixed 15 minutes for the formation of the alcoholic second solution. The first solution was added drop by drop to the alcoholic solution under stirring. The molar ratios of the polymeric titania sol was 1:0.057:2:52 (TTIP:HNO_3:H_2O:EtOH). The particle size distribution of the polymeric TiO_2 sol was determined by Zetasizer-DLS. The coated TiO_2 hydrosol layer was coated with the polymeric titania sol. The polymeric titania sol was coated for 10 seconds. The coated NF layer was dried at room temperature for 24 hours. The dried NF layer was heated at 400°C in the furnace. The furnace was heated from room temperature to 400 °C with 1 °C/min heating rate. The tube was dwelled at 400 °C for 1 h in the furnace.

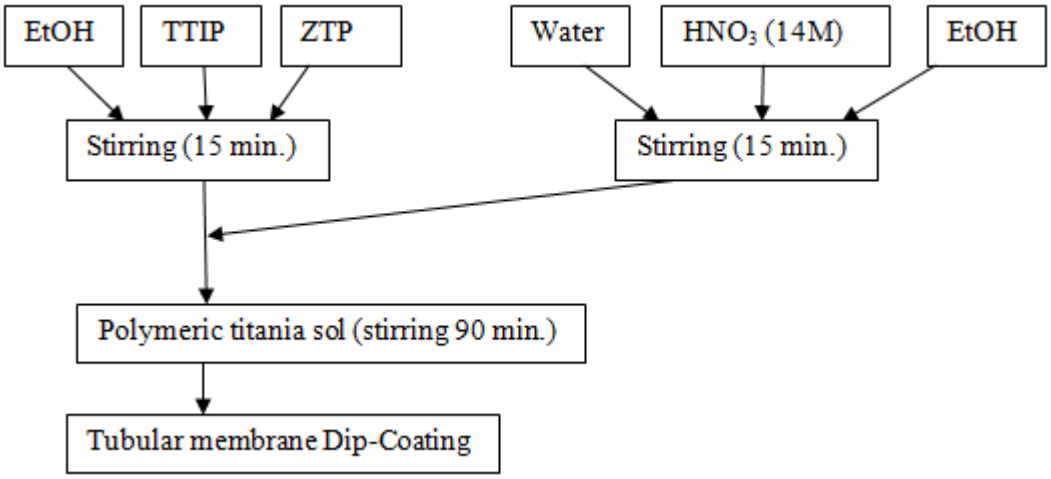

Figure 5.8. Schematic representation of the polymeric titania-zirconia layer preparation.

The other NF layer was prepared by using polymeric titania-zirconia sol. The polymeric titania-zirconia sol was prepared by using two different solvents. The first route utilized EtOH. Two separate solutions was prepared for this first route. TTIP, ZTP and EtOH were mixed 15 minutes for the formation of the first solution. Nitric acid (14 M), ethanol and water were mixed for 15 minutes for the preparation of the second alcoholic solution. The first solution was added dropwise to the alcoholic solution under stirring. The molar ratios of the polymeric titania sol was 0.8:0.2:0.057:2:52 (TTIP:ZTP:HNO_3:H_2O:EtOH). The particle size distribution of the polymeric titania-

zirconia sol was determined by Zetasizer-DLS. The polymeric TiO_2 coated layer was coated with the polymeric titania-zirconia sol. The polymeric titania-zirconia sol was coated for 10 seconds. The coated NF layer was dried at room temperature for 24 hours. The dried NF layer was heat treated at 400°C in the furnace. The furnace was heated from room temperature to 400°C with 1°C/min heating rate. The tubular membranes were dwelled at 400°C about 1 h in the furnace.

5.2.2. Thermal Behaviour of Selective Layer

There are some important parameters for the formation of defect-free selective layers with high performances such as the dip-coating process parameters, heat treatment temperature and the heating rate. Unsupported membrane selective layers were prepared by drying the α-alumina, disperal, titania hydrosol, polymeric titania sols at room temperature. The shrinkage/densification behaviour of the unsupported membranes dry pressed at 140 MPa were determined by Linzeis L76150B-1600 dilatometer. Dilatometric characterizations were conducted from room temperature to 1500 °C.

5.2.3. Filtration Experiments

A cross flow filtration set-up was used for the filtration experiments conducted at room temperature and this filtration set-up is shown in Figure 5.9. The most important parts of this set-up are the membrane module which was made of stainless steel contruction and pump. The membrane module has two membrane holding flanges at both sides. This module also has two cylindrical rubber rings for the prevention of liquid leakage under high pressure. The flow which was in the system can be changed by using the high pressure pump. The needle valves were used to adjust the pressure. The system was generally operated at low TMP levels in the 1-3 bar range but the system can be operated at TMP levels up to 25 bars.

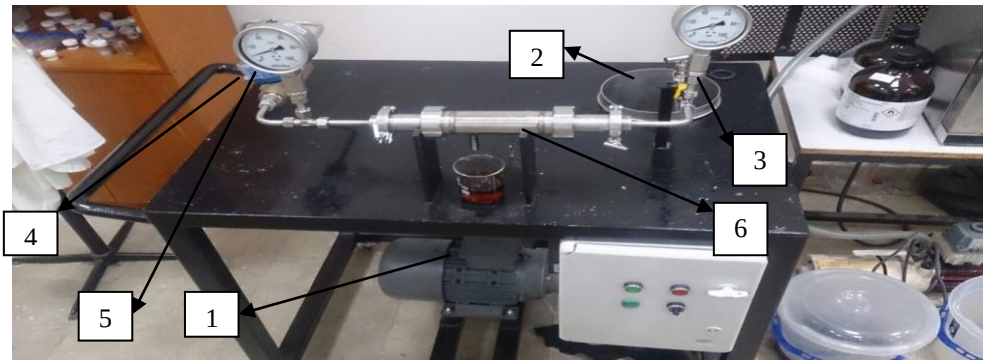

Figure 5.9. The cross flow filtration set-up (1-pump, 2-feed tank, 3- recycle, 4-gauge, 5-flowmeter, 6-cross-flow membrane module).

The textile wastewater before biological treatment was supplied by Sun Tekstil, İzmir in February 2017. The textile wastewater was characterized and the TOC, TSS, COD, color, pH, conductivity parameters were determined by Hach Lange DR 3900 spectrophotometer and Hach HQ40d conductivity/pH meter. Color characterizations can be conducted at different wavelengths/methods. The Pt-Co values were measured at 455 nm and 465 nm. Other color parameters were measured by Admi method at three different wavelengths (423 nm, 525 nm and 620 nm) and their units were m^{-1}. The suspended solids of the wastewater samples were measured at 810 nm in mg/l unit.

The determination of a pretreatment method involved the optimum amount of $Al_2(SO_4)_3$ addition for coagulation and the proper choice of a suitable filter paper for the filtration of the coagulated wastewater. The optimum amount of aluminium sulfate addition determination was based on the lowest filtrate color measurements. The uncoated tubular alumina supports were also used in the cross flow filtration set-up for the pretreatment of the wastewater before biological treatment. The textile wastewater was filtered by using three different filter papers [3-5 μm (Filtrak), 12-15 μm (Filtrak) and 20-25 μm (Whatman)] for selection of the pretreatment filter paper. The membrane fouling and concentration polarization are important parameters for membrane separations.

There are dye particles/molecular species with various morphologies/sizes present in textile wastewater which necessitates pretreatment to prevent excessive fouling problems during membrane treatment. $Al_2(SO_4)_3$ was used for coagulation pretreatment of textile wastewater. $Al_2(SO_4)_3$ precipitated the particles/species in the textile wastewater forming relatively large flocculates/agglomerates significantly larger than the original size of the particles/species present in textile wastewater. Various

amounts of $Al_2(SO_4)_3$ were added (30 mg, 50 mg, 100 mg, 150 mg, 200 mg, 250 mg, 300 mg, 350 mg, 400 mg, 450 mg, 500 mg and 550 mg) to the textile wastewater and the flocculated mixture were filtered through the filter paper. Color, turbidity and Pt-Co values of the filtrate were determined and used for the determination of the proper addition level of the flocculant.

Clean water and textile wastewater fluxes of the tubular membranes [support, MF (α-alumina), AKP-50, UF-1 (disperal+P2), UF-2 (titania hydrosols) and NF (titania polymeric sol+titania-zirconia polymeric sol)] were determined at different transmembrane pressures. The system was operated under constant pressure (4 bar) so that the flux decline can be analyzed. Feed, permeate and retentate samples during the filtration experiments were characterized. The variation of the TSS, color (Pt-Co and Admi at various wavelengths), TOC, and conductivities of the permeate and retentate samples were recorded as a function of filtration time (about 60 minutes). Membrane flux declines were determined by using textile wastewater and clean water filtration fluxes. The equations given in Table 5.2 were used for flux decline analysis.

Table 5.2. The flux decline analysis equations.

Formula	**Type/cause of flux decline**
$\frac{J_{cwi} - J_{ww}}{J_{cwi}}$	Total
$\frac{J_{cwf} - J_{ww}}{J_{cwf}}$	Concentration Polarization
$\frac{J_{cwi} - J_{cwf}}{J_{cwi}}$	Fouling(Irreversible+reversible)
$\frac{J_{cwc} - J_{cwf}}{J_{cwc}}$	Reversible Fouling
$\frac{J_{cwi} - J_{cwc}}{J_{cwi}}$	Irreversible Fouling

Textile wastewater and clean water fluxes of the membrane were defined as J_{ww} ($l/m^2.h$) and J_{cwi} ($l/m^2.h$), respectively. The clean water flux of the fouled membrane and the clean water flux of the cleaned membrane were defined as J_{cwf} ($l/m^2.h$) and J_{cwc} ($l/m^2.h$), respectively.

CHAPTER 6

RESULTS AND DISCUSSION

6.1. Preparation of The Selective Layers

The tubular α-alumina supports used for membrane formation are shown in Figure 6.1. The asymmetric ceramic membranes were prepared by successive dip-coating of the α-alumina supports with intermediate MF, UF-1, UF-2 and NF top layers along with appropriate heat treatments after each coating.

Figure 6.1. The extruded tubular α-alumina supports.

The tubular α-alumina supports were coated with α-alumina suspensions for MF layers (CT3000SG and AKP-50 powder suspensions), boehmite (dispersal and P2) sols for UF-1 layers, titania hydrosol for UF-2 layer and titania, titania/zirconia mixed oxide polymeric sols for the final top NF layers.

6.1.1. Characterization of Ceramic Asymmetric Membrane Layers

The tubular α-alumina supports coated with a number of selective layers were characterized by SEM. The top surface and cross-sectional areas of the MF layers are given in Figure 6.2. The surface of the MF layer was smooth and crack free. PVA (polyvinyl alcohol M_w=9000-10000) addition to the sols may effectively control drying which also may provide defect free MF surfaces for the preparation of the successive layers. The average thickness of the MF layer was determined to be in the 40-50 μm range.

The MF coated tubular ceramic membrane was coated with disperal and P2 sols and these layers were called as UF-1. The top surface SEM images of the UF-1 layer are given in Figure 6.3. The surface of the UF-1 layer was mostly smooth but had a pinhole and a crack. There were some cracks and these may partially be related to the mechanical forces applied during tube breakage necessary for SEM sample preparation. The average thickness of the UF-1 layer was determined as 3 μm.

The UF-1 coated tubular ceramic membrane was coated with titania hydrosols and and these layers were called as UF-2. The top surface and cross-sectional views of the UF-2 layer are given in Figure 6.4. The surface of the UF-2 layer was smooth and crack free. The average thickness of the UF-2 layer was determined to be 733 nm.

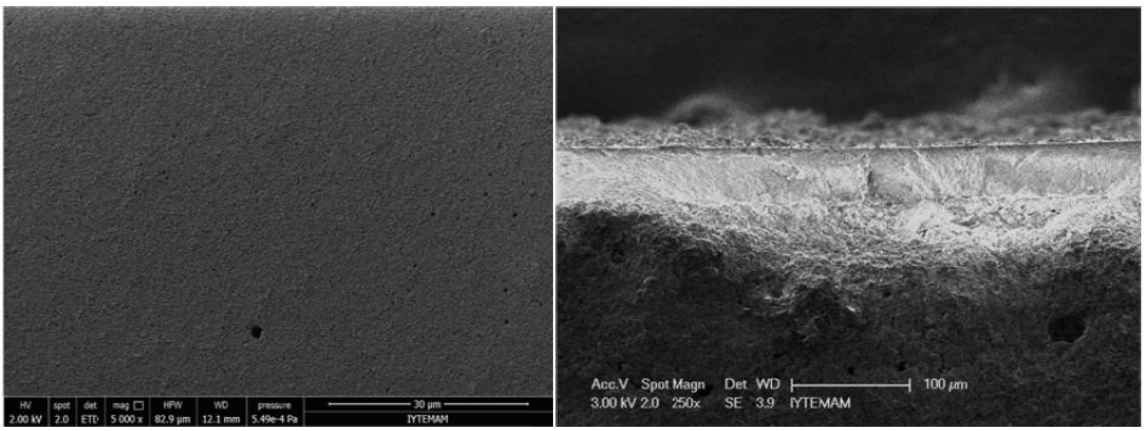

Figure 6.2. Top surface and cross-sectional SEM images of the MF layer.

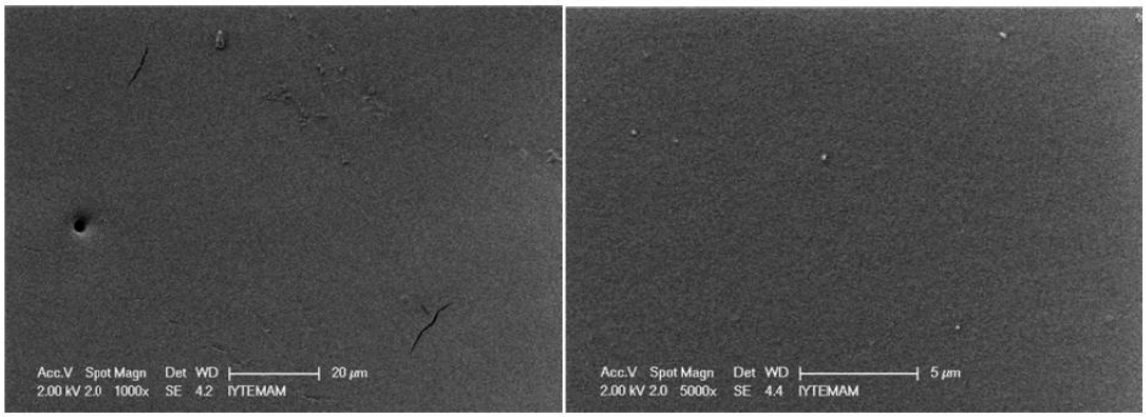

Figure 6.3. Top surface SEM images of the UF-1 selective layer.

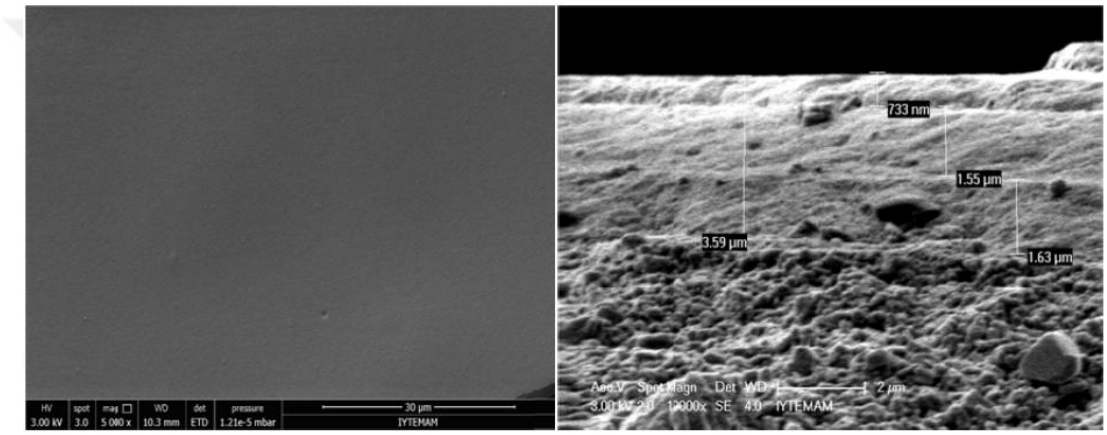

Figure 6.4. Top surface and cross-sectional SEM images of the UF-2 selective layer.

6.1.2. Characterization of the Dip-Coating Sols

The selective MF layer was prepared by using colloidal α-alumina powder (CT3000 SG powder) suspensions and a representative particle size distribution of these α-alumina colloidal suspensions is shown in Figure 6.5. The second MF layer formed in between first MF and UF-1 layers was prepared by using stable colloidal suspensions of AKP-50 α-alumina powders and a representative particle size distribution of these colloidal suspensions is given in Figure 6.6. The selective UF-1 layer was prepared by using boehmite (disperal) powder colloidal sols and a representative particle size distribution of the disperal colloidal sol is given in Figure 6.7. Disperal (P2) layer which was in between UF-1 and UF-2 was prepared by using disperal (P2) powder sols and a typical particle size distribution of the P2 colloidal sol is given in Figure 6.8. The

selective UF-2 layer was prepared by using TTIP and TTB sols and their representative particle size distributions are given in Figures 6.9 and 6.10. The top layer was prepared by using TTIP/ZTP generated polymeric sol. The top layer was called NF. The particle size distribution of the polymeric sol is given in Figure 6.11.

The average particle size of the CT3000SG α-alumina, AKP-50 α-alumina, disperal, P2 colloidal sols; TTIP, TTB hydrosols and titania/zirconia polymeric sols were determined as 522 nm, 175 nm, 42 nm, 16 nm, 14 nm, 4.9 nm and 3.6 nm respectively. The pore sizes in the corresponding selective layers prepared by using these sols would be expected to be proportional to these particle sizes (the pore size may be about 40% of the packed particles/spheres in simple cubic packing).

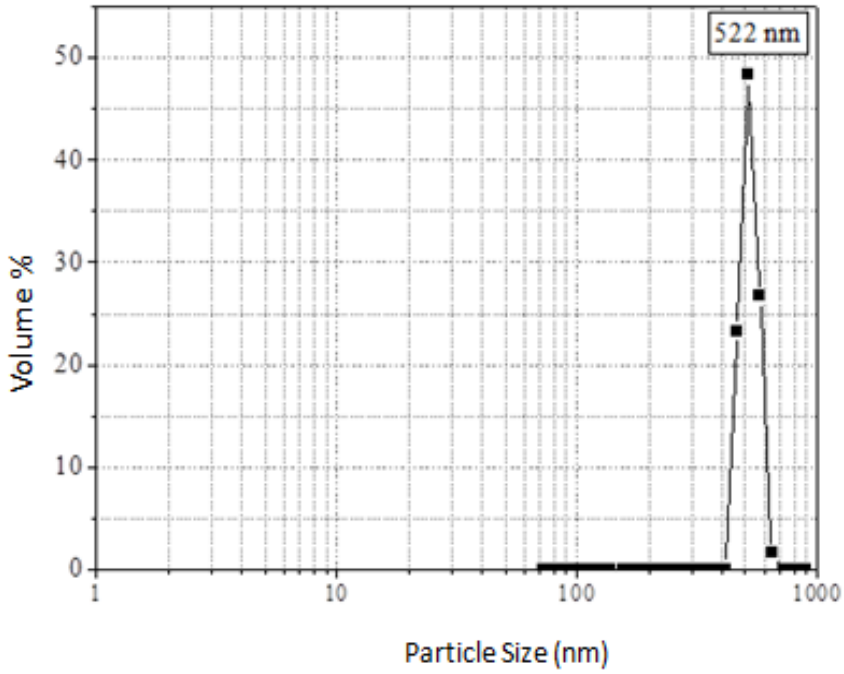

Figure 6.5. The particle size distribution of the CT3000SG α-alumina colloidal suspension (wt 7% α-alumina, 0.8% PVA).

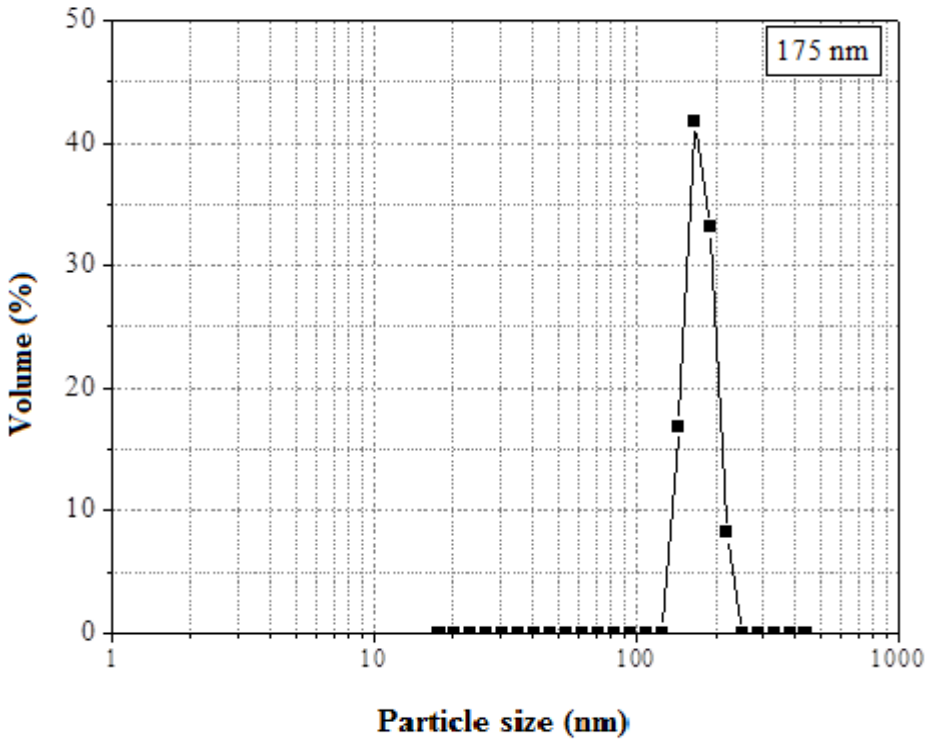

Figure 6.6. The particle size distribution of the AKP-50 colloidal suspension (wt 7% AKP-50).

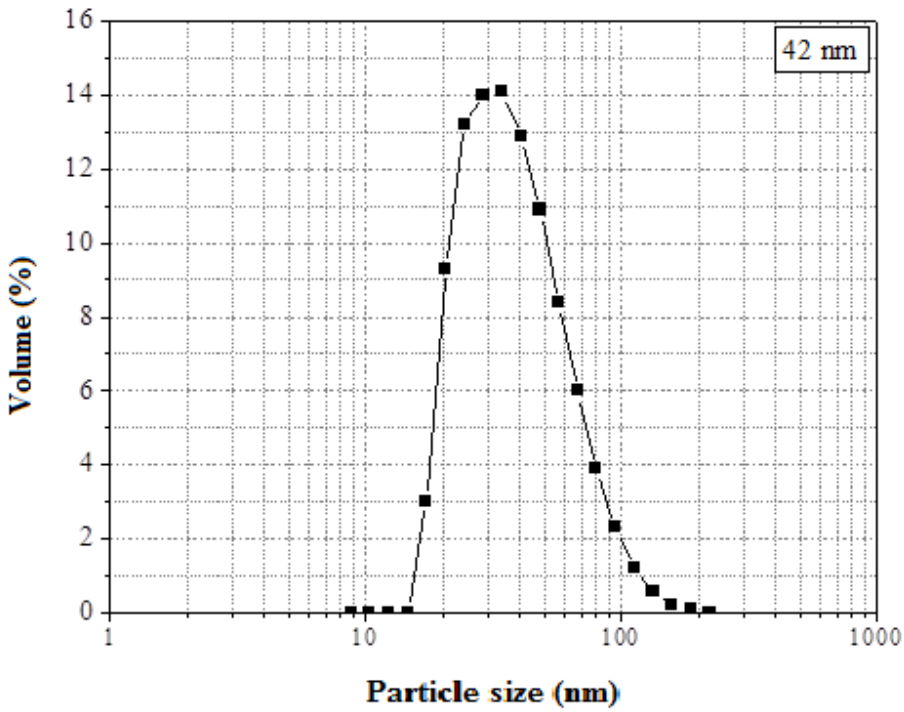

Figure 6.7. The particle size distribution of the disperal colloidal suspension (wt 0.6% Boehmite (disperal), 0.8% PVA).

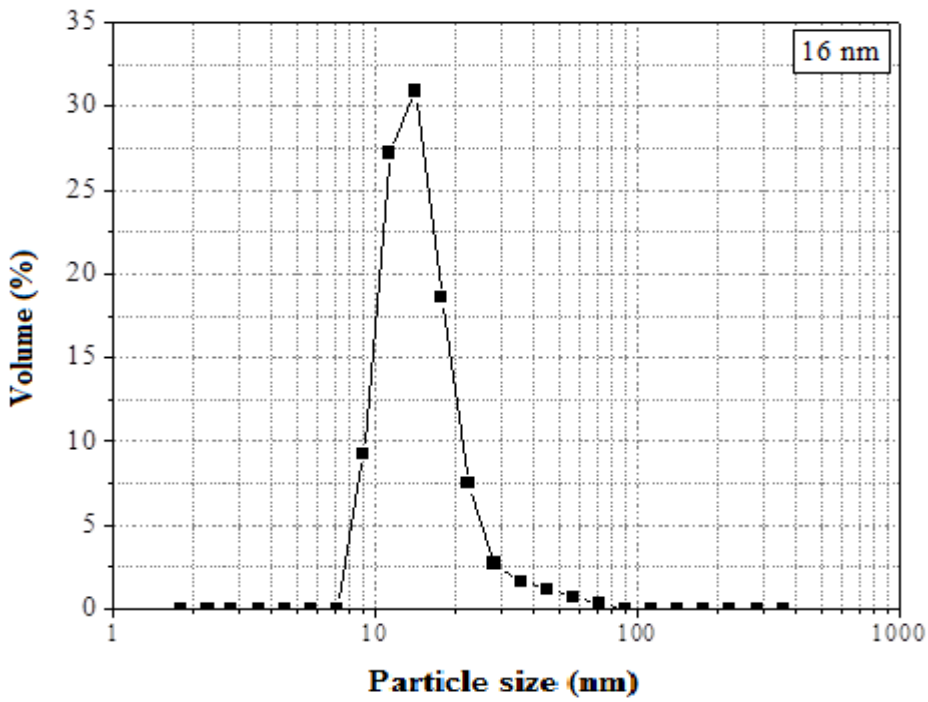

Figure 6.8. The particle size distribution of the P2 colloidal suspension (wt 0.6% P2).

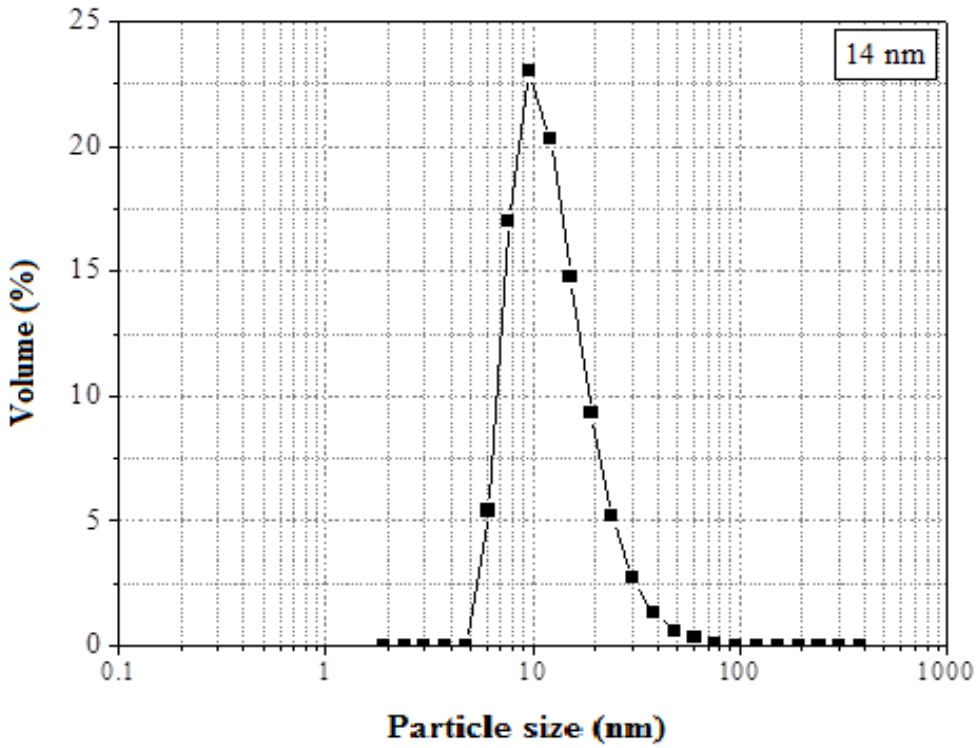

Figure 6.9. The particle size distribution of the TTIP hydrosol (TTIP:DEA:HNO_3:H_2O:Propanol 1:0.8:2.4:1000:10).

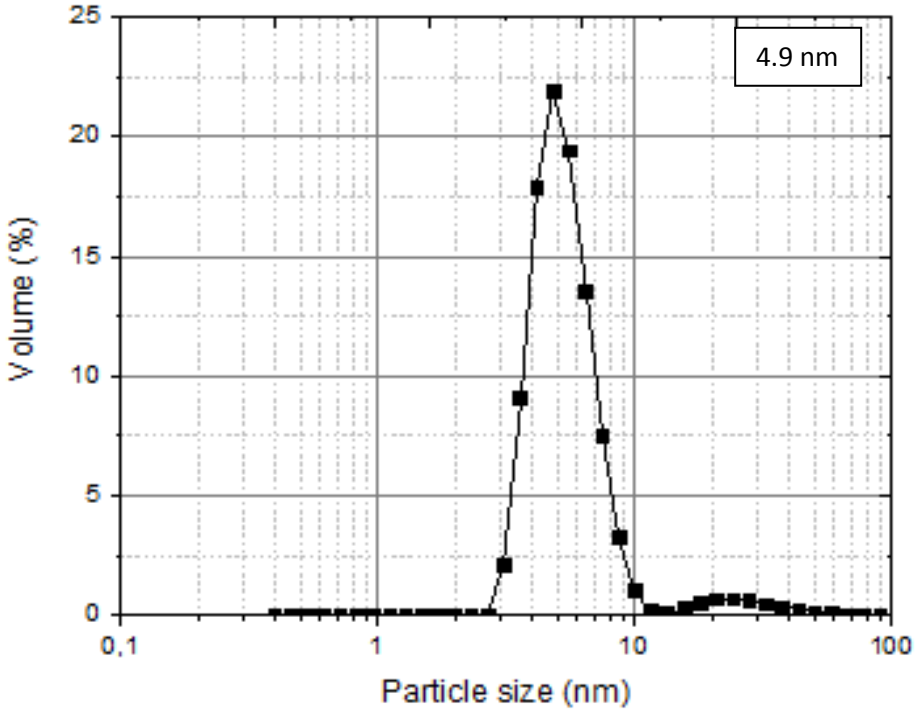

Figure 6.10. The particle size distribution of the TTB hydrosol.

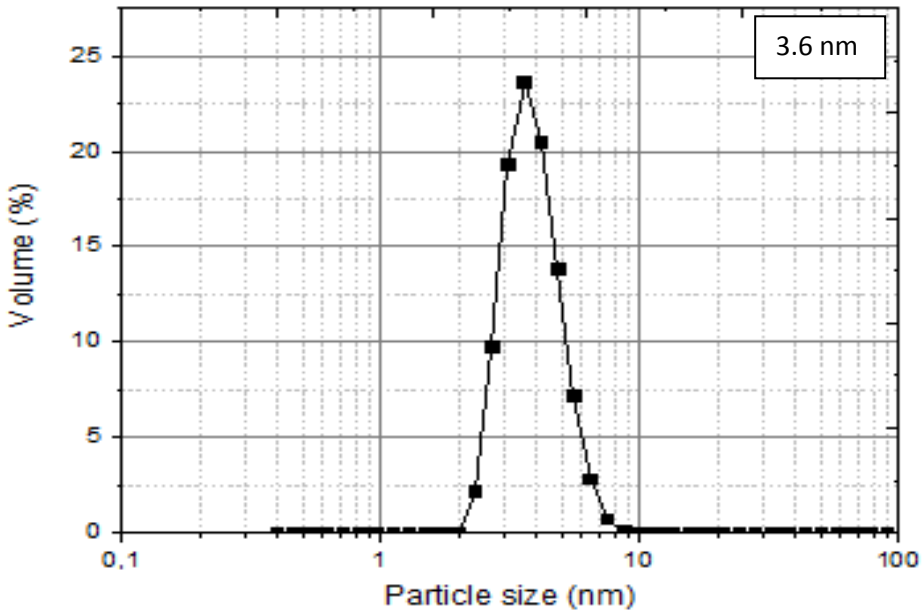

Figure 6.11. The particle size distribution of the titania/zirconia polymeric sols.

6.2. Characterization of Textile Wastewater

The characterization results of textile wastewater (SUN Textile) are given in Table 6.1. The Color (Pt-Co, 455 nm and 465 nm) values for the wastewater were determined to be about 7960 and 8070, respectively. The Admi Color (m^{-1}, 436 nm, 525 nm and 620 nm) values for the wastewater were determined to be about 109, 91.4 and 79.5, respectively. The suspended solids content was determined as 260 mg/L. The COD and TOC values were determined as 329 mg/L and 477 mg/L, respectively.

Table 6.1. Textile wastewater characterization results.

Parameter	**Wastewater**
Pt-Co (410 nm)	2110
Pt-Co (455 nm)	7960
Pt-Co (465 nm)	8070
Color (m^{-1}) 436 nm 525 nm 620 nm	 109 91.4 79.5
Suspended Solids (810 nm, mg/L)	260
Conductivity (mS/cm)	8.36
pH	8.74
TOC (mg/L)	477
COD (448 nm, mg/L)	329

6.3. Determination of the Pre-treatment Methods

6.3.1. Analyses of Filter Papers

There were three kinds of available filter papers with pore sizes of 3-5 μm (Filtrak), 12-15 μm (Filtrak) and 20-25 μm (Whatman). The cumulative percent suspended solids, color and turbidity rejections were obtained for textile wastewater

which was filtered by using these filter papers. These findings are given as bar graphs in Figures 6.12 to 6.16. These plots clearly show that filtering through 3-5 µm is the most effective pretreatment for textile wastewater. The cumulative percent rejection values of the filter papers are given in Table 6.2. The pretreatment had no detectible effects on pH and conductivity levels.

Table 6.2. The percent rejection values of the filter papers.

Parameter	**Filter Papers**		
	20-25 µm	**12-15 µm**	**3-5 µm**
Pt-Co (410 nm)	30.04	35.45	52.36
Pt-Co (455 nm)	29.02	34.07	50.96
Pt-Co (465 nm)	28.62	33.68	50.69
Color (m^{-1})			
436 nm	29.17	34.31	51.28
525 nm	29.54	34.79	52.51
620 nm	30.56	36.85	54.71
Suspended Solid (810 nm, mg/L)	53.84	66.15	84.61

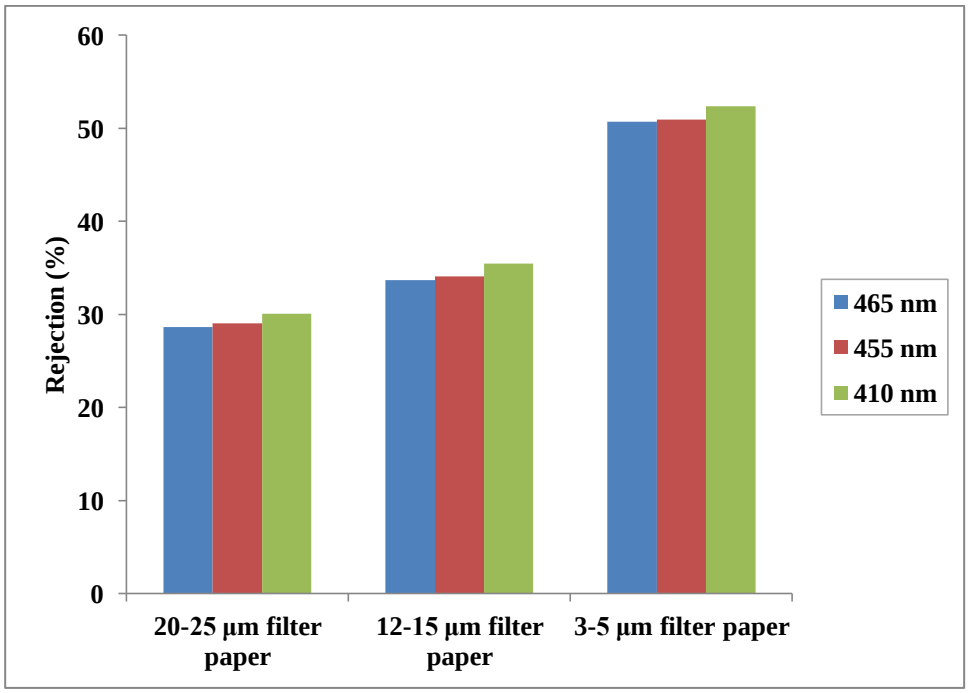

Figure 6.12. The rejection percentage of Color (Pt-Co) after filter paper pretreatment.

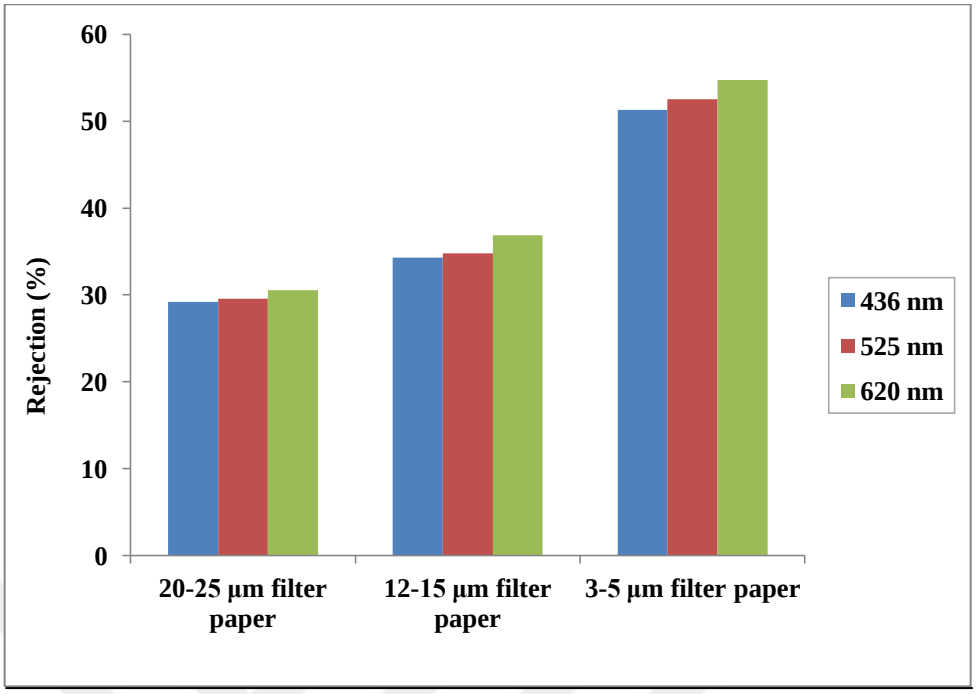

Figure 6.13. The rejection percentage of Admi Color (m^{-1}) after filter paper pretreatment.

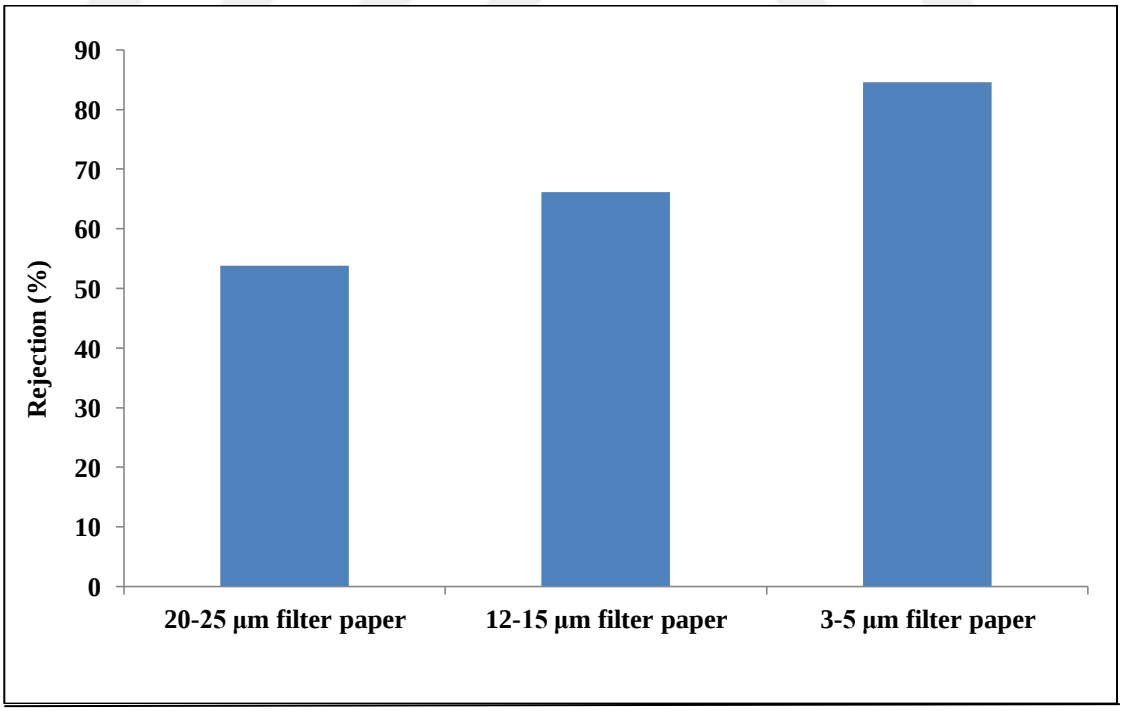

Figure 6.14. The rejection percentage of Suspended Solids (mg/L) after filter paper pretreatment.

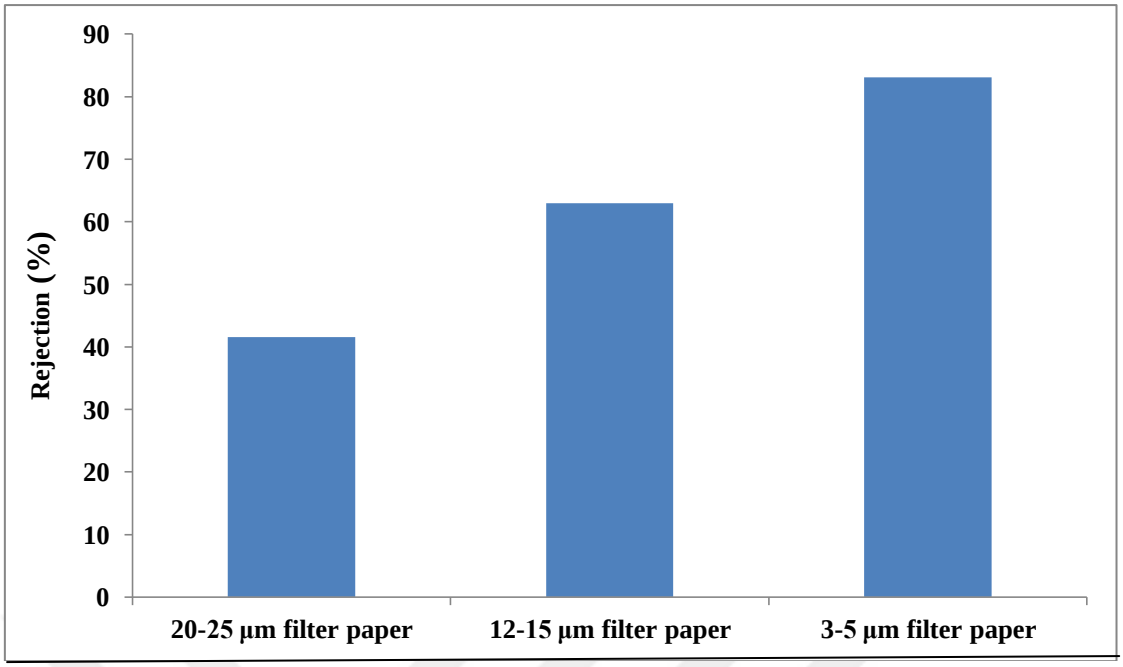

Figure 6.15. The rejection percentage of Turbidity (NAU) after filter paper pretreatment.

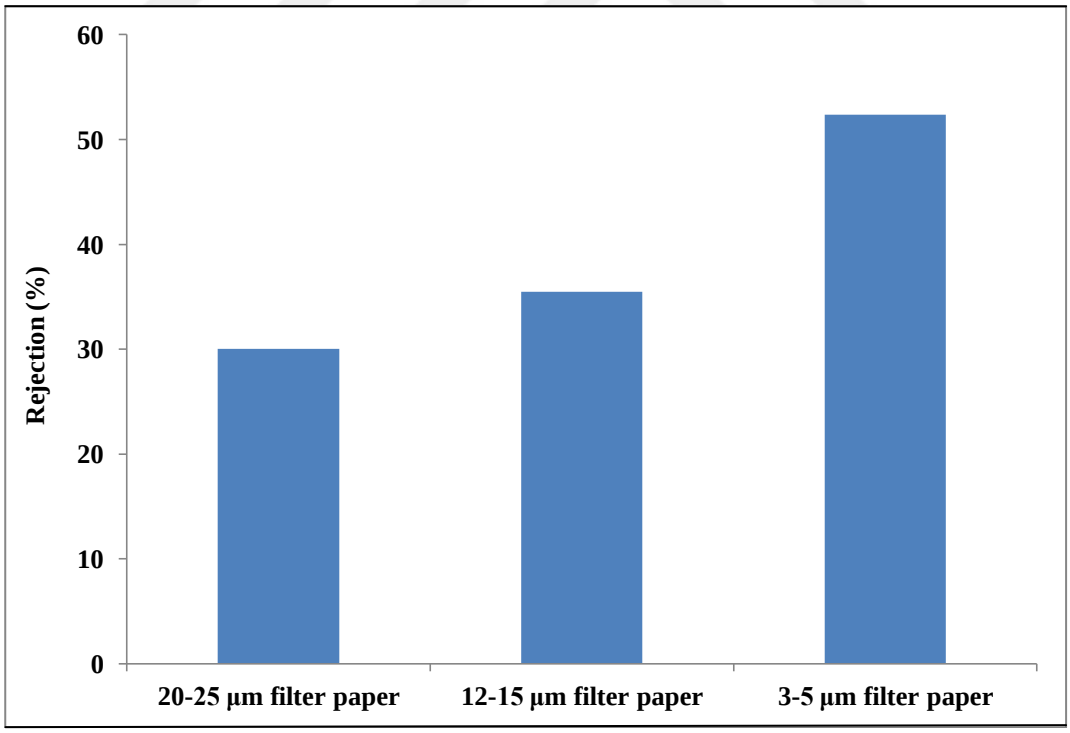

Figure 6.16. The rejection percentage of Pt-Co 410 Color (mg/L) after filter paper pretreatment.

6.3.2. Determination of the effective $Al_2(SO4)_3$ coagulant addition in pretreatment

The various amounts of $Al_2(SO_4)_3$ was added to 100 ml of textile wastewater (30 mg, 50 mg, 100 mg, 150 mg, 200 mg, 250 mg, 300 mg, 350 mg, 400 mg, 450 mg, 500 mg and 550 mg) for the determination of the optimum level of $Al_2(SO_4)_3$ coagulant addition. The cumulative percent suspended solids, color, and turbidity rejections of the filtrates were determined by filtering the coagulated textile wastewater through 3-5 μm filter paper for each coagulant addition level. The characterization results are plotted in Figures 6.17 to 6.21 as a function of coagulant addition level. These results clearly demonstrate that 350 mg $Al_2(SO_4)_3$/100 ml wastewater was the most effective and lowest coagulant amount for pretreatment. The rejection values decrease after that level due to the increase in the ionic strength of the suspensions/solutions and the resulting decreases in the thicknesses of the electrical double layers on the solid phases. This may start decreasing the electrical interactions between the particles/polymeric species forming a more stable colloidal suspension which decreases the rejection values. The cumulative percent rejection values at various $Al_2(SO_4)_3$ coagulant amounts are also given Table 6.3.

Table 6.3. The variation of percent rejection values with $Al_2(SO_4)_3$ addition level.

Parameter	The Amount of $Al_2(SO_4)_3$ (mg/100ml)											
	30 mg	50 mg	100 mg	150 mg	200 mg	250 mg	300 mg	350 mg	400 mg	450 mg	500 mg	550 mg
Pt-Co (410 nm)	59.52	60.28	65.45	74.64	73.60	83.88	88.43	90.09	90.56	90	88.05	87.67
Pt-Co (455 nm)	57.76	58.92	63.01	74.72	75.50	83.92	87.33	90.07	89.83	89.89	86.56	86.21
Pt-Co (465 nm)	59.04	60.17	63.77	75.65	75.67	84.31	87.32	90.27	89.87	90.11	86.54	86.25
Color (m^{-1})												
436 nm	58.44	59.90	64.49	74.95	76.97	84.31	88.25	90.36	90.45	90.18	87.61	87.24
525 nm	59.62	62.14	64.66	77.78	74.28	85.12	86.76	90.60	89.44	90.42	86.21	85.88
620 nm	63.14	71.94	69.18	86.91	76.22	93.43	87.45	96.13	89.89	95.22	89.77	89.34
Suspended Solid	90.38	91.53	96.92	97.69	98.84	99.23	99.23	99.23	99.23	99.23	98.84	98.46

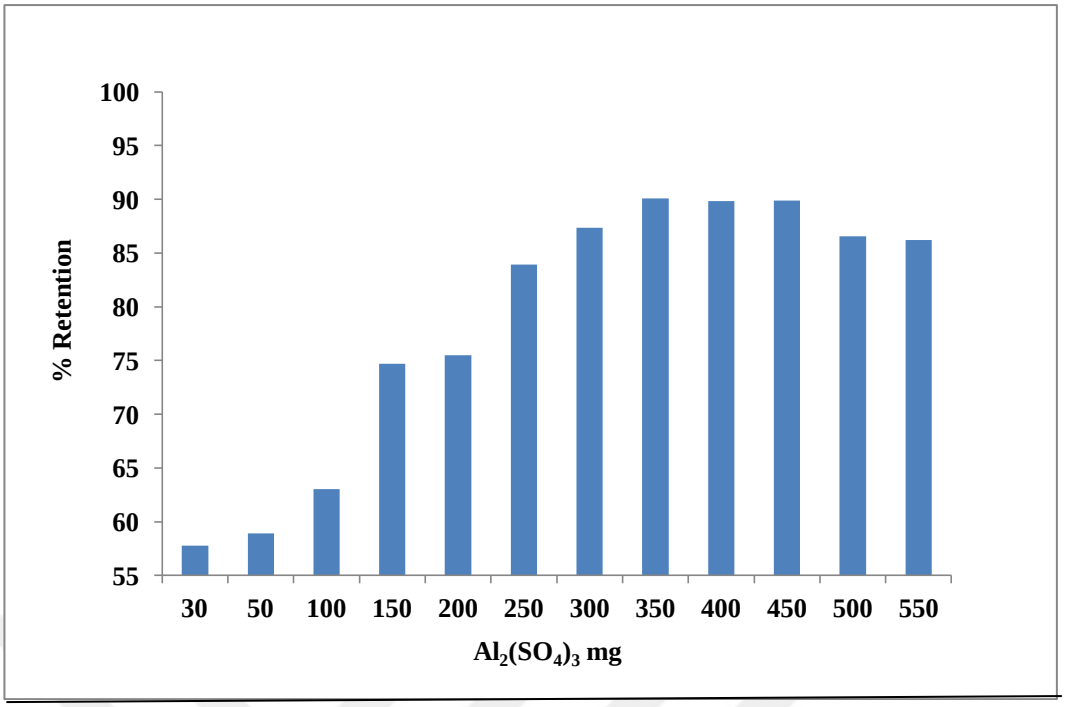

Figure 6.17. The variation of the rejection percentage of 455 Pt-Co color values with coagulant addition level.

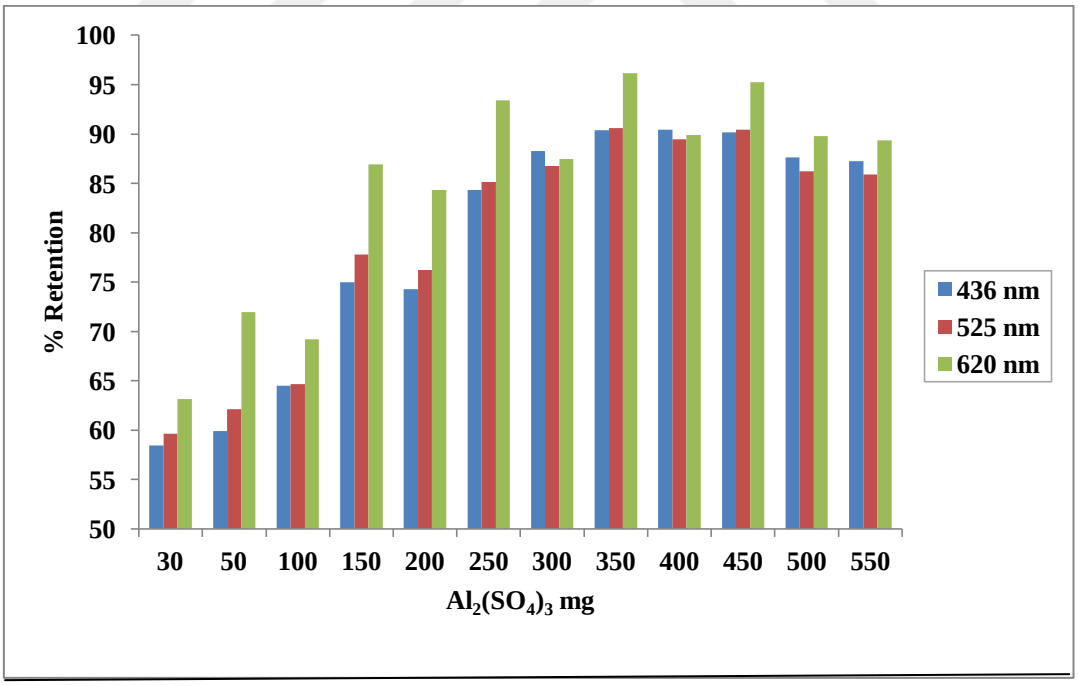

Figure 6.18. The variation of rejection percentage of Admi color (m^{-1}) with coagulant amount.

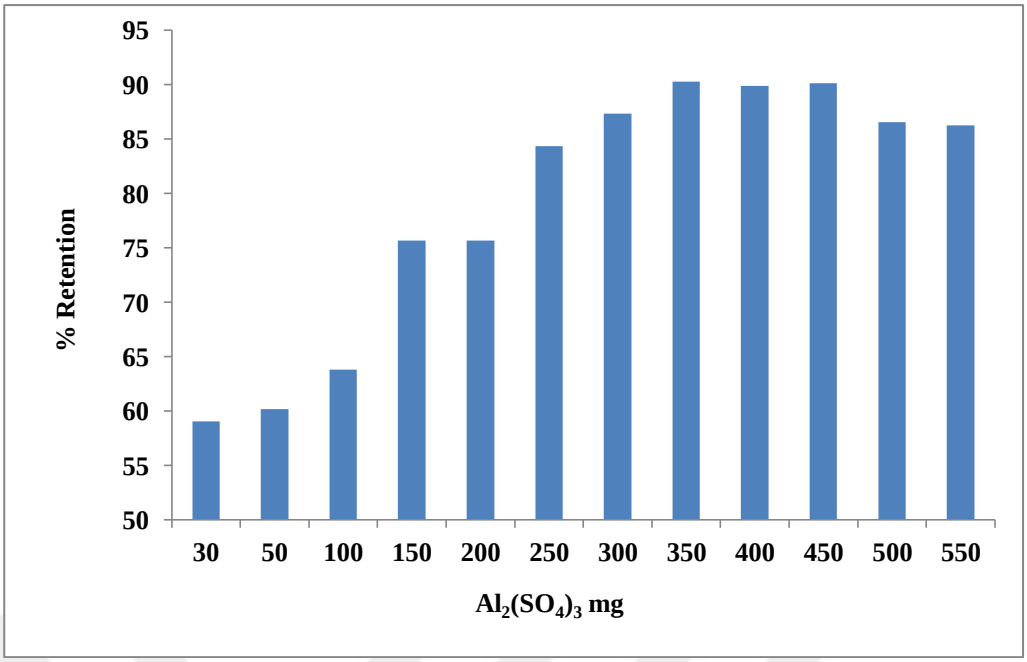

Figure 6.19. The variation of rejection percentage of Pt-Co color with coagulant amount.

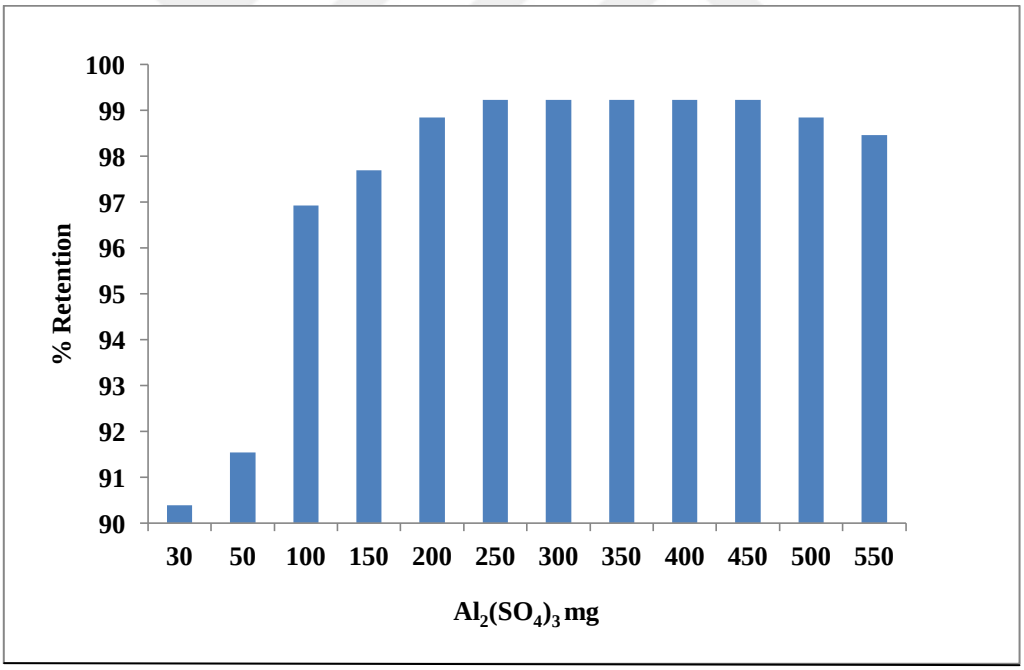

Figure 6.20. The variation of rejection percentage of turbidity with coagulant amount.

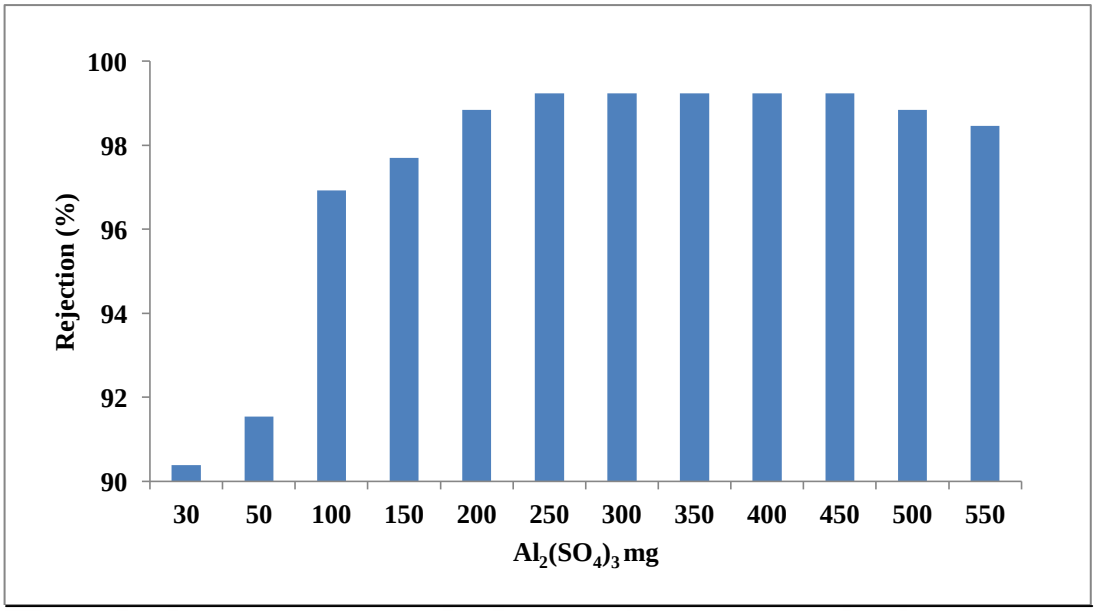

Figure 6.21. The variation of rejection percentage of Suspended Solids (mg/L) with coagulant amount.

6.4. Membrane Performance

6.4.1. Effect of Pre-treatment on Membrane Performance For the First tubular membrane set

The variation of the J_{cwi} (clean water flux) of support, MF (α-alumina and AKP-50), UF-1 (disperal and P2), UF-2 (TTIP and TTB) and NF (zirconia+titania) at TMP-2 are given in Figures 6.22 and 6.23. The clean water flux decreases with decreasing pore size as expected. The support presented the highest flux because of its pore size which was determined to about 1.5-2 μm in previous studies. The clean water flux of support was about 1800 L/m^{2}h. The NF membranes which were coated once, twice, three times, four times and five times presented the lowest flux due to their pore sizes. The clean water flux of NF membrane (five layer) is about 25 L/m^{2}h. Clean water flux stayed almost constant and was independent of time.

The wastewater fluxes of the membranes with pre-treatment are shown in Figures 6.24 and 6.25. Filter papers (3-5 μm) were used for removing coagulates/particles after $Al_2(SO_4)_3$ (0.35 g) coagulation. The TMP was 2 during these experiments. The fluxes of uncoated and coated (α-alumina, AKP-50, disperal, P2, TTIP, TTB and NF layers) membranes were stable with time due to the presence of a very low level of

species/particles which may cause membrane fouling due to the effective pre-treatment utilized. The filtration tests had a continuous nature during the experiments.The permeate from support filtration was fed as feed to the microfiltration membrane.The permeate obtained during the microfiltration was fed as feed for the succeeding membrane filtration. The filtration experiments were conducted in series with the AKP-50/ UF-1 (disperal)/UF-1 (P2)/UF-2 (TTIP)/UF-2 (TTB)/NF/NF/NF/NF (four layers) membranes where the permeate from the previous filtration was fed as the feed for the following membrane filtration.

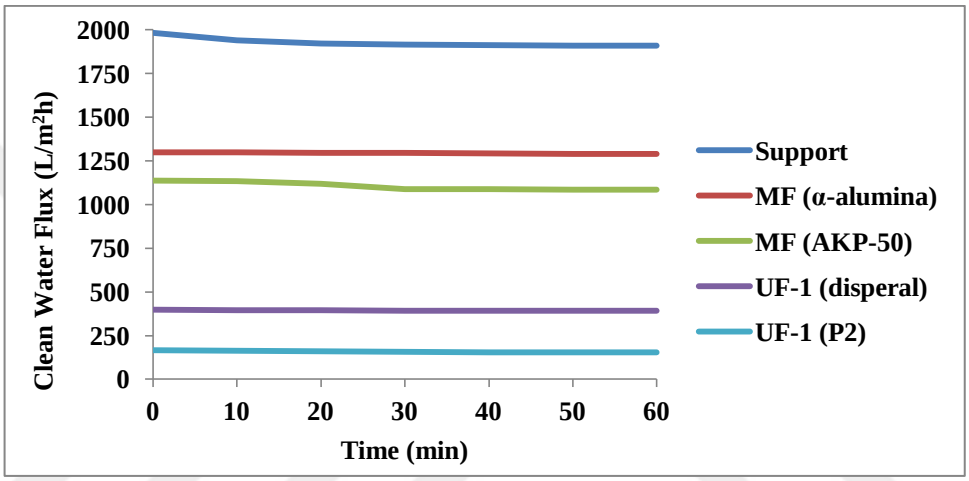

Figure 6.22. Variation of clean water flux at TMP-2 (support, α-alumina, AKP-50, disperal and P2).

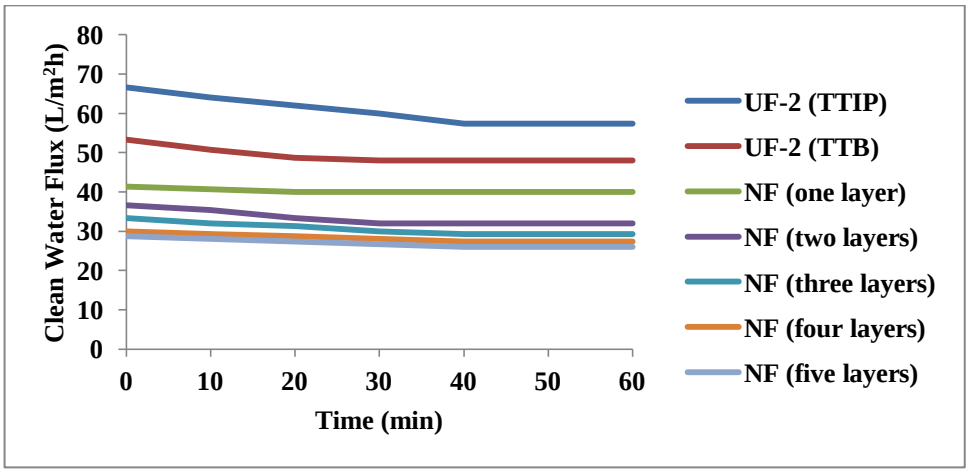

Figure 6.23. Variation of clean water flux at TMP-2 (TTIP, TTB, NF (one, two, three, four and five layers)).

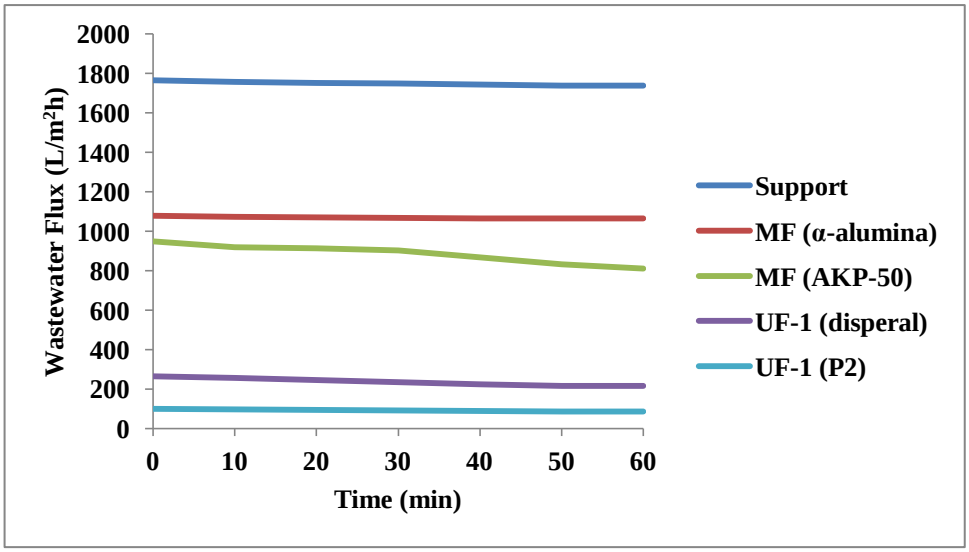

Figure 6.24. Wastewater flux decline of membranes at TMP-2 (support, α-alumina, AKP-50, disperal and P2).

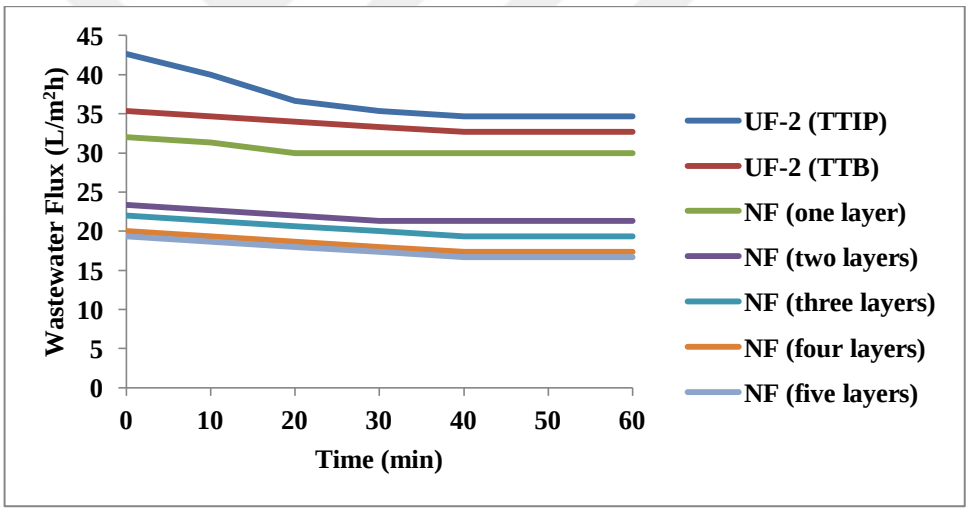

Figure 6. 25. Wastewater flux decline of membranes at TMP-2 (TTIP, TTB, NF (one, two, three, four and five layers)).

The filtered solid content of the coagulated wastewater was determined to be 0.55%. The suspended solids content of wastewater was decreased 99.23% after the pre-treatment with $Al_2(SO_4)_3$. The fluxes of the membranes increased considerably by pre-treatment which decreased the membrane fouling significantly. The cumulative percent rejection values of the wastewater with pre-treatment after the NF (five layers) treatment are given in Table 6.4. These results are also presented as bar graphs in Figures 6.26 to 6.32.

Table 6.4. The cumulative percent rejection values of the wastewater with pre-treatment after the NF (five layers) treatment.

Parameter	Wastewater with pre-treatment	The values of wastewater with pre-treatment
Pt-Co (410 nm)	97.78	70
Pt-Co (455 nm)	97.56	215
Pt-Co (465 nm)	97.72	210
Color (m^{-1}) 436 nm 525 nm 620 nm	 97.86 98.58 99.80	 3.39 1.7 0.4
Suspended solid (mg/L, 810 nm)	100	0
Conductivity (mS/cm)	37.79	5.20
COD (mg/L)	100	0
TOC (mg/L)	89.11	51.94

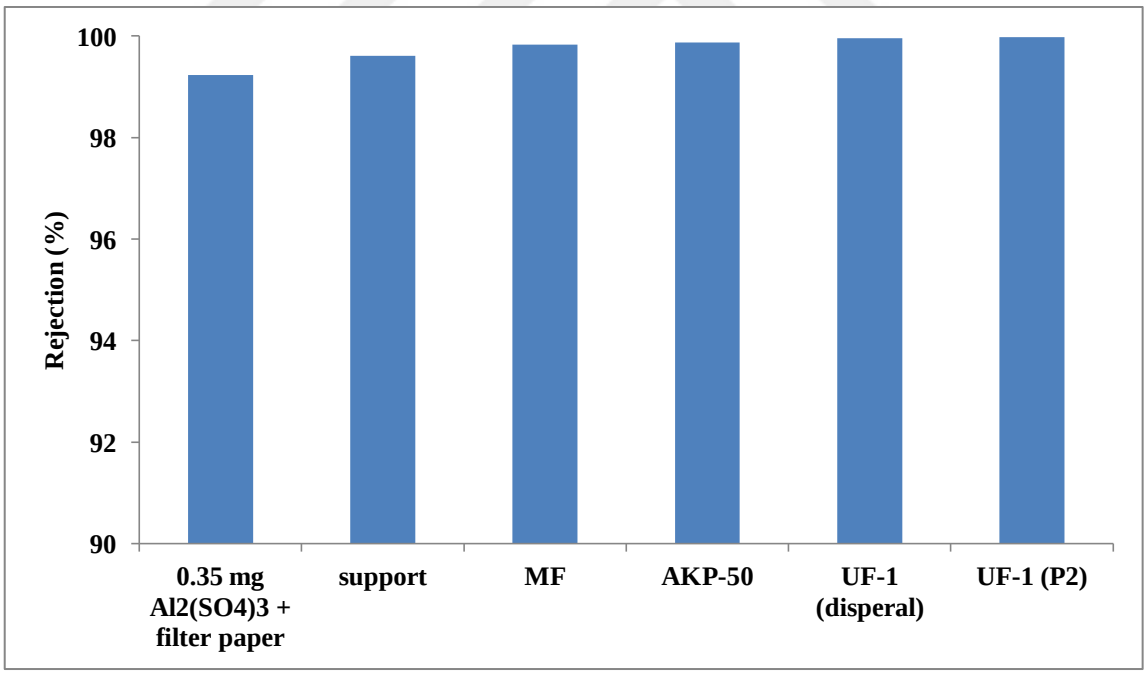

Figure 6.26. Rejection percentage of suspended solids (wastewater with pre-treatment).

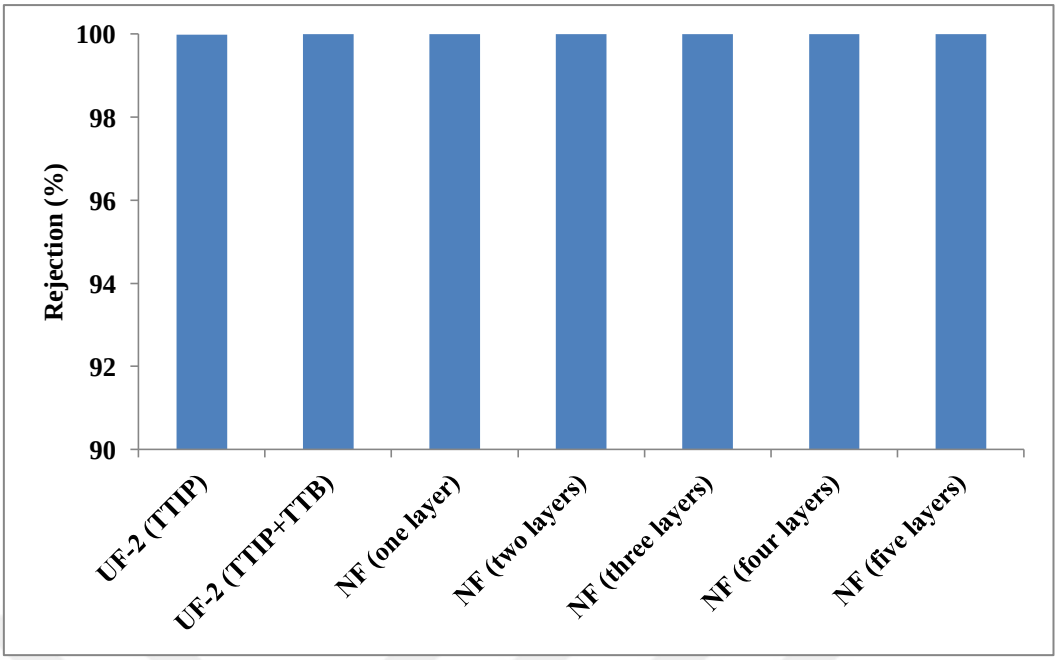

Figure 6.27. Rejection percentage of suspended solids (wastewater with pre-treatment).

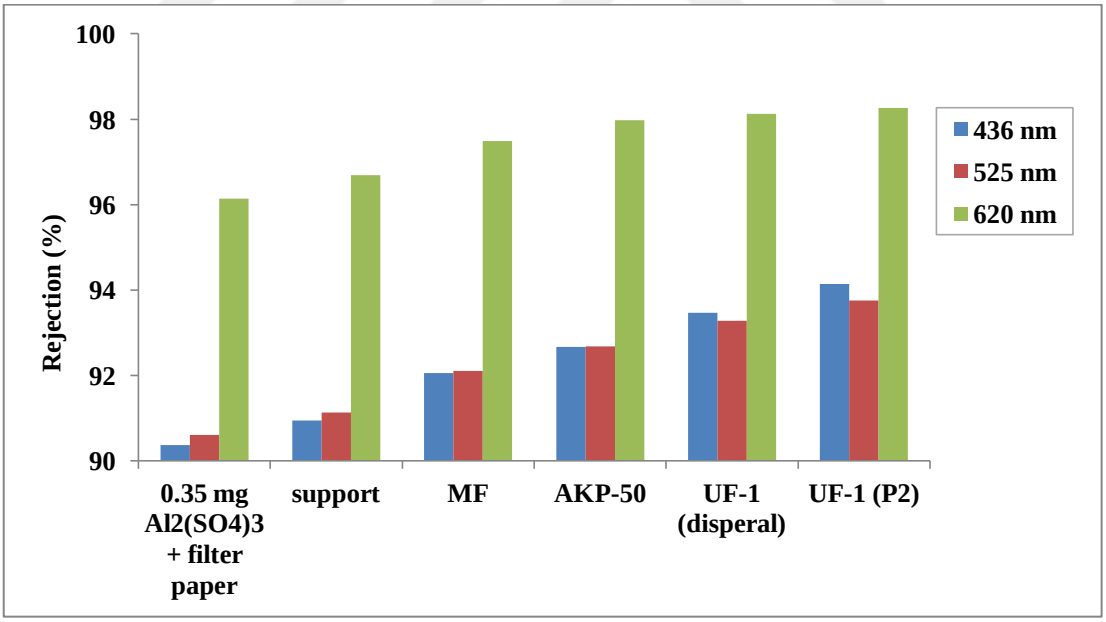

Figure 6.28. Rejection percentage of Admi Color (m^{-1}) of wastewater with pre-treatment.

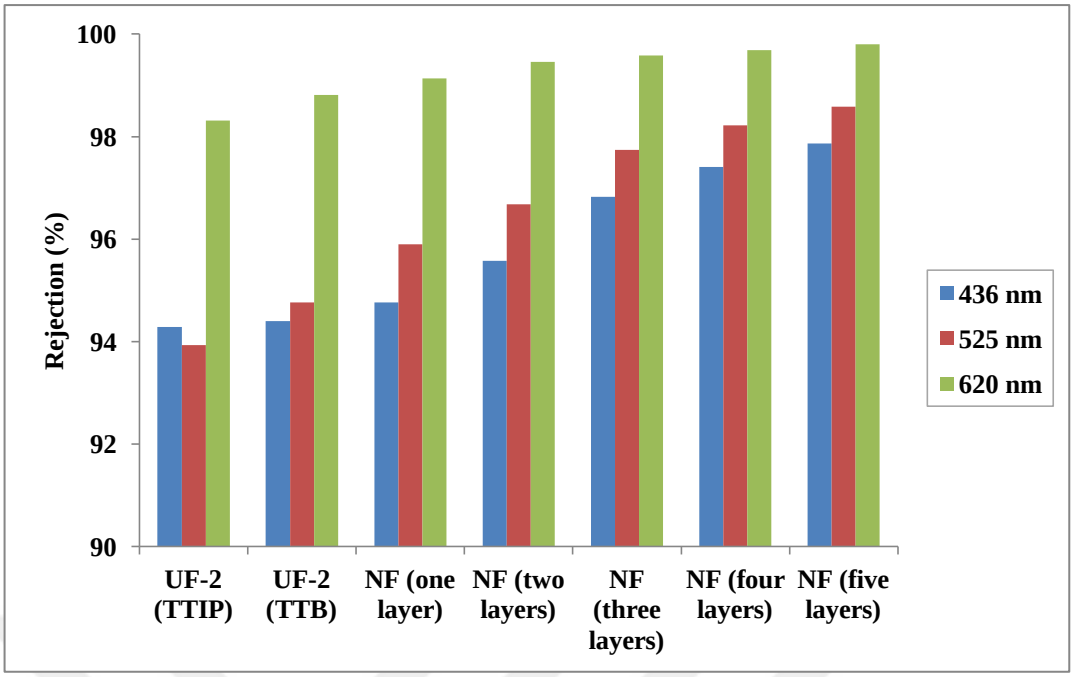

Figure 6.29. Rejection percentage of Admi Color (m^{-1}) of the wastewater with pre-treatment.

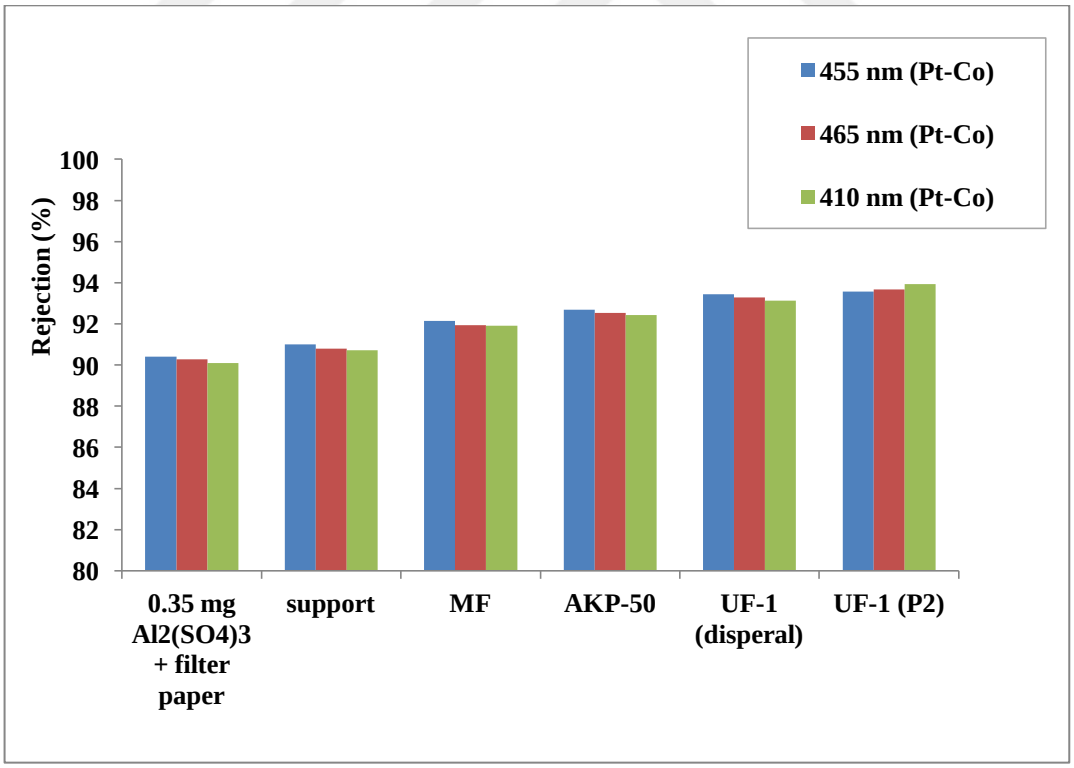

Figure 6.30. Rejection percentage of Color (Pt-Co) of the wastewater with pre-treatment.

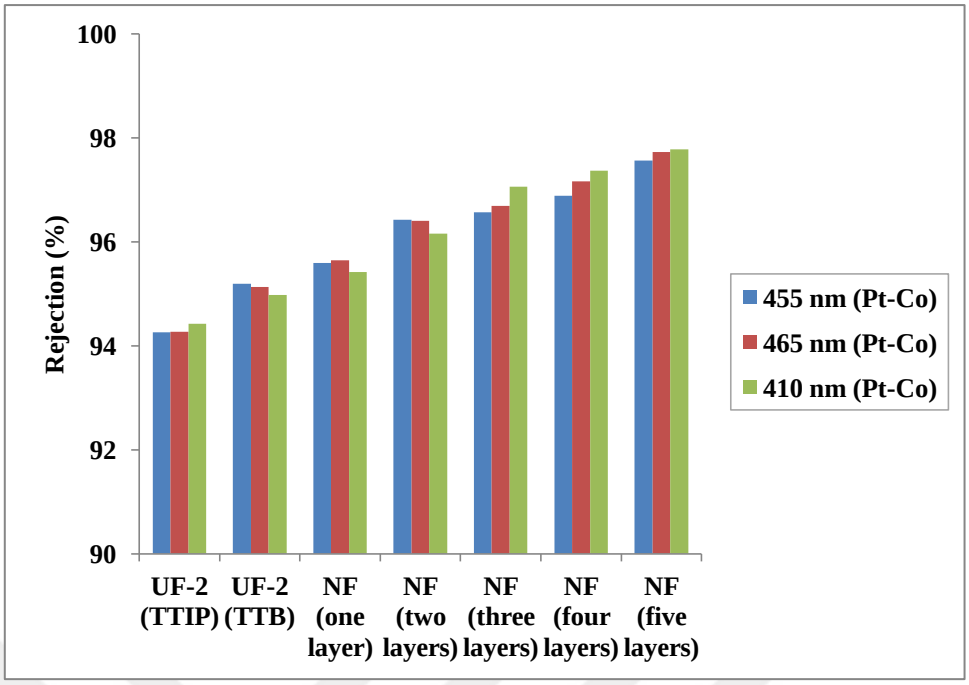

Figure 6.31. Rejection percentage of Color (Pt-Co) of the wastewater with pre-treatment.

a

b

Figure 6.32. The color change of wastewater (with pre-treatment) (from left to right; for a; original wastewater, $Al_2(SO_4)_3$+fitler paper, support, MF, AKP-50, UF-1 (disperal and P2),for b; UF-2 (TTIP and TTB), NF (one, two, three, four and five layers), respectively).

6.4.1.1. Analyses of Membrane Fouling with Pre-treatment

The flux decline of the support, MF, AKP-50, UF-1(disperal), UF-1(P2), UF-2 (TTIP), UF-2(TTB), NF (coated once, twice, three times, four times and five times) membranes in textile wastewater membrane filtration with pre-treatment at TMP=2 are given in Table 6.5. Membrane flux as expected was the highest for the uncoated support and decreased gradually in the membrane series till the final NF coated asymmetric membranes due to the decrease in pore sizes of the intermediate/selective membrane layers.

Table 6.5. The various fluxes and flux recoveries of the membranes (support, MF, AKP-50, UF-1 (disperal and P2), UF-2 (TTIP and TTB) and NF (one, two, three, four and five layers)).

Membrane Type	**Flux (L/m^2h)**				
	Clean Water			**Wastewater (J_{ww})**	**Flux Recovery (J_{cwc}/J_{cwi}) (%)**
	Initial (J_{cwi})	**Final (J_{cwf})**	**Cleaned (J_{cwc})**		
Support	1910	1800	1806	1738	94.5
MF	1290	1255	1271	1065	98.5
AKP-50	1085	927	1051	811	96.8
UF-1 (disperal)	393	313	351	215	89.3
UF-1 (P2)	153	109	124	87	81
UF-2 (TTIP)	57	48	52	35	91.2
UF-2 (TTB)	48	40	45	33	93.7
NF (one layer)	40	33	35	30	87.5
NF (two layers)	32	26	30	21	93.7
NF (three layers)	29	23	29	19	100
NF (four layers)	27	22	26	17	96.3
NF (five layers)	26	21	25	16	96.1

The flux recovery was higher for membranes with the AKP-50 MF layer when compared to the membrane with the UF-1 (disperal) selective layers since the pore size of the AKP-50 selective layer was larger than the UF-1 (disperal) selective layer. The fouling of all of the membranes were determined to be at a low level mostly due to the coagulation pretreatment of the wastewater where the flux recoveries obtained were above 80% as listed in Table 6.5. The flux recovery for the final NF (five layers) membrane was determined as 96%. The J_{cwc} (the clean water flux of the cleaned

membrane) of this final NF membrane was very close to the J_{cwi} (initial clean water flux) (25 and 26 L/m^{2}h respectively).

The results of the flux decline analyses (the irreversible+reversible fouling and concentration polarization) for all of the membranes are given in Table 6.6. The difference between J_{cwf} (clean water flux of the fouled membrane) and J_{ww} (wastewater flux) is a measure of concentration polarization. The difference of J_{cwi} and J_{cwf} is a measure of total fouling (irreversible+reversible fouling).

Table 6.6. The fouling (irreversible, reversible) and concentration polarization flux decline percentages of Support, MF, AKP-50, UF-1 (disperal and P2), UF-2 (TTIP and TTB) and NF (one, two, three, four and five layers) membranes with pre-treatment.

Membrane Type	**Flux Decline (%)**				
			Fouling		
	Total (J_{cwi}-J_{ww})/J_{cwi}	**Concentration Polarization (J_{cwf}-J_{ww})/J_{cwf}**	**Total (J_{cwi}-J_{cwf})/J_{cwi}**	**Reversible (J_{cwc}-J_{cwf})/J_{cwc}**	**Irreversible (J_{cwi}-J_{cwc})/J_{cwi}**
Support	9	3.44	5.75	0.33	5.44
MF	17.41	15.13	2.68	1.25	1.44
AKP-50	25.19	12.44	14.56	11.85	3.07
UF-1 (disperal)	45.42	31.48	20.34	10.81	10.67
UF-1 (P2)	43.47	20.24	29.13	12.36	19.13
UF-2 (TTIP)	39.53	27.77	16.27	7.69	9.3
UF-2 (TTB)	31.94	18.33	16.66	10.44	6.94
NF (one layer)	25	10	16.66	5.66	11.66
NF (two layers)	33.33	17.94	18.75	13.33	6.25
NF (three layers)	34.09	17.14	20.45	18.6	2.27
NF (four layers)	36.58	21.21	19.51	13.15	7.31
NF (five layers)	35.89	21.87	17.94	13.51	5.12

The highest flux decline due to concentration polarization was determined to be 31.48% for UF-1 (disperal) membrane which also had the highest total flux decline of 45.42%. The level of concentration polarization had a determining effect on total flux decline. The concentration polarization contributes to membrane fouling significantly during wastewater treatment. The estimation of the membrane resistance is important for evaluating membrane performance/application. Various resistances of all the

membranes including R_{total}, R_m, R_{cp} and R_f were calculated by using the obtained flux data (J_{ww}, J_{cwi}, J_{cwc} and J_{cwf}) and these results are tabulated in Table 6.7. The filtration resistances of the membranes varied due to the different levels of fouling and concentration polarization. The calculated filtration resistances are further given in Table 6.7 and plotted in Figures 6.33 and 6.34 with respect to the various membranes used in this work.

Table 6.7. The filtration resistance of Support, MF, AKP-50, UF-1 (disperal and P2), UF-2 (TTIP and TTB) and NF (one, two, three, four and five layers) membranes with pre-treatment.

Membrane Type	**$R_{total}=R_m+R_{cp}+R_f$**	**R_m**	**R_{cp}**	**R_f**		
				R_f	**R_{rf}**	**R_{if}**
Support	4.11E+11	3.73E+11	1.18E+10	2.62E+10	1.43E+09	2.47E+10
MF	6.74E+11	5.57E+11	1.02E+11	1.54E+10	7.20E+09	8.18E+09
AKP-50	8.86E+11	6.62E+11	1.10E+11	1.13E+11	9.19E+10	2.10E+10
UF-1 (disperal)	3.35E+12	1.83E+12	1.05E+12	4.66E+11	2.48E+11	2.18E+11
UF-1 (P2)	8.29E+12	4.69E+12	1.68E+12	1.93E+12	8.18E+11	1.11E+12
UF-2 (TTIP)	2.07E+13	1.25E+13	5.76E+12	2.44E+12	1.15E+12	1.29E+12
UF-2 (TTB)	2.20E+13	1.50E+13	4.03E+12	2.99E+12	1.88E+12	1.12E+12
NF (one layer)	2.40E+13	1.80E+13	2.40E+12	3.59E+12	1.22E+12	2.37E+12
NF (two layers)	3.37E+13	2.25E+13	6.05E+12	5.18E+12	3.68E+12	1.50E+12
NF (three layers)	3.72E+13	2.45E+13	6.37E+12	6.30E+12	5.73E+12	5.70E+11
NF (four layers)	4.15E+13	2.63E+13	8.79E+12	6.37E+12	4.30E+12	2.08E+12
NF (five layers)	4.31E+13	2.76E+13	9.43E+12	6.05E+12	4.55E+12	1.49E+12

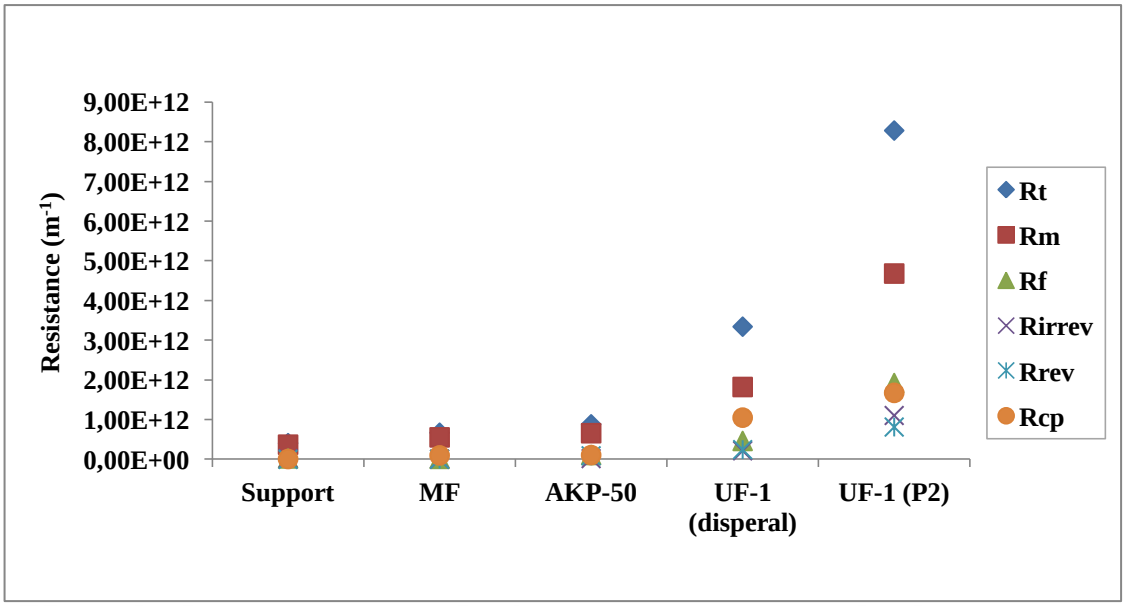

Figure 6.33. The variation of the filtration resistance for wastewater with pre-treatment with membrane type.

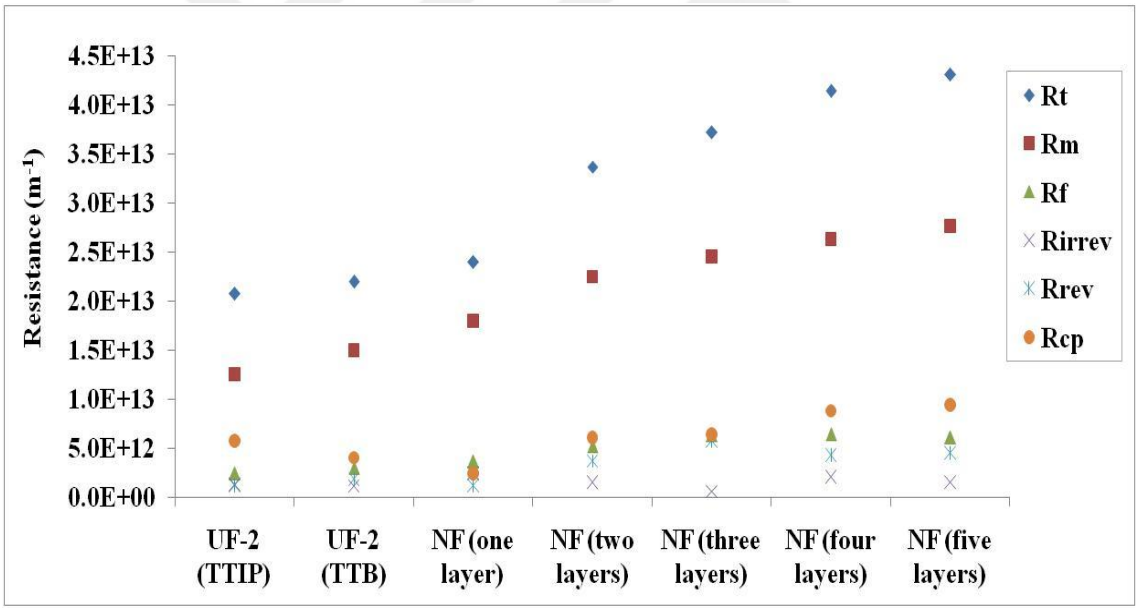

Figure 6.34. The variation of the filtration resistance for wastewater with pre-treatment with membrane type.

6.4.2. Textile Wastewater Treatment With/Without Pre-Treatment For The Second Tubular Membrane Series

Textile wastewater treatment was conducted through two routes by using the second tubular membrane set. The first wastewater membrane treatment route involved

the use of the membrane series without pretreatment. The second route involved using a pre-treatment involving $Al_2(SO_4)_3$ coagulation and filtering through selected filter paper which was followed by [UF-1 (P2) followed by NF(four layer)] membrane wastewater treatment.

Route1:

The variation of the J_{cwi} (clean water flux) of UF-1 (disperal and P2), UF-2 (TTB) and NF (zirconia+titania) tubular membranes at TMP=2 are given in Figure 6.35. The clean water flux decreases with decreasing pore size as expected. The UF-1 (disperal) presented the highest flux because it has the largest pore size. The clean water flux of UF-1 (disperal) is about 163 L/m^2h. The NF membranes which were coated once, twice, three times and four times presented the lowest flux due to their pore sizes. The clean water flux of NF membrane (four layers) is about 77 L/m^2h. The flux remained almost constant after the first 30 minutes of filtration.

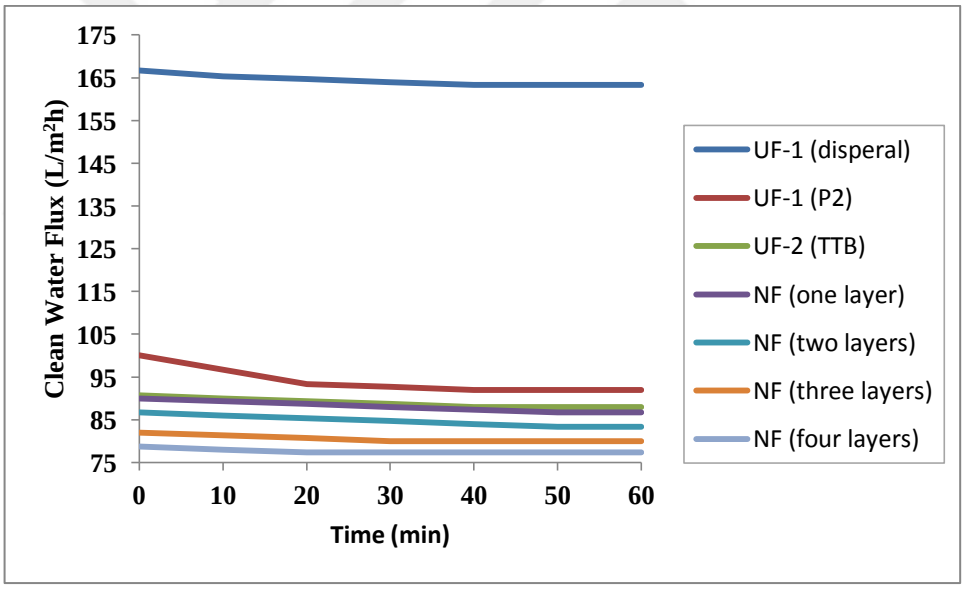

Figure 6.35. Variation of clean water flux at TMP=2 (UF-1 (disperal), UF-1 (P2), UF-2 (TTB), NF (one, two, three and four layers)) (without pre-treatment).

The variation of wastewater flux for all tubular membranes without pre-treatment with time are shown in Figure 6.36. The TMP was 2 during these experiments. The fluxes of disperal and P2 coated membranes significantly decreased with time due to extensive fouling due to the heavy particle/polymeric species load of the original wastewater and the absence of a pretreatment. The wastewater treatment was successive

in nature where permeate from the previous membrane was fed as the feed to the following membrane treatment [permeate from the UF-1 (disperal) filtration was fed as feed to UF-1 (P2), the permeate of UF-1 (P2) treatment was fed as feed to UF-2 (TTB)membrane , UF-2 (TTB) permeate was fed as feed to the NF (one layer) membrane treatment, NF (one layer) permeate was fed as feed to the NF (two layers) filtration, NF (two layer) permeate was fed as feed to the NF (three layers) filtration, NF (three layers) permeate was fed as feed to the NF (four layers)]. The final stabilized fluxes of the NF membranes were about 80 L/m^{2}h for the wastewater without pre-treatment.

The solids/salt content of wastewater without pre-treatment was gravimetrically determined to be about 0.57%. The wastewater suspended solids content was reduced 99.18% after the UF-1 (disperal) membrane treatment and to 100% after the UF-1 (P2) treatment. The UF-1 (disperal) and UF-1 (P2) increased the fluxes/performances of the successive UF-2 (TTB) and NF (one, two, three and four layers) membranes through the prevention of significant levels of fouling.

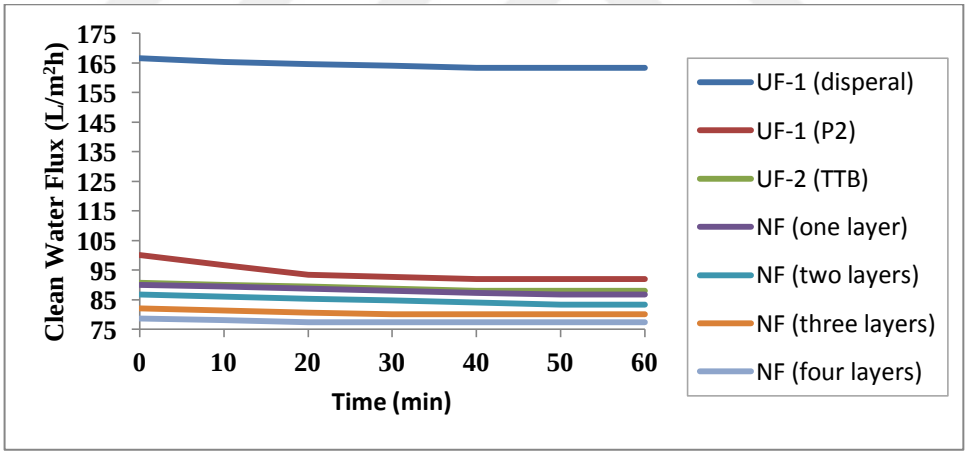

Figure 6.36. Wastewater flux variation of membranes at TMP-2 with time (UF-1 (disperal), UF-1 (P2), UF-2 (TTB) and NF (one, two, three and four layers)) (without pre-treatment).

The cumulative percent rejection values of the wastewater parameters without pre-treatment after the NF (four layers) membrane treatment are given in Table 6.8. The rejections were determined to be in the 99-100% range for important wastewater parameters such as suspended solids, all color values, and TOC. These results are also presented as bar graphs in Figures 6.37 to 6.39. Significant rejection in conductivity was

also obtained which may be due to the removal of dissolved ions/salts adsorption on retained particles/polymeric species on membrane surfaces. The photographs of the original and membrane treated wastewaters are given in Figure 6.40. The final treated wastewater sample in the bottle had a Pt-Co 455 value of 15 which may raise a reuse possibility in the plant.

Table 6.8. The cumulative percent rejection values of the wastewater without pre-treatment after the NF (four layers) treatment.

Parameter	Wastewater	The values of wastewater (without pre-treatment)
Pt-Co (410 nm)	99.5	5
Pt-Co (455 nm)	99.64	15
Pt-Co (465 nm)	99.63	15
Color (m^{-1}) 436 nm 525 nm 620 nm	 99.76 99.77 99.94	 0.213 0.131 0.064
Suspended Solid (810 nm, mg/L)	100	0
Conductivity (mS/cm)	87.5	1.045
pH	9.26	7.93
TOC (mg/L)	100	0
COD (448 nm, mg/L)	93.5	21.38

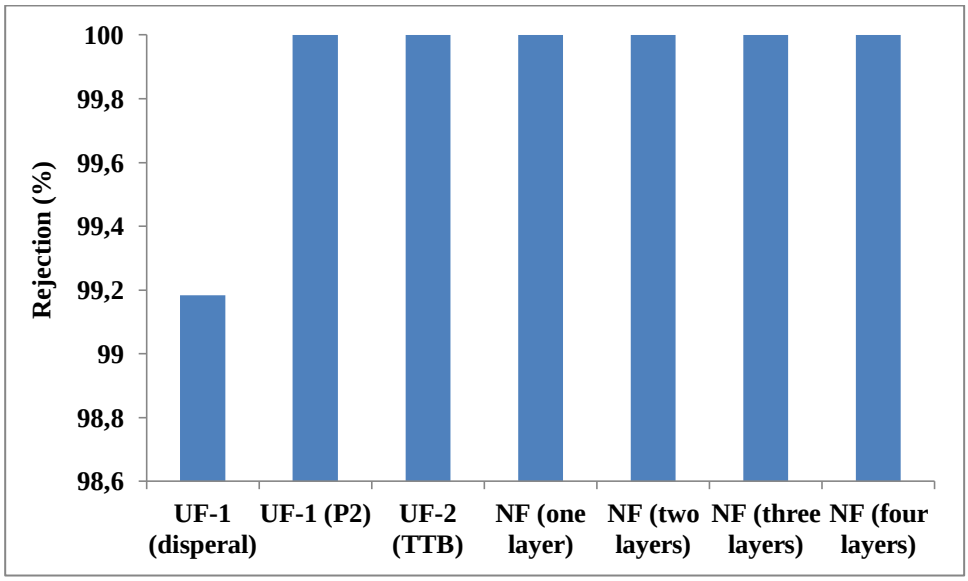

Figure 6.37. Rejection percentage of suspended solids (without pre-treatment).

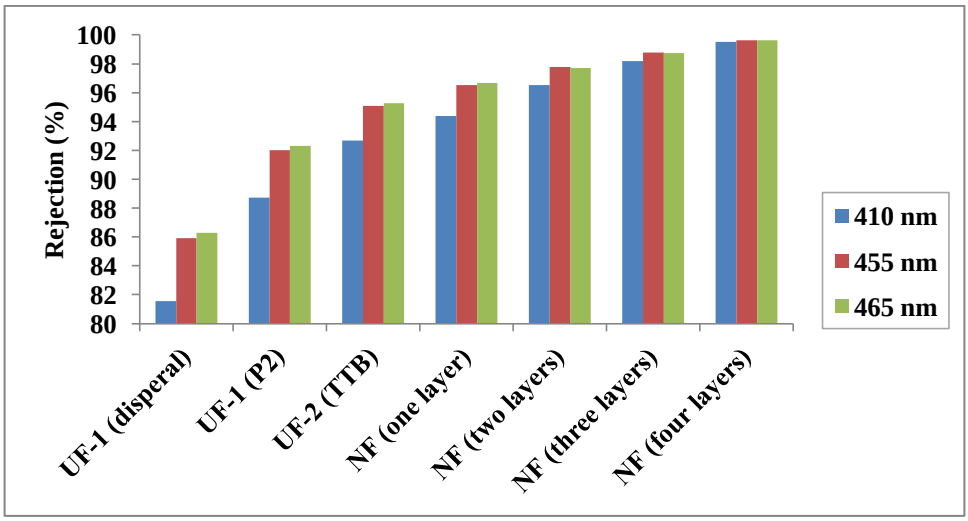

Figure 6.38. Rejection percentage of Color (Pt-Co) (without pre-treatment).

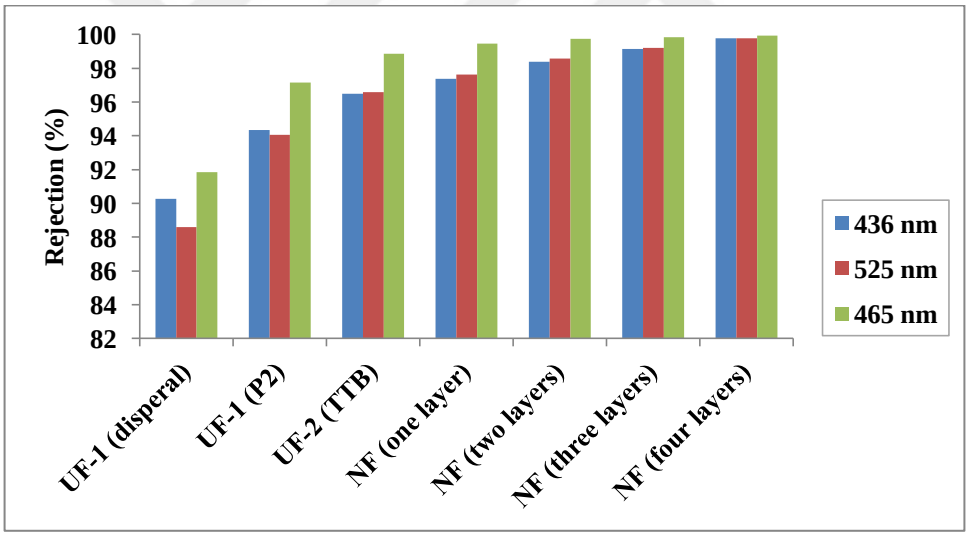

Figure 6.39. Rejection percentage of Admi Color (m^{-1}) (without pre-treatment).

Figure 6.40. Color change of wastewater (without pre-treatment) (from left to right; original wastewater, UF-1 (disperal, P2), UF-2 (TTB), NF (one, two, three and four layers, respectively)).

Route 2:

The variation of the clean water fluxes (J_{cwi})of UF-1 (P2) and NF (zirconia+titania) membranes at TMP=2 with time in 60 minutes are given in Figure 6.41. The clean water flux decreases with decreasing pore size as expected. The UF-1 (P2) presented the highest flux because of larger pore size. The clean water flux of UF-1 (P2) is about 92 L/m^{2}h. The membranes with four NF layers presented the lowest flux due to its smaller pore size. The clean water flux of NF membrane (four layers) was about 77 L/m^{2}h. The flux remained almost constant after the first 30 minutes of filtration.

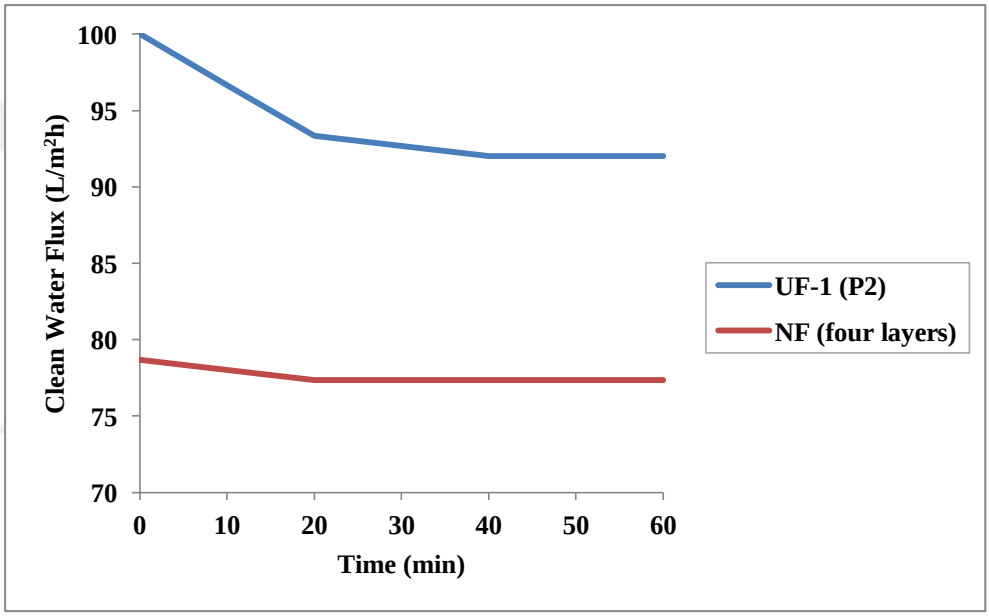

Figure 6.41. Variation of clean water flux at TMP=2 (P2 and NF(four layers)).

The variation of wastewater flux with time for UF-1 (P2) and NF (four layers) membranes with pre-treatment are shown in Figure 6.42. The TMP was 2 during these experiments. The flux of coated P2 membrane was not decreased with time due to pretreatment. Permeate of the UF-1 (P2) membrane wastewater treatment was fed as feed to the NF (four layers) membrane treatment. The wastewater fluxes of UF-1 (P2) and NF membrane (four layers) were about 14 L/m^{2}h and 72 L/m^{2}h, respectively. The wastewater flux of the first membrane was considerably lower than its clean water flux.

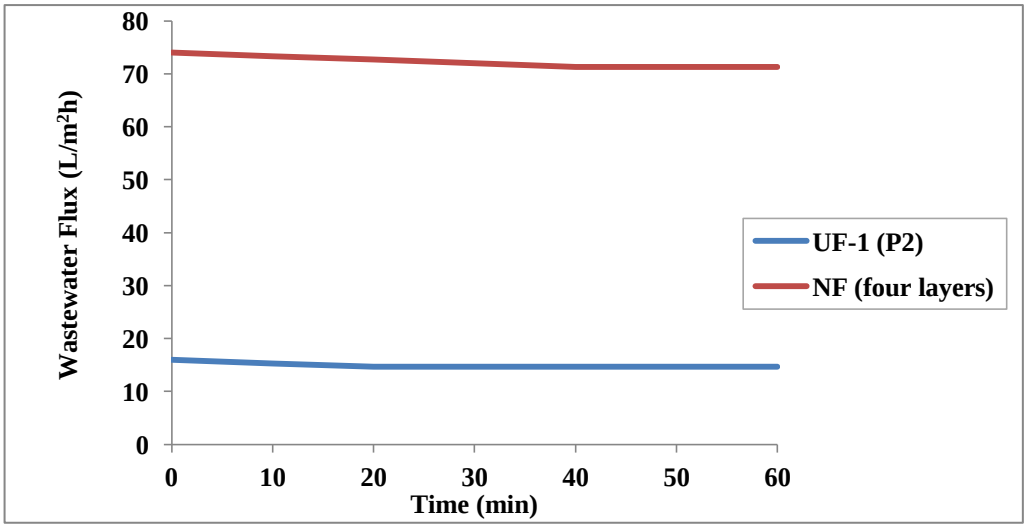

Figure 6.42. Wastewater flux decline of membranes at TMP-2 (UF-1 (P2) and NF (four layers)) (with pre-treatment).

The solids content of wastewater with pre-treatment was 0.55%. The wastewater suspended solids content was reduced 98.77 % after the pre-treatment ($Al_2(SO_4)_3$ + filter paper) filtration. The suspended solids content was reduced 100% after the UF-1 (P2) membrane wastewater treatment. The pre-treatment ($Al_2(SO_4)_3$ + filter paper) increased the flux/performance of the NF (four layers) membrane through fouling prevention. The UF-1 (P2) membrane flux was significantly reduced due to fouling

The cumulative percent rejection values of the wastewater with pre-treatment after the NF (four layers) treatment are given in Table 6.9. The cumulative percent suspended solids, color (436, 525, 620 nm), Pt-Co (410, 455, 465 nm), conductivity, TOC and COD rejections were measured as 100%, 99.66% (436 nm), 99.82% (525 nm), 99.97% (620 nm), 99.51% (410 nm), 99.69% (455nm), 99.72% (465 nm), 76 %, 100%, 91.53%, respectively. These results are also given as bar graphs in Figures 6.43 to 6.45 and a picture of the untreated/treated wastewater samples is given in Figure 6.46. Final treated wastewater with similar properties to the previous membrane treatment was obtained.

Table 6.9. The cumulative percent rejection values of the wastewater with pre-treatment after the NF (four layers) treatment.

Parameter	Wastewater	The values of wastewater (with pre-treatment)
Pt-Co (410 nm)	99.51	9
Pt-Co (455 nm)	99.69	24
Pt-Co (465 nm)	99.72	23
Color (m^{-1}) 436 nm 525 nm 620 nm	 99.66 99.82 99.97	 0.358 0.201 0.025
Suspended Solid (810 nm, mg/L)	100	0
Conductivity (mS/cm)	76	2.0064
pH	7.69	8.06
TOC (mg/L)	100	0
COD (448 nm, mg/L)	91.53	27.86

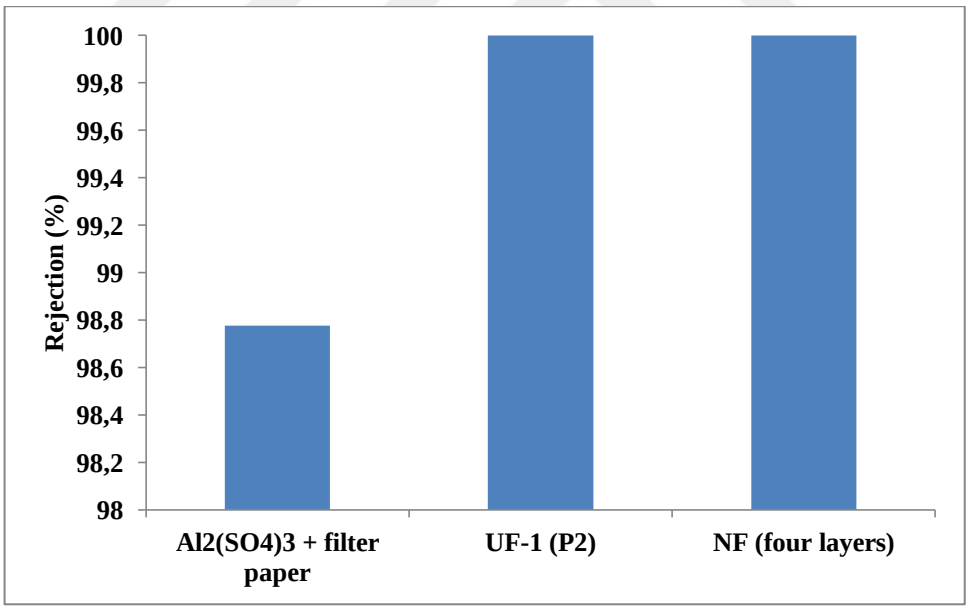

Figure 6.43. Rejection percentage of Suspended solids (with pre-treatment).

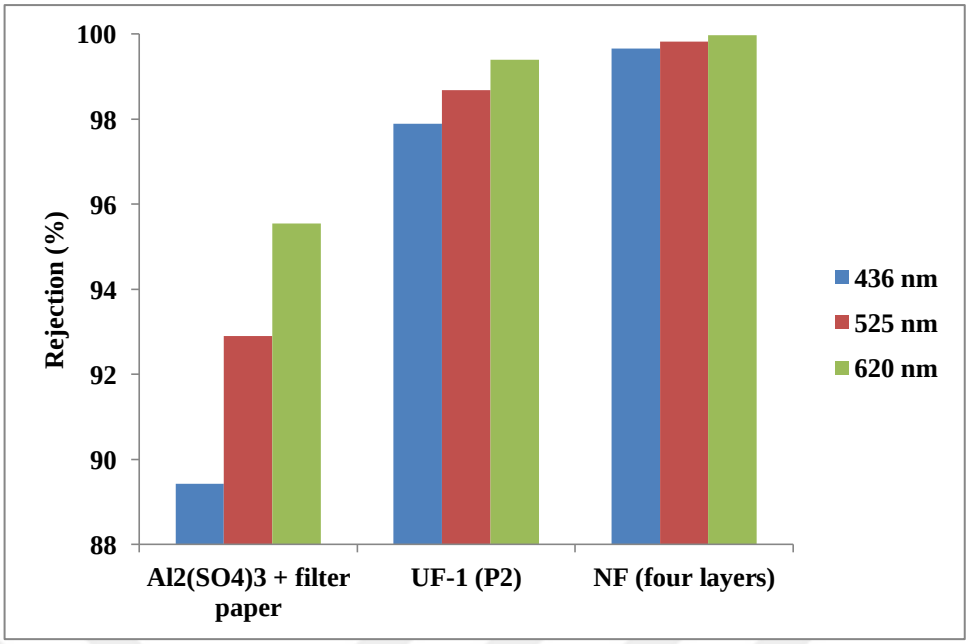

Figure 6.44. Rejection percentage of Admi Color (m^{-1}) (with pre-treatment).

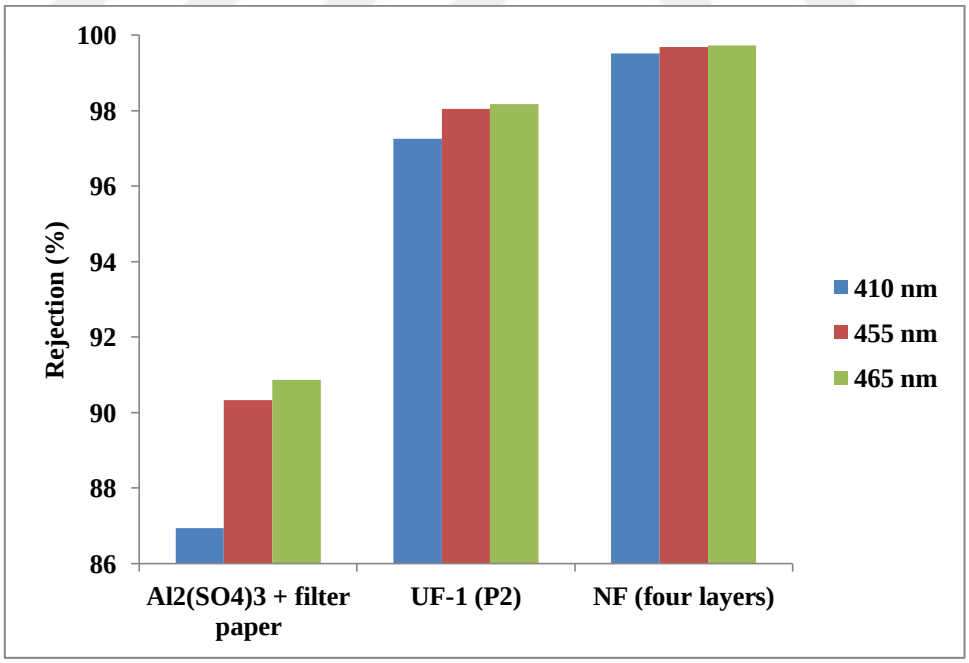

Figure 6.45. Rejection percentage of Color (Pt-Co) (with pre-treatment).

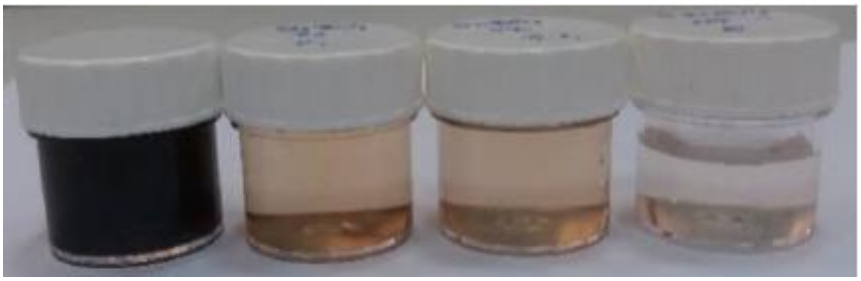

Figure 6.46. Color change of wastewater (with pre-treatment) (from left to right; original wastewater, $Al_2(SO_4)_3$+filter paper, UF-1 (P2), NF (four layers)).

6.4.2.1. Fouling Analyses of the Textile wastewater treatment with/without pre-treatment for the second tubular membrane series

Route 1:

The flux decline of the UF-1 (disperal), UF-1(P2), UF-2(TTB), NF (coated once, twice, three times and four times) membranes in the membrane treatment of the textile wastewater without pre-treatment are given in Table 6.10 at TMP=2. The clean water flux decreased from UF-1 (disperal) to NF layer coated membranes as a result of the nature of the pore structure of the membrane layers. The wastewater fluxes and the flux recoveries on the otherhand was the lowest for the first membrane in the series and increased gradually till the final NF membrane.

The tubular coated UF-1 (disperal) membrane had the highest clean water flux because the pore size of this membrane was designed to be the highest. The NF (four layers) is a top layer on the membrane and this membrane had the lowest clean water flux since it has the smallest pore size. The flux decline of the NF membranes was at about the same level due to the similarity in their pore sizes/structures. The presence of a high level of fouling in the first two membranes can be clearly seen from the data given in Table 6.10. The flux recovery (%) was also calculated 100 for NF (four layers). The comparison of the J_{cwc} fluxes with J_{cwi} initial clean water fluxes for the membrane series [UF-1 (disperal): 163 to 101, UF-1 (P2): 92 to 71, UF-2 (TTB): 88 to 82, NF (one layer): 87 to 86, NF (two layers): 83 to 83, NF (three layers): 80 to 76, NF (four layers): 77 to 77] also indicates that the first membranes in the series which are coming into contact with the most contaminated wastewater were fouled to a higher extent. These two fluxes were very close to each other especially for UF-2(TTB) and NF (one, two, three and four layers) membranes. The (J_{cwf}-J_{ww}) difference is a measure of

concentration polarization whereas (J_{cwi}-J_{cwf}) is a measure of fouling (irreversible+reversible fouling).

Table 6.10. The flux decline of the membranes (UF-1 (disperal and P2), UF-2 (TTB) and NF (one, two, three and four layers)) (without pre-treatment).

Membrane Type	**Flux (L/m^2h)**				
	Clean Water			**Wastewater**	**Flux Recovery (J_{cwc}/J_{cwi}) (%)**
	Initial (J_{cwi})	**Final (J_{cwf})**	**Cleaned (J_{cwc})**		
UF-1 (disperal)	163	60	101	18	61.96
UF-1 (P2)	92	61	71	46	77.17
UF-2 (TTB)	88	69	82	63	93.18
NF (one layer)	87	85	86	82	98.85
NF (two layers)	83	82	83	80	100
NF (three layers)	80	74	76	74	95
NF (four layers)	77	75	77	72	100

The flux decline analysis results (the fouling and concentration polarization) are given in Table 6.11. The highest flux decline due to concentration polarization was about 70% for UF-1 (disperal) membrane. The concentration polarization was determined to be the dominant mechanism in the total flux decline. The highest total flux decline was 88.97% for UF-1 (disperal). The filtration resistance is important for the evaluation of membrane performance. R_{total}, R_m, R_{cp} and R_f were calculated from the values of J_{ww}, J_{cwi}, J_{cwc} and J_{cwf} and these results are given in Table 7.12. The filtration resistance varied due to the different extents fouling and concentration polarization. The estimate filtration resistances are further illustrated in Figure 6.43.

Table 6.11. The flux decline and its distribution with fouling (irreversible, reversible) and concentration polarization of membranes without pre-treatment.

Membrane Type	**Flux Decline (%)**				
	Total	**Concentration Polarization**	**Fouling**		
	Total		**Total**	**Reversible**	**Irreversible**
	$(J_{cwi}-J_{ww})/J_{cwi}$	**$(J_{cwf}-J_{ww})/J_{cwf}$**	**$(J_{cwi}-J_{cwf})/J_{cwi}$**	**$(J_{cwc}-J_{cwf})/J_{cwc}$**	**$(J_{cwi}-J_{cwc})/J_{cwi}$**
UF-1 (disperal)	88.97	70	63.26	40.78	37.95
UF-1 (P2)	50	25	33.33	14.01	22.46
UF-2 (TTB)	28.03	8.65	21.21	15.44	6.81
NF (one layer)	5.38	3.14	2.30	1.55	0.76
NF (two layers)	4	2.43	1.6	0.8	0.8
NF (three layers)	7.5	0.89	6.66	1.75	5
NF (four layers)	6.89	4.42	2.58	1.73	0.86

Table 6.12. The filtration resistances of the membranes without pre-treatment.

Membrane Type	**$R_{total}=R_m+R_{cp}+R_f$**	**R_m**	**R_{cp}**	**R_f**		
				R_f	**R_{rf}**	**R_{if}**
UF-1 (disperal)	3.99E+13	4.40E+12	2.79E+13	7.58E+12	2.69E+12	4.88E+12
UF-1 (P2)	1.56E+13	7.81E+12	3.90E+12	3.93E+12	1.64E+12	2.26E+12
UF-2 (TTB)	1.13E+13	8.16E+12	9.82E+11	2.20E+12	1.60E+12	5.97E+11
NF (one layer)	8.76E+12	8.29E+12	2.76E+11	1.96E+11	1.32E+11	6.43E+10
NF (two layers)	8.98E+12	8.62E+12	2.19E+12	1.4E+11	7.07E+10	6.95E+10
NF (three layers)	9.71E+12	8.98E+12	8.67E+10	6.42E+11	1.69E+11	4.73E+11
NF (four layers)	9.97E+12	9.29E+12	4.42E+11	2.46E+11	1.66E+11	8.08E+10

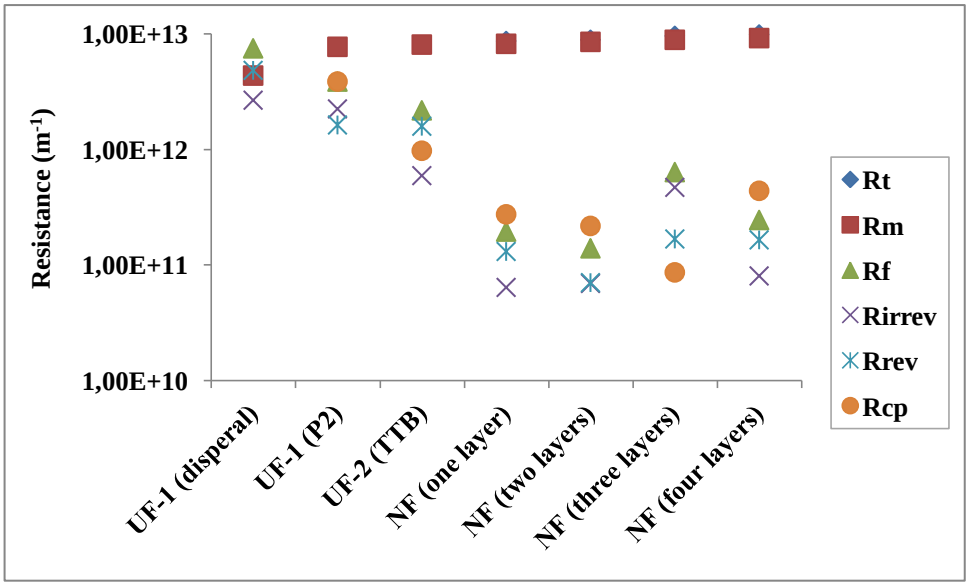

Figure 6.47. The distribution of the resistances for the second tubular membrane series without pre-treatment (Route 1).

Route 2:

The flux decline of the UF-1 (P2) and NF (four layers) membranes in the textile wastewater filtration with pre-treatment are given in Table 6.13 at TMP=2. The flux decreased gradually starting from UF-1 (P2) to NF (four layers) layer due to the variation in the membrane selective layer pore structures.

Table 6.13. The fluxes and flux recovery for the UF-1 (P2) and NF (four layers) membranes with pre-treatment.

Membrane Type	**Flux (L/m^{2}h)**				
	Clean Water			**Wastewater (J_{ww})**	**Flux Recovery (J_{cwc}/J_{cwi}) (%)**
	Initial (J_{cwi})	**Final (J_{cwf})**	**Cleaned (J_{cwc})**		
UF-1 (P2)	92	28	39	14.66	42.39
NF (four layers)	77	73	75	71	97.40

The tubular coated UF-1 (P2) membrane had a higher clean water flux than the NF (four layers) membrane due to its larger pore size. The level of membrane fouling was planned to be reduced with the applied pretreatment by using only two membranes successively instead of 7 membranes used in route 1. The flux decline of the UF-1 (P2)

and NF (four layers) membranes are given in Table 6.14. The flux recovery (%) was also calculated 97.40 for NF (four layers). The J_{cwc} was considerably lower than the J_{cwi} for UF-1 (P2) membrane due to fouling of the pore structure of the UF-1 (P2) membrane with the small particles/species present in the wastewater. The J_{cwc} was almost equal to the J_{cwi} for NF (four layers) membrane. The difference between J_{cwf} and J_{ww} is a measure of concentration polarization where the difference between J_{cwi} and J_{cwf} is similarly a measure of the fouling (irreversible+reversible fouling).

The flux decline analyses (the fouling and concentration polarization) are given in Table 6.14. The highest flux decline due to concentration polarization is 47.61% for UF-1 (P2). The concentration polarization affected the total flux decline. The highest total flux decline is 84.05% for UF-1 (P2). R_{total}, R_m, R_{cp} and R_f were calculated from the values of J_{ww}, J_{cwi}, J_{cwc} and J_{cwf} and these results are given in Table 6.15. The filtration resistance varied due to the nature of membrane fouling and concentration polarization. The filtration resistances are also illustrated in Figure 6.48. These results clearly indicated the importance of pretreatment and membrane system combination for a certain wastewater treatment process for discharge and reuse.

Table 6.14. The flux decline distribution with fouling (irreversible, reversible) and concentration polarization of UF-1 (P2) and NF (four layers) membranes with pre-treatment.

Membrane Type	**Flux Decline (%)**				
	Total	**Concentration Polarization**	**Fouling**		
	$(J_{cwi}-J_{ww})/J_{cwi}$	**$(J_{cwf}-J_{ww})/J_{cwf}$**	**Total $(J_{cwi}-J_{cwf})/J_{cwi}$**	**Reversible $(J_{cwc}-J_{cwf})/J_{cwc}$**	**Irreversible $(J_{cwi}-J_{cwc})/J_{cwi}$**
UF-1 (P2)	84.05	47.61	69.56	27.58	57.97
NF (four layers)	7.75	2.72	5.17	1.78	3.44

Table 6.15. The filtration resistance of UF-1 (P2) and NF (four layers) membranes with pre-treatment.

Membrane Type	$R_{total}=R_m+R_{cp}+R_f$	R_m	R_{cp}	R_f		
				R_f	R_{rf}	R_{if}
UF-1 (P2)	4.90E+13	7.81E+12	2.33E+13	1.79E+13	1.08E+13	7.08E+12
NF (four layers)	1.01E+13	9.29E+12	2.75E+11	5.07E+11	3.32E+11	1.75E+11

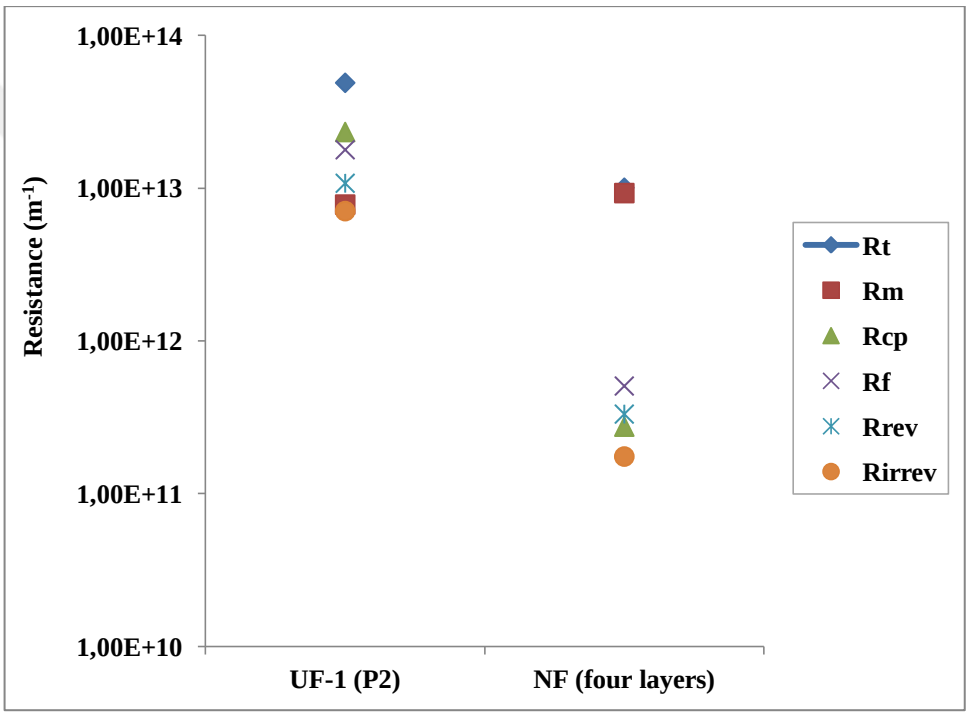

Figure 6.48. The distribution of the filtration resistance for wastewater with pre-treatment (UF-1(P2) and NF (four layers)).

CHAPTER 7

CONCLUSIONS

Tubular alumina supports were formed through the extrusion of alumina pastes. The tubular alumina supports were coated by dip coating with α-alumina, boehmite and titania stable suspensions/sols. The selective MF layers were prepared by two α-alumina colloidal suspensions. The selective UF-1 layers were prepared by disperal and P2 colloidal suspensions. The UF-2 and NF layers were formed as the top layers. The UF-2 layers were prepared by dip-coating with TTIP and TTB hydrosols. The NF layers were prepared by dip-coating the membranes with titania/zirconia polymeric sols.

The distribution of the particle sizes of the sols were determined by DLS-Zetasizer. The heating rates and heat treatment temperatures of the selective layers were determined by dilatometric investigation of room temperature dried unsupported membranes. The structure/thickness of the membrane layers were determined by SEM. The separation performance and clean water permeability of ceramic membranes were measured by cross-flow filtration. The COD, TOC, colors, suspended solids and turbidity of the permeates and wastewaters were measured by a spectrophotometer.

The selective microfiltration layers were formed by using α-alumina CT3000SG/AKP-50 suspensions. The average particle size of α-alumina CT3000SG powder colloidal suspension was determined as 522 nm. This α-alumina MF layer was dried at room temperature and heat treated at 1200 °C. The second α-alumina MF layer was prepared by using AKP-50 powder colloidal suspension. The average particle size of AKP-50 colloidal suspension was determined as 175 nm. These second MF membrane layers were heat treated at 1000 °C. The selective UF-1 layers were prepared by using disperal and P2 sols. The average particle sizes of disperal and P2 sols were 42 nm, 16 nm, respectively. The dried disperal and P2 membranes were heat treated at 600 °C. The UF-2 layers was prepared by using titania hydrosols (TTIP and TTB). The average particle sizes of the TTIP and TTB hydrosols were 14 nm, 4.9 nm, respectively. The dried titania layers were heat treated at 400 °C.

The clean water fluxes of the first set of tubular membranes [supports, microfiltration, AKP-50, UF-1(disperal), UF-1(P2), UF-2(TTIP), UF-2(TTB), NF (one

layer), NF (two layers), NF (three layers), NF (four layers) and NF (five layers) coated] varied in the 1910-26 L/m^{2}h range at TMP 2. The corresponding wastewater fluxes of these membranes were measured to be in the 1738-16 L/m^{2}h range with pre-treatment at TMP 2. Wastewater suspended solids (SS) contents were reduced by about 99% after the pre-treatment [$Al_2(SO_4)_3$ coagulation and successive filtration of the coagulates by using a filter paper]. The pre-treatment decreased MF, UF-1 (disperal, P2), UF-2 (TTIP, TTB) and NF (one, two, three, four and five layers) fouling. Cumulative percent retentions of SS, Pt-Co and Admi colors , TOC, COD and conductivity of the wastewater were obtained as 100%, 97-99%, 89%, 100% and 37%, respectively. The flux declines due to the concentration polarization were determined to be the highest for (31.48%) UF-1 (disperal) membrane and lowest for the (3.44%) uncoated support. The flux recoveries (%) varied in the 81-100 % range with the lowest value (81%) for the UF-1 membrane which also had the highest irreversible fouling level.

The clean water fluxes (route 1 and route 2) of the second set of membranes were determined to be in the 163-77 L/m^{2}h. The wastewater fluxes (route 1) of the membranes were measured to be in the 18-72 L/m^{2}h range (without pre-treatment). Wastewater (route-1) SS contents were reduced by about 99% after the UF-1 (disperal) filtration treatment. The UF-1 (disperal) filtration treatment also decreased UF-1 (P2), UF-2 (TTB) and NF (one, two, three and four layers) fouling. Cumulative percent retention of SS, colors, TOC, COD and conductivity of the wastewater (route-1) were obtained as 100%, 99%, 100%, 93.5% and 87.5%, respectively. The flux declines due to the concentration polarization were 70% for UF-1 (disperal), 25% for UF-1 (P2), 8.65% for UF-2 (TTB), 3.14% for NF (one layer), 2.43% NF (two layers), 0.89% NF (three layers) and 4.42% for NF (four layers). The flux recovery (%) of the UF-1 (disperal), UF-1 (P2), UF-2 (TTB), NF (one, two, three and four layers) were 61.96%, 77.17%, 93.18%, 98.85%, 100%, 95% and 100%, respectively.

The wastewater fluxes (route-2) of UF-1 (P2) and NF (four layers) coated membranes were measured as 14 and 71 L/m^{2}h (with pre-treatment) with the second membrane set at TMP 2. Wastewater (route-2) SS contents were reduced by about 98% after the coagulation pre-treatment . Membrane fouling was decreased significantly by pre-treatment in the UF-1 (P2) and NF (four layers) membranes. Cumulative percent retention of SS, colors, TOC, COD and conductivity of the wastewater were obtained as 100%, 99%, 100%, 91% and 76%, respectively. The flux declines due to the concentration polarization were 47.61% for UF-1 (P2) and 2.72% for NF (four layers).

The flux recovery of the UF-1 (P2) was 42.39% whereas it was about 97% for NF (four layers).

In conclusion, membrane fouling was significatly reduced by using coagulation pre-treatment. The Pt-Co 455 color value which is one of the most important wastewater parameters was determined to be 215 at the end of first tubular membrane set with $Al_2(SO_4)_3$ coagulation pre-treatment. The Pt-Co 455 color values of second tubular membrane set with/without pre-treatment were 24 and 15, respectively. These are in the discharge and reuse criteria range of Pt-Co 455 color value of textile wastewater which are 260-280 and 0, respectively. The results of this work indicated that the ceramic membrane treatment may be an effective method in textile wastewater treatment.

REFERENCES

Anderson MA, Gieselmann MJ and Xu Q (1988). Titania and alumina ceramic membranes. *Journal of Membran Science, 243-258.* doi: http://dx.doi.org/10.1016/S0376-7388(00)80932-1

A. Chemseddine, T. M., Eur. J. . (1999). Nanostructuring Titania: Control over Nanocrystal Structure, Size, Shape, and Organization.

Barredo-Damas, S., Alcaina-Miranda, M. I., Bes-Piá, A., Iborra-Clar, M. I., Iborra-Clar, A., & Mendoza-Roca, J. A. (2010). Ceramic membrane behavior in textile wastewater ultrafiltration. *Desalination, 250*(2), 623-628. doi:http://dx.doi.org/10.1016/j.desal.2009.09.037

Barredo-Damas, S., Alcaina-Miranda, M. I., Iborra-Clar, M. I., & Mendoza-Roca, J. A. (2012). Application of tubular ceramic ultrafiltration membranes for the treatment of integrated textile wastewaters. *Chemical Engineering Journal, 192*, 211-218. doi:http://dx.doi.org/10.1016/j.cej.2012.03.079

Benito, J. M., Conesa, A., Rubio, F., & Rodríguez, M. A. (2005). Preparation and characterization of tubular ceramic membranes for treatment of oil emulsions. *Journal of the European Ceramic Society, 25*(11), 1895-1903. doi:http://dx.doi.org/10.1016/j.jeurceramsoc.2004.06.016

Cai, Y., Wang, Y., Chen, X., Qiu, M., & Fan, Y. (2015). Modified colloidal sol–gel process for fabrication of titania nanofiltration membranes with organic additives. *Journal of Membrane Science, 476*, 432-441. doi:http://dx.doi.org/10.1016/j.memsci.2014.11.034

Capar, G., Yilmaz, L., & Yetis, U. (2006). Reclamation of acid dye bath wastewater: Effect of pH on nanofiltration performance. *Journal of Membrane Science, 281*(1-2), 560-569. doi:10.1016/j.memsci.2006.04.025

Capar, G., Yilmaz, L., & Yetis, U. (2008). A membrane-based co-treatment strategy for the recovery of print- and beck-dyeing textile effluents. *Journal of Hazardous Materials, 152*(1), 316-323. doi:http://dx.doi.org/10.1016/j.jhazmat.2007.06.100

Debik, E., Kaykioglu, G., Coban, A., & Koyuncu, I. (2010). Reuse of anaerobically and aerobically pre-treated textile wastewater by UF and NF membranes. *Desalination, 256*(1–3), 174-180. doi:http://dx.doi.org/10.1016/j.desal.2010.01.013

Fersi, C., & Dhahbi, M. (2008). Treatment of textile plant effluent by ultrafiltration and/or nanofiltration for water reuse. *Desalination, 222*(1), 263-271. doi:http://dx.doi.org/10.1016/j.desal.2007.01.171

Fersi, C., Gzara, L., & Dhahbi, M. (2009). Flux decline study for textile wastewater treatment by membrane processes. *Desalination, 244*(1), 321-332. doi:http://dx.doi.org/10.1016/j.desal.2008.04.046

Katoch, A., Kim, H., Hwang, T., & Kim, S. S. (2012). Preparation of highly stable TiO2 sols and nanocrystalline TiO2 films via a low temperature sol-gel route. *Journal of Sol-Gel Science and Technology*, *61*(1), 77-82. doi:10.1007/s10971-011-2593-6

Kırkbaş, Ö. (2016). *Preparation and Characterization of Ceramic Micro/Ultra/Nanofiltration Membranes for Separation Processes and Wastewater Treatment.* İzmir Institute of Technology.

Kurt, E., Koseoglu-Imer, D. Y., Dizge, N., Chellam, S., & Koyuncu, I. (2012). Pilot-scale evaluation of nanofiltration and reverse osmosis for process reuse of segregated textile dyewash wastewater. *Desalination*, *302*, 24-32. doi:http://dx.doi.org/10.1016/j.desal.2012.05.019

Mohammadi, M. R. (2014). Semiconductor TiO2–Al2O3 thin film gas sensors derived from aqueous particulate sol–gel process. *Materials Science in Semiconductor Processing*, *27*, 711-718. doi:http://dx.doi.org/10.1016/j.mssp.2014.07.051

Mohammadi, M. R., Fray, D. J., & Mohammadi, A. (2008). Sol-gel nanostructured titanium dioxide: Controlling the crystal structure, crystallite size, phase transformation, packing and ordering. *Microporous and Mesoporous Materials*, *112*(1-3), 392-402. doi:10.1016/j.micromeso.2007.10.015

Moliner-Salvador, R., Deratani, A., Palmeri, J., & Sanchez, E. (2012). Use of nanofiltration membrane technology for ceramic industry wastewater treatment. *Boletin De La Sociedad Espanola De Ceramica Y Vidrio*, *51*(2), 103-110. doi:10.3989/cyv.152012

Puhlfurss, P., Voigt, A., Weber, R., & Morbe, M. (2000). Microporous TiO2 membranes with a cut off < 500 Da. *Journal of Membrane Science*, *174*(1), 123-133. doi:10.1016/s0376-7388(00)00380-x

Schrank, S. G., Santos, J. N. R. d., Souza, D. S., & Souza, E. E. S. (2007). Decolourisation effects of Vat Green 01 textile dye and textile wastewater using H2O2/UV process. *Journal of Photochemistry and Photobiology A: Chemistry*, *186*(2–3), 125-129. doi:http://dx.doi.org/10.1016/j.jphotochem.2006.08.001

Sekulic, J., ten Elshof, J. E., & Blank, D. H. A. (2004). A microporous titania membrane for nanofiltration and pervaporation. *Advanced Materials*, *16*(17), 1546-+. doi:10.1002/adma.200306472

Sh. Akbarnezhad, S. M. M. a. R. S. (2010). Sol-gel synthesis of alumina-titania ceramic membrane: Preparation and characterization. *Indian Journal of Science and Technology*.

Shi, X., Tal, G., Hankins, N. P., & Gitis, V. (2014). Fouling and cleaning of ultrafiltration membranes: A review. *Journal of Water Process Engineering*, *1*, 121-138. doi:http://dx.doi.org/10.1016/j.jwpe.2014.04.003

Tang, C., & Chen, V. (2002). Nanofiltration of textile wastewater for water reuse. *Desalination*, *143*(1), 11-20. doi:http://dx.doi.org/10.1016/S0011-9164(02)00216-3

Uzal, N., Yilmaz, L., & Yetis, U. (2009). Microfiltration/ultrafiltration as pretreatment for reclamation of rinsing waters of indigo dyeing. *Desalination*, *240*(1), 198-208. doi:http://dx.doi.org/10.1016/j.desal.2007.10.092

Uzal, N., Yılmaz, L., & Yetis, U. (2010). Nanofiltration and Reverse Osmosis for Reuse of Indigo Dye Rinsing Waters.

Van der Bruggen, B., Vandecasteele, C., Van Gestel, T., Doyen, W., & Leysen, R. (2003). A review of pressure-driven membrane processes in wastewater treatment and drinking water production. *Environmental Progress*, *22*(1), 46-56. doi:10.1002/ep.670220116

Van Gestel, T., Kruidhof, H., Blank, D. H. A., & Bouwmeester, H. J. M. (2006). ZrO2 and TiO2 membranes for nanofiltration and pervaporation - Part 1. Preparation and characterization of a corrosion-resistant ZrO2 nanofiltration membrane with a MWCO < 300. *Journal of Membrane Science*, *284*(1-2), 128-136. doi:10.1016/j.memsci.2006.07.020

Vitaliy Gidis, G. R. (2016) *Ceramic Membranes: New Opportunities and Practical Applications*.

Yılmaz, K. (2016). *Rheological Characterization and Extrusion of Alumina Based Pastes for The Preparation of Tubular Ceramic Membrane Supports.* İzmir Institute of Technology.

Zeidler, S., Puhlfürß, P., Kätzel, U., & Voigt, I. (2014). Preparation and characterization of new low MWCO ceramic nanofiltration membranes for organic solvents. *Journal of Membrane Science*, *470*, 421-430. doi:http://dx.doi.org/10.1016/j.memsci.2014.07.051